Reference

REPORT NO. DOT-TSC-CG-72-1

A TECHNIQUE FOR MEASURING THE BEHAVIOR OF A NAVIGATIONAL BUOY

L.V. BABB AND R.W. WILMARTH
TRANSPORTATION SYSTEMS CENTER
55 BROADWAY
CAMBRIDGE, MA. 02142

SEPTEMBER 1971
TECHNICAL REPORT

Prepared for
U.S. COAST GUARD
WASHINGTON, D.C. 20591

The contents of this report reflect the views of the Transportation System Center which is responsible for the facts and the accuracy of the data presented herein. The contents do not necessarily reflect the official views or policy of the Department of Transportation. This report does not constitute a standard, specification or regulation.

1. Report No.	2. Government Accession No.	3. Recipient's Catalog No.
DOT-TSC-CG-72-1		

4. Title and Subtitle	5. Report Date
A Technique for Measuring the Behavior of a Navigational Buoy	Sept. 1971
	6. Performing Organization Code: TER
7. Author(s): L.V. Babb, R.W. Wilmarth	8. Performing Organization Report No.: DOT-TSC-CG-72-1
9. Performing Organization Name and Address: U.S. Department of Transportation, Transportation Systems Center, Cambridge, MA 02142	10. Work Unit No.: CG01
	11. Contract or Grant No.
12. Sponsoring Agency Name and Address: U.S. Department of Transportation, U.S. Coast Guard, Washington, DC 20591	13. Type of Report and Period Covered: Technical Report, Nov 1970-July 1971
	14. Sponsoring Agency Code

15. Supplementary Notes

16. Abstract: A prototype instrumentation system has been developed and fabricated to furnish stability information about a moored navigational buoy. The parameters necessary to define this stability are listed and the electro-mechanical transducers selected to measure these parameters are discussed. By utilizing a command and data transmission telemetry system, analog data were recorded and used to determine the types of instrumentation best suited to this application. A discussion of the results of testing and project recommendations conclude the report.

17. Key Words	18. Distribution Statement
Buoy Behavior Telemetry Control	Availability is Unlimited. Document may be Released To the National Technical Information Service, Springfield, Virginia 22151, for Sale to the Public.

19. Security Classif. (of this report)	20. Security Classif. (of this page)	21. No. of Pages	22. Price
Unclassified	Unclassified	118	

PREFACE

The authors are indebted to Cmdr. R. Baetsen, Chief, Navigation Aids Branch and Cmdr. G. Budridge of the Office of Research and Development, U. S. Coast Guard and to Dr. Gene G. Mannella, Mr. L. W. Roberts and Mr. C. M. Veronda of the Transportation Systems Center for their support and encouragement. The authors also would like to acknowledge Mr. Charles Dunne and Mr. James Reardon for constructing the instrumentation.

TABLE OF CONTENTS

TABLE OF CONTENTS (CONT.)

LIST OF ILLUSTRATIONS

LIST OF ILLUSTRATIONS (CONT.)

LIST OF ILLUSTRATIONS (CONT.)

LIST OF TABLES

1.0 INTRODUCTION

The use of a buoy as a marine navigational aid has long been established. Buoys provide information by their shape, colors, markings, and the devices carried by them, such as lights, bells and radar reflectors. For these latter devices to be most effective it is important that the motions of the buoy remain within certain limits a high percentage of the time. When the motion of the buoy exceeds a given envelope, the probability of detection and recognition is reduced and its utility as an aid decreases. The stability of present buoys is due to a great extent to their sheer size and bulk. For example a buoy used widely today is the Coast Guard standard 8x26 type and is shown in figure 1. The number is directly related to its size which measures 8 feet in diameter and 26 feet high. When placed in water the position of the buoy is constrained by a mooring chain attached to a massive concrete sinker. The weight of a single buoy system including the buoy, mooring chain, and sinker, often exceeds ten tons. While this buoy has proven to be reliable with desirable stability characteristics it does require extensive maintenance. Buoys are generally serviced once a year at which time the entire system must be removed sufficiently from the water to be inspected and any necessary repairs made. Because of the extreme environmental conditions experienced by the buoy it is common for corrosion of the exterior, marine fouling of the mooring chain, and physical damage of the active devices on board to have taken place. Normal service also includes checking the position of the buoy and replacement of the battery packs and light bulbs. In addition to the annual maintenance, every lighted buoy is taken ashore at three year intervals for a complete overhaul.

With many hundreds of buoys in service is is necessary for the Coast Guard to employ a sizable fleet of specially equipped boats, called buoy tenders, on a continuing basis. Needless-to-say, this is an expensive program which accounts for an appreciable portion of the Coast Guard's budget. To reduce the cost, a new series of plastic buoys are being given serious consideration. The advantages of using anti-corrosion materials with weight savings of at least one-third are attractive from two viewpoints. First, with anti-corrosion materials the maintenance should be reduced along with increasing the length of maintenance intervals. Secondly, the lighter weight should ease the equipment requirements while allowing for a safer operation. Presently the stability of the buoys is unknown, i.e., how do their motions compare

Figure 1. 8x26 Standard Buoy

to those of the standard 8x26 buoy currently used. Figures 2 through 5 illustrate these buoys which are not only different from the standard but different from each other. One would intuitively expect the catamaran buoy to behave quite differently from the standard since it is a surface device while the standard is certainly a deep draft device. To resolve these buoy motion questions a program was sponsored by the Coast Guard (at the Transportation Systems Center) to develop and fabricate an instrumentation and data handling system.

This document is the final report on this program which was concluded in June 1971 with simulated tests on a standard 8x26 buoy.

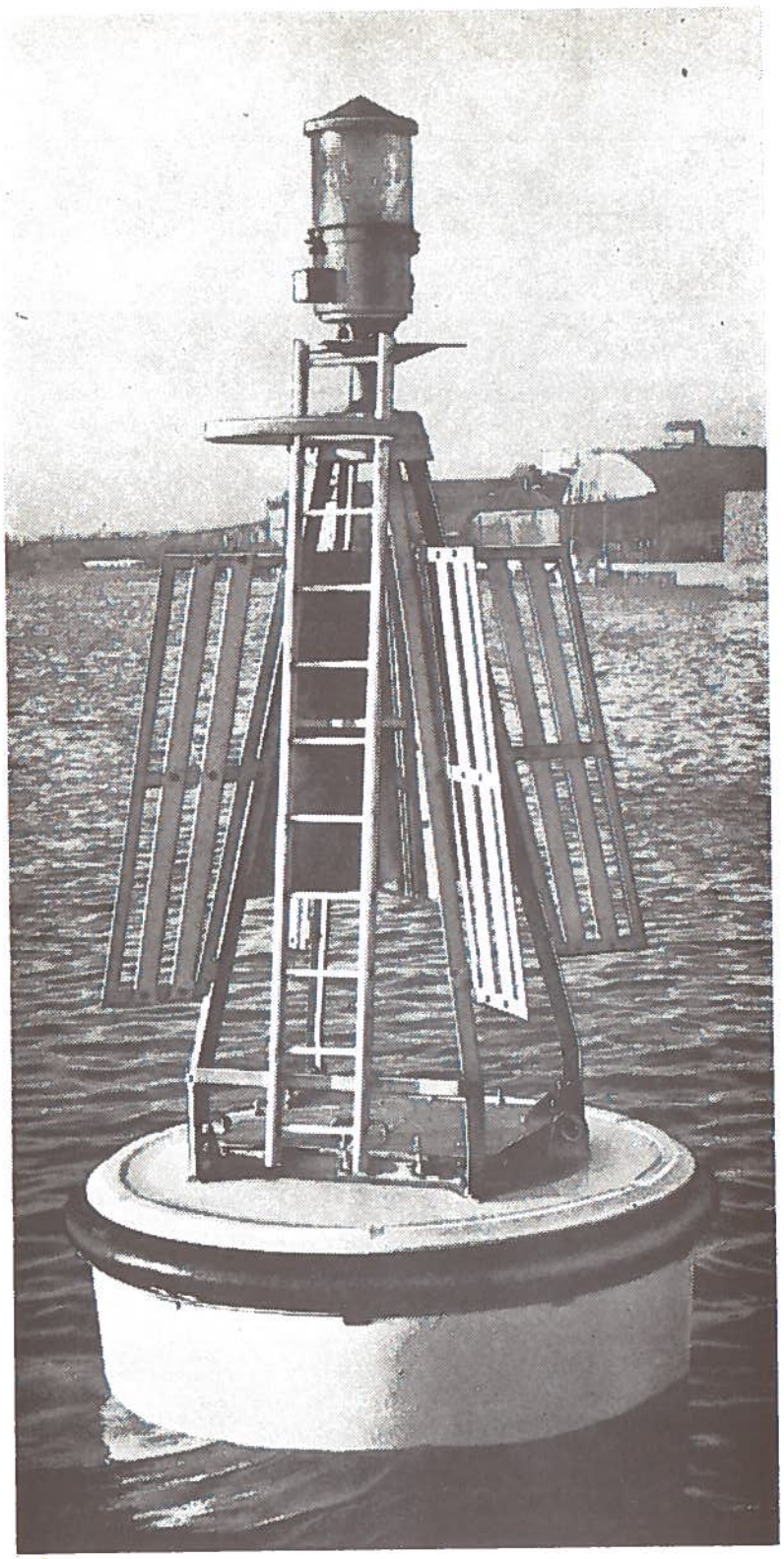

Figure 2. Osprey Buoy

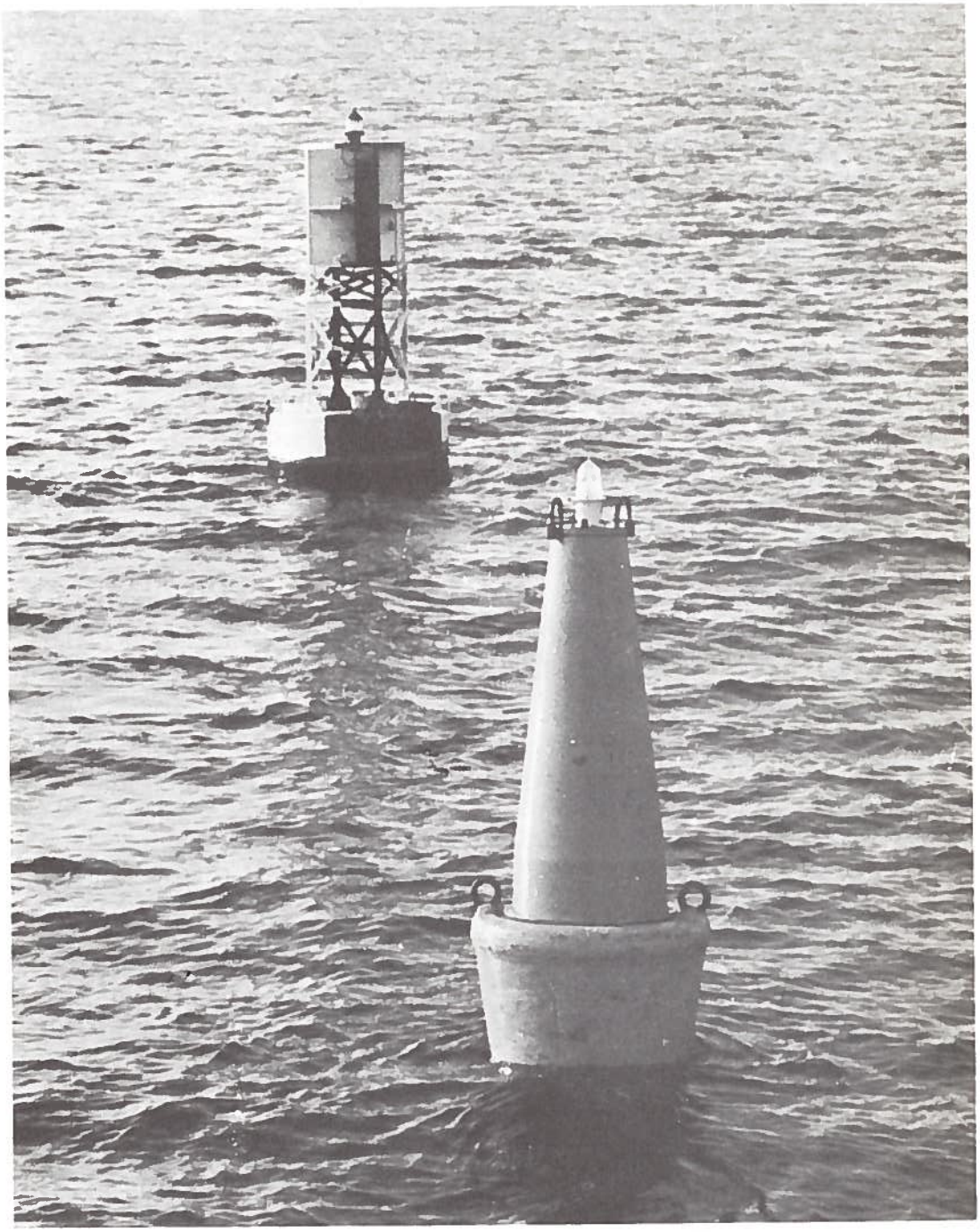

Figure 3. Standard Coast Guard 8x26 Steel Buoy (left) and Canun Buoy (right)

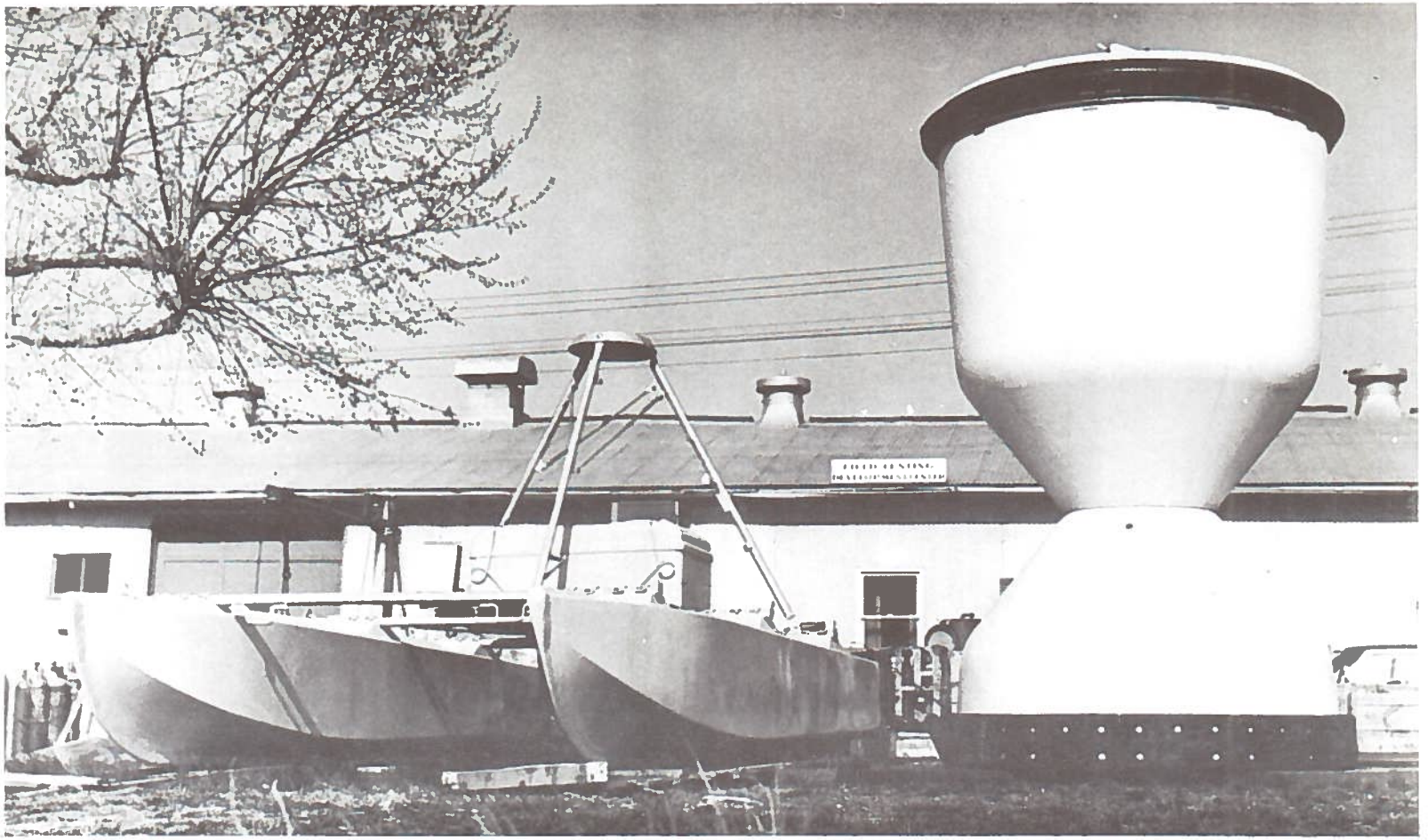

Figure 4. Catamaran Buoy (left) and Lower Portion of Osprey Buoy

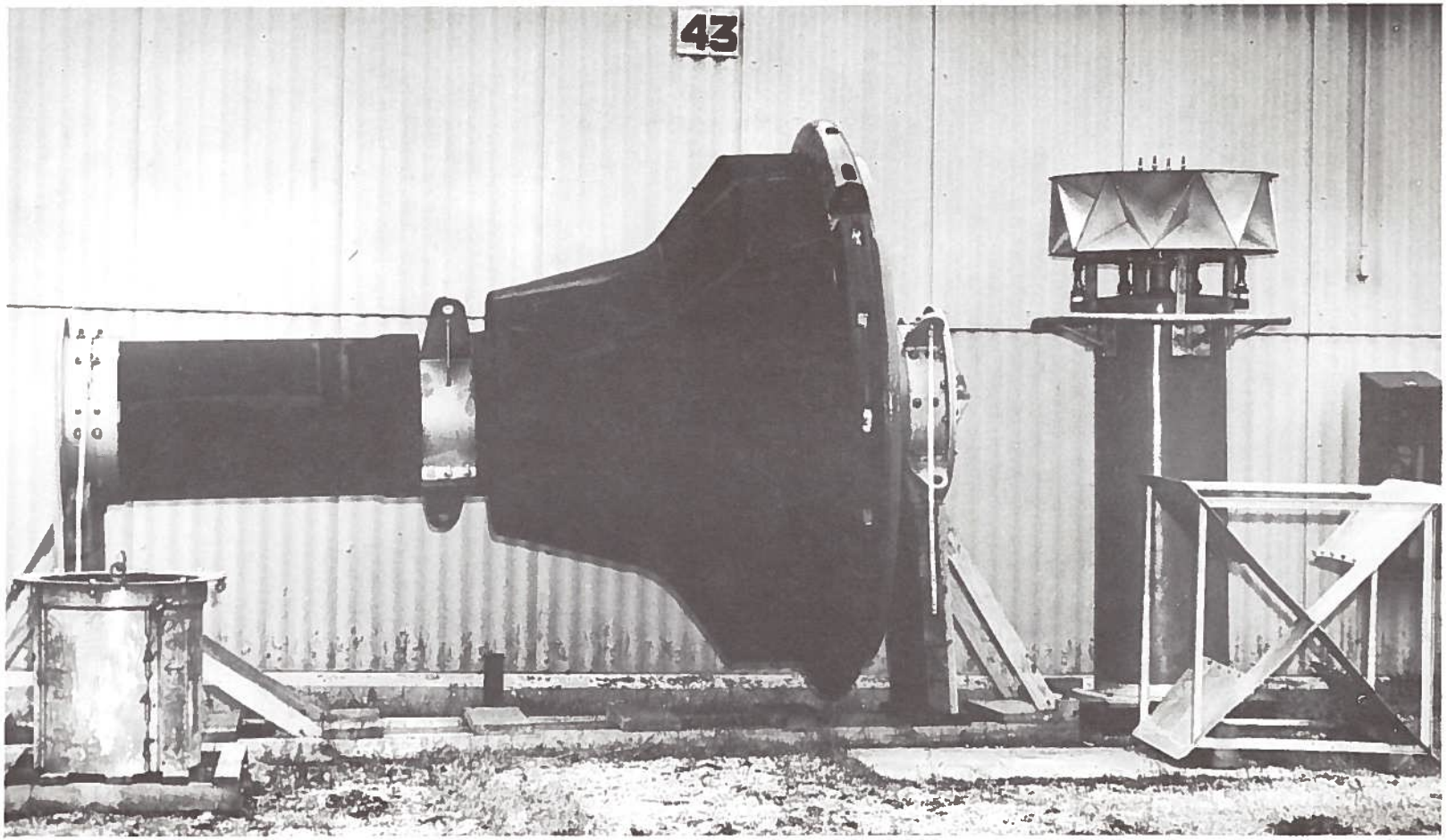

Figure 5. Tidelands Buoy, Disassembled

2.0 STABILITY PARAMMETERS

To accurately describe the stability of a buoy, the following parameters were measured:

a. Double displacement in vertical direction (heave movement) from 0 through 60 feet with an accuracy of 0.5 feet.

b. Heave rate.

c. Neutral pitch angle (the neutral position inclination of the vertical axis of the buoy about the lateral axis) from 0 through 10 degrees with an accuracy of 0.5 degrees and from 10 through 30 degrees with an accuracy of 2 degrees.

d. Neutral roll angle (the neutral position inclination of the vertical axis of the buoy about the longitudinal axis) to the same accuracy as preceding.

e. Pitch excursions

f. Roll excursions

g. Pitch rate

h. Roll rate

i. Mooring line tension with 50 pound accuracy

In addition to the above parameters, information concerning the sea conditions during tests is also important and will ultimately be utilized in buoy motion predictions. Although the effect of the varying conditions is not included in this report, parameters that must be considered include:

a. Current direction

b. Current speed

c. Wind direction

d. Wind speed

e. Sea state

f. Wave height

g. Wave celerity

h. Wave period

i. Barometric pressure

j. Water temperature

k. Air temperature

3.0 TRANSDUCERS IN THE PROTOTYPE UNIT

To measure the parameters specified above, electro-mechanical transducers were chosen to interface with the telemetry system. The selection of the transducers was governed by accuracy, frequency response, power requirements, weight, size, expected life, and of course, cost. The transducers chosen include accelerometers, pendulum inclinometers, vertical gyros, and a strain gage tension load cell. A brief description of these instruments is given followed by a discussion of the system as a whole.

Accelerometers are equivalent second-order spring-mass systems. Using straightforward mathematics, it can be shown that for a sinusoidal input with frequency, ω:

$$Z = \frac{(\omega/\omega_n)^2 Y}{\sqrt{[1 - (\omega/\omega_n)^2]^2 + [2\zeta\ \omega/\omega_n]^2}} \qquad (1)$$

where Z = relative displacement of the mass to the case

$\omega_n = \sqrt{k/m}$ = natural frequency of spring-mass system

$\zeta = c/C_c$ = damping ratio where $C_c = 2$ km

If ω/ω_n is small, the denominator approaches unity and

$$Z = \frac{\omega^2 Y}{\omega_n^2} = \frac{\text{Acceleration of case}}{\omega_n^2}$$

In an undamped accelerometer, the useful frequency range is quite limited because $1 - (\omega/\omega_n)^2$ decreases rapidly as ω increases. But by adding damping approximately equal to 70% of the critical value, this diminishing term is compensated for by the remaining denominator term, $2\zeta(\omega/\omega_n)$. The sum of these terms approaches unity over a wider frequency range and the utility of the device is increased. Figure 6 is a plot of the response of a second order system to a sinusoidal input acceleration for various values of ζ.

The damping ratio is also important in determining the phase relationships between the input and output accelerations. To accurately reproduce an acceleration input, the phase of all harmonic components must be shifted equally along the time axis. This can be accomplished if the phase angle, ϕ, is a linear function of the frequency. A damping factor of 0.7

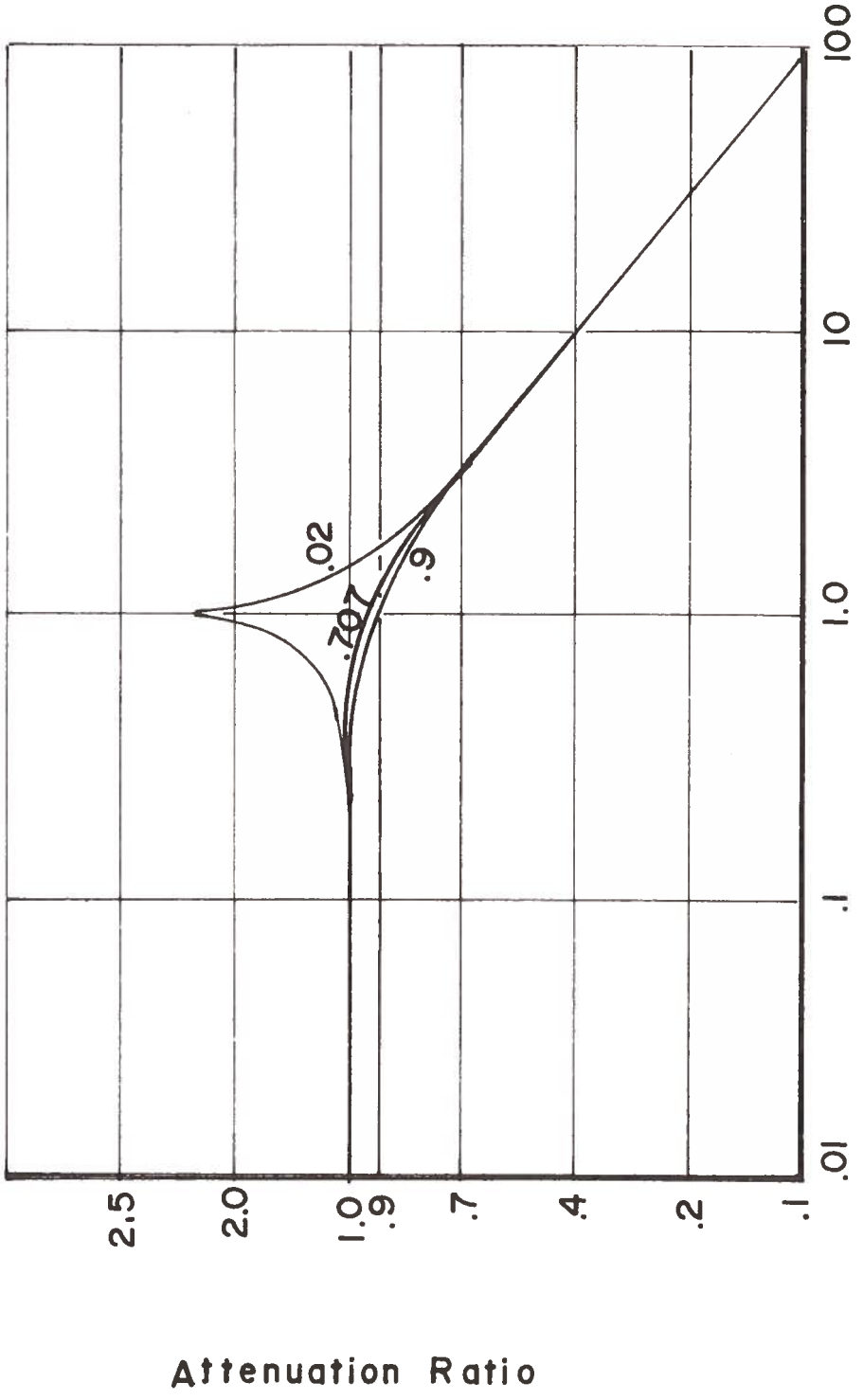

Figure 6. Response of a Second Order System

satisfies this condition as shown in figure 7 where

$$\phi = \tan^{-1} \frac{2\zeta(\omega/\omega_n)}{1 - (\omega/\omega_n)^2}$$

or

$$\phi = \pi/2(\omega/\omega_n) \text{ for } \zeta = .707$$

By properly choosing the natural frequency and damping ratio, a flat frequency response from 0 to 20 Hz was obtained with a time lag of less than 0.013 second.

The accelerometers chosen for the prototype unit were potentiometric devices manufactured by Edcliff Instruments, Model Number 7-101, with a range of ±5 G's. Table 1 details the remaining specifications of this unit.

For comparison purposes, a variable reluctance accelerometer with a range of ±1 1/2 G was included in the instrument package. The primary advantage of this unit is the electrical pick-off. The relative movement of the mass with respect to the case is sensed by a change in electrical field instead of a wiper arm movement across a resistor in the potentiometer type. This results in a decrease in friction within the unit and allows the resolution to be continuous. Table 2 lists these specifications.

Table 1. Accelerometer Specifications Edcliff 7-101

Range	± 5 G	
Max. Static Error Band	± 1.5%FR	.15G
Linearity	± .5%	.05
Resolution	.6%	.06
Hysteresis	.6%	.06
Friction	.6%	.06
Threshold	.8%	.08

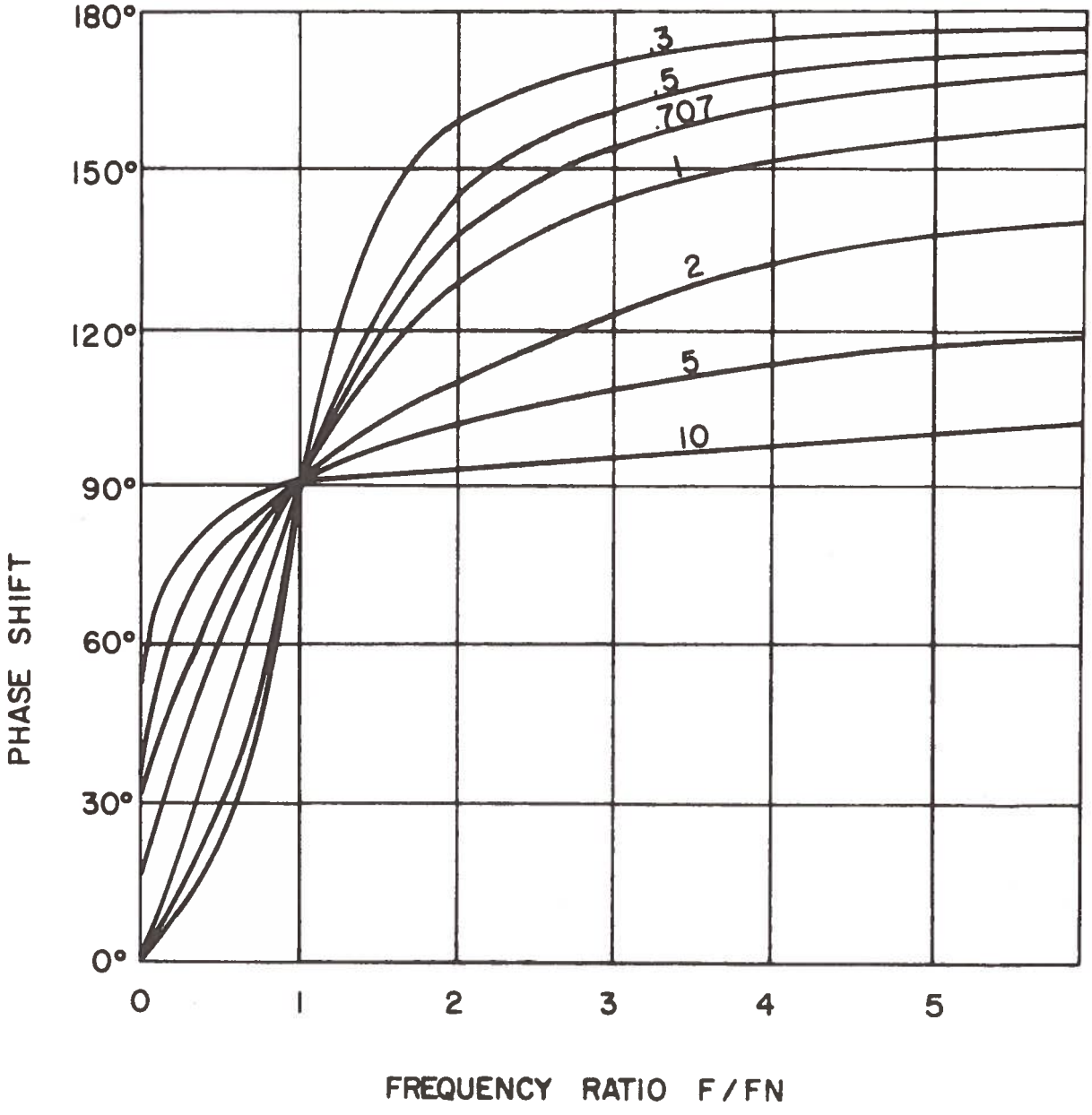

Figure 7. Phase Response of a Second Order System

Table 2. Accelerometer Specifications, Wianco A-1110

Range	± 1.5G	
Linearity	± 1.0% FR	.03G
Hysteresis	.1%	.003G
Resolution	Continuous	
Friction	< .6%	
Threshold	< .8%	

The basic elements of an inclinometer include a pendulum, case, and potentiometer type read-out in which the angular deviation is proportional to the change in resistance. On a non-accelerating platform with the pivot of the inclinometer located at the center of rotation of the platform, the accuracy of the device is limited only by the inherent bearing and potentiometer friction and by the linearity and resolution of the resistance element. However, if the instrument is accelerated, an error in angle measurement is introduced. It can be shown that for an acceleration input, $\ddot{x}$, in Figure 8

$$\tan\theta = \ddot{x}/g \sqrt{\frac{1}{[1 - (\omega/\omega_n)^2]^2 + [2\zeta\ \omega/\omega_n]^2}} \qquad (2)$$

$$\omega_n = \sqrt{g/l}$$

$$\zeta = C/C_c \text{ where } C_c = 2ml\sqrt{gl}$$

By referring again to figure 6, the bracketed term approaches unity under the same conditions as the accelerometer and the angular error introduced by lateral accelerations is given by Eq. 3,

$$\theta_{error} = \text{Arctan } \ddot{x}/g \qquad (3)$$

or

$$\theta_{error} \tilde{=} \ddot{x}/g \text{ for } \ddot{x}<g.$$

or

$$\theta_{error} \tilde{=} 0 \text{ for } \ddot{x}<<g.$$

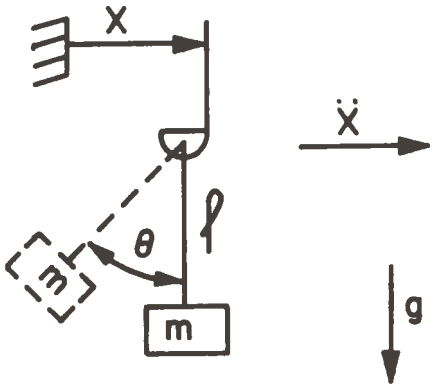

Figure 8. Acceleration Effects On a Pendulum

The use of pendulum inclinometers for angular measurements is therefore dependent upon the magnitude of "$\ddot{x}$" in an ocean environment. The simplicity of operation and minimum power requirements dictated that the instruments be included in the prototype package for evaluation.

The unit chosen was a dual axis type manufactured by Edcliff Instruments, Model 5-900. The advantage of a dual axis unit is that each pendulum is located in a gimbal so the axis of rotation remains in the horizontal plane and the pendulum is free to align with the gravity field. For this reason a reference with respect to local vertical is always obtained. The specifications of this unit are shown in Table 3.

Table 3. Inclinometer Specifications, Edcliff No. 5-900.

Range	±45°	
Linearity	± .4% FR	.36°
Resolution	.1%	.09°
Damping	.65±.1 crit.	
Nat. Freq.	3 hz.	

Vertical gyros were included in the package to "smooth" the data from the inclinometers so the magnitude of the lateral accelerations could be ascertained. Basically, a vertical gyro is a spinning rotor that is mounted in a two degree of freedom gimbal which isolates the rotor from base rotations. The physics of a spinning rotor dictate that in the absence of external torques, the spin axis remains in a stabilized orientation in space. By using an additional sensor, this orientation may be chosen as vertical and by utilizing pick-offs on the gimbals, the angular orientation of the base with respect to the vertical may be described. The mechanism by which the gyro obtains the vertical reference is termed the erection system. This system makes use of the law of gyroscopic precession and introduces torques about the appropriate axes to rotate (precess) the spin axis into the desired orientation. Numerically,

$$\vec{T} = \vec{\omega}_\rho \times \vec{H} \qquad (4)$$

where $\vec{H} = I\omega_s$ = Angular Momentum
I = Rotor Inertia
$\vec{\omega}_s$ = Rotor Velocity (Spin)
$\vec{\omega}_\rho$ = Precession Velocity
$\vec{T}$ = Torque

Referring to figure 9, a force, $\vec{F}_1$, applied as shown exerts a torque about the pitch axis. Using equation 4, it is apparent that the spin axis will rotate about the roll axis as noted in the figure.

The gyros purchased for the prototype package were Summers, Model 69. This model differs from a conventional vertical gyro in that the spin axis is erected to vertical in the outer axis and to the case of the instrument in the inner axis. Figure 10 is a simplified sketch of this gyro. The rotor is a motor with the armature shaft attached to a balanced hemispherical fly wheel (shaded). Erection to vertical is accomplished by a pendulum with its center of rotation coincident with the outer gimbal axis, but free to rotate with respect to the rotor. Attached to the pendulum is a small friction pad that is in contact with the fly wheel. If the pad is aligned with the spin axis the system is in equilibrium and no correction torque is introduced. However, misalignment of the pad with the spin axis results in relative sliding which in turn creates a friction force, $\vec{F}$, as shown. This force produces a torque, $\vec{T}$, about the roll axis, and recalling the law of gyroscopic precession, the rotor is forced to precess about the pitch axis until the spin axis is aligned with the friction pad. The precession velocity, $\vec{\omega}_\rho$, can be varied from 4°/min to 24°/min by adjusting the pressure of the friction pad.

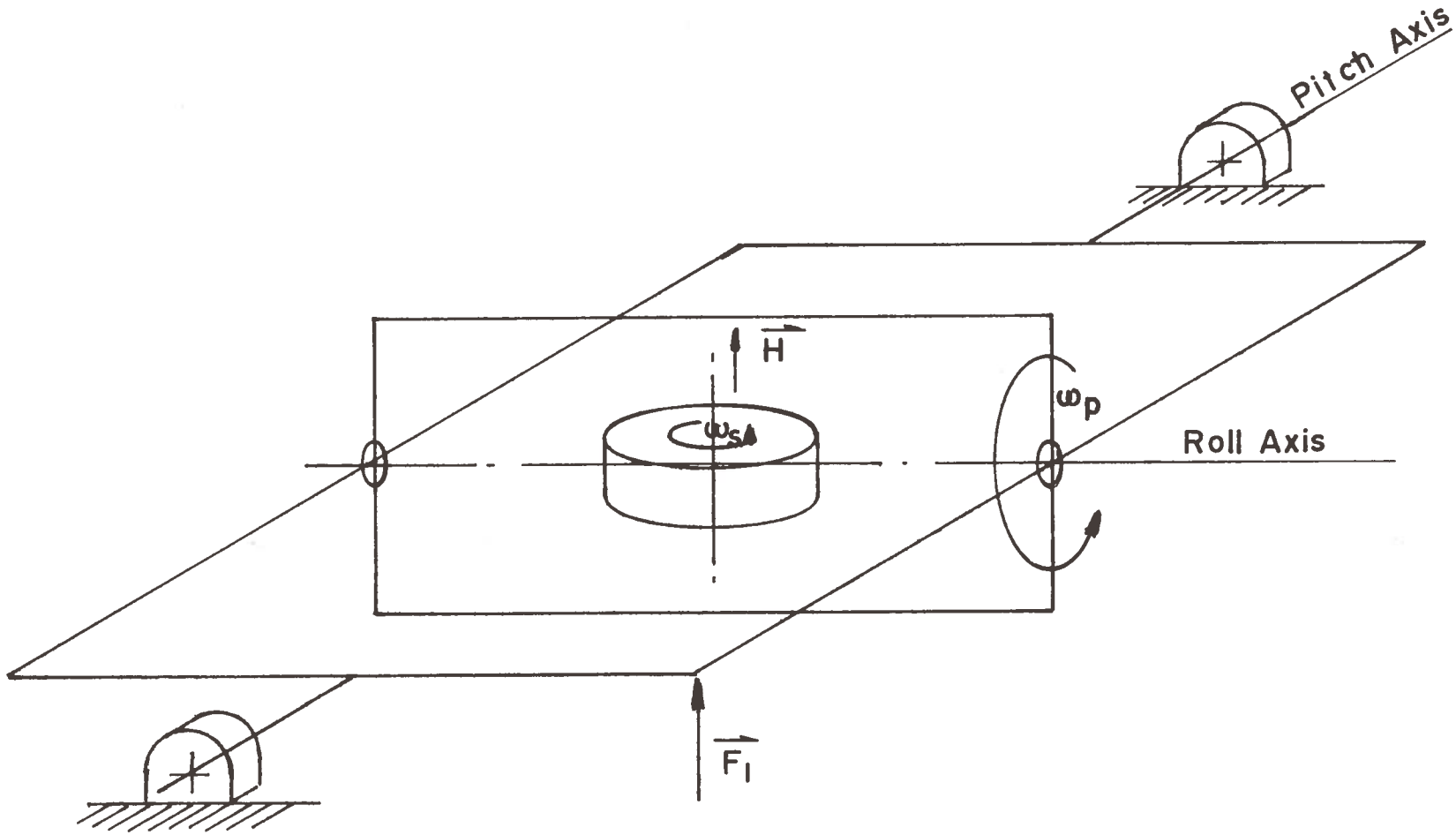

Figure 9. Simplified Sketch of Gyro

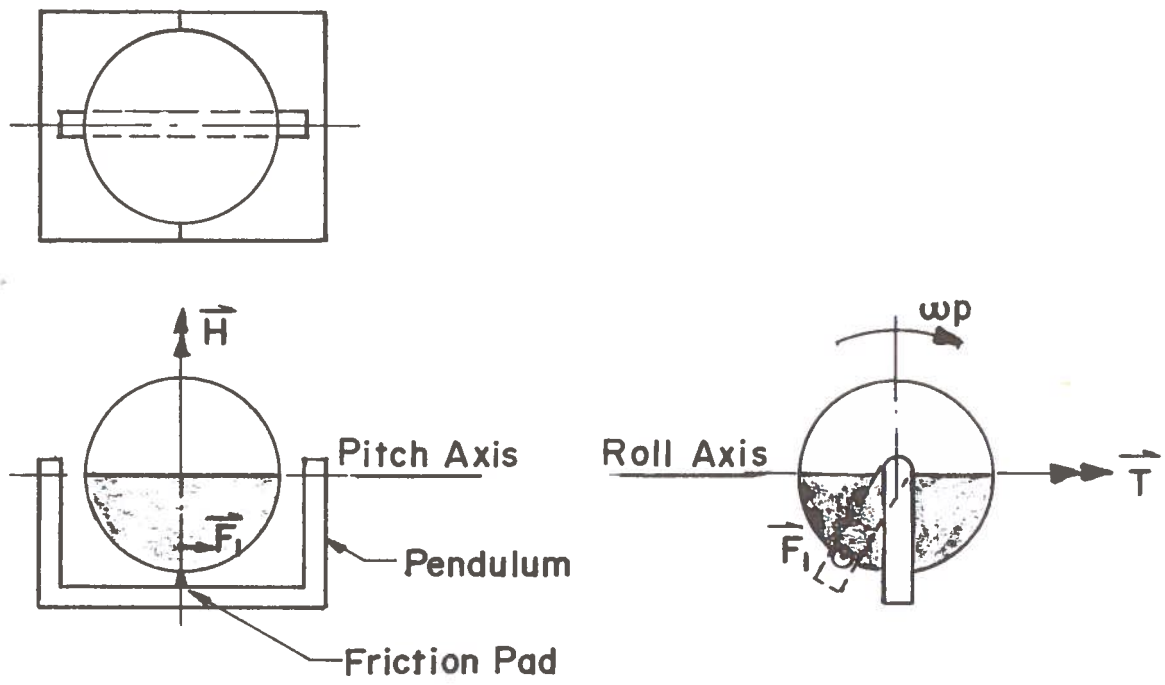

Figure 10. Pendulum Erection Vertical Reference

A disadvantage of this operational simplicity is that vertical erection does not occur in the roll axis. When the gyro experiences a roll motion, the pendulum is also constrained to roll, thus misaligning the friction pad with the spin axis as shown in figure 11. A torque is created about the pitch axis until the rotor axis aligns with the pad. A vertical reference no longer exists in the roll plane and if yaw motions are present, this loss of reference is translated to the pitch plane. However, if the precession rate of the gyro is minimized (4°/min in this case), the response to oscillations created by the wave motion can be minimized. The maximum error introduced is equal to the non-vertical alignment of the spin axis. Ideally, the inclinometers will be used to define the pitch and roll motions while the gyros will be used to "smooth" the inclinometer data in the presence of lateral accelerations. Figure 12 illustrates the output of the two devices simultaneously subjected to low frequency pitching motion with higher frequency lateral acceleration components. The gyro is, by design, less sensitive to these high frequency components.

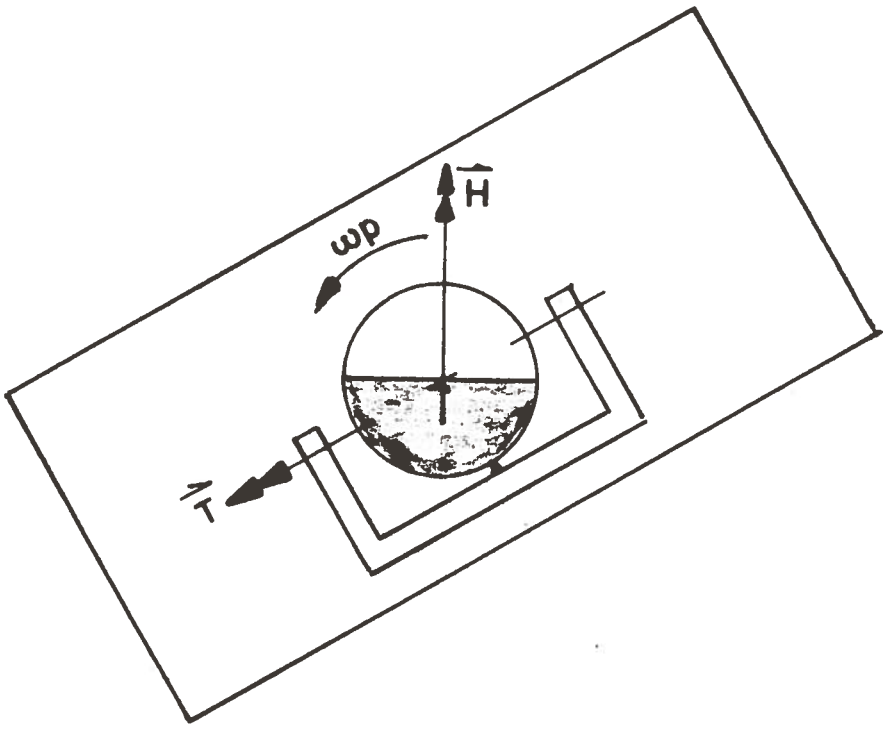

Figure 11. Pendulum Erection Case Reference

A strain gage tension link was inserted in the mooring chain to furnish loading data. Its operation is based on the principle that the electrical resistance of a conductor changes proportionally when it is subjected to a mechanical deformation (Eq. 5). By mounting a strain gage on a carefully machined specimen, the output of the gage may be related to the tensile force in the specimen.

$$\varepsilon = \frac{1}{F}\frac{\Delta R}{R} \qquad (5)$$

ε = Strain
F = Gage Factor
ΔR = Change in Resistance
R = Total Resistance

For an axially loaded specimen

$$E = \frac{\sigma}{\varepsilon} = \frac{P}{A}\frac{1}{\varepsilon} \qquad (6)$$

E = Young's Modulus
σ = Stress
P = Force
A = Cross Sectional Area

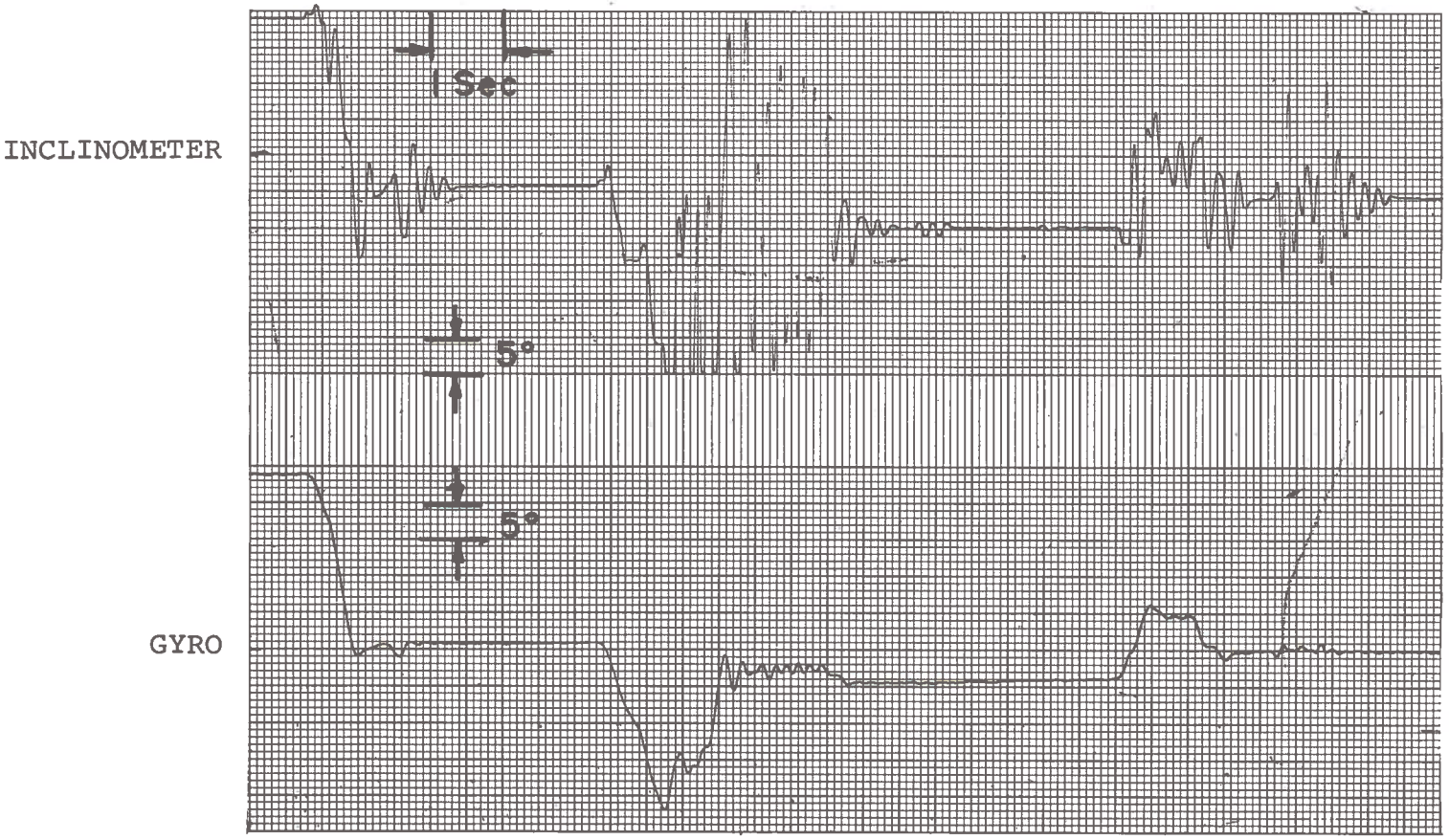

Figure 12. Comparison of Inclinometer and Gyro Data

By substitution

$$P = \frac{EA\Delta R}{FR} = K\Delta R \qquad (7)$$

The load cell used on the prototype package was purchased from Gentran, Inc., and has a range of 0-20,000 pounds. To estimate the response of the load cell, it was approximated by a spring mass system. The deflection of the load cell is .005 inches for a 20,000 pound load. Therefore $K=4x10^6$ lb/in. Assuming m equal to the weight of a typical mooring chain or 5000 pounds,

$$F_n = \frac{1}{2\pi}\sqrt{k/m} \cong 88 \text{ Hz}$$

Since it is expected that the dominant forces in the chain will be caused by wave action, it is safe to assume that $F/F_n<<1$ and that the load cell will exhibit unity response, again referring to figure 6 which is the response of the second-order spring mass system.

The system equations are derived using figure 13 as a reference and assuming the availability of three orthagonal accelerations and two vertically referenced angles. Point "O" is the center of rotation of the buoy with the instrument package placed a distance "R" from this center. The output of the inertial instrumentation is therefore a function of the translational accelerations A_1, A_2, A_3 and the rotational accelerations, $\ddot{\phi}_R$ and $\ddot{\phi}_P$. Yaw motions are not considered because the package is placed along the buoy axis of symmetry. An accelerometer triad, A_P, A_R, A_V, hard-mounted to the buoy furnishes analog information about accelerations along the buoy axes while angular displacements with respect to a vertical reference are used to find the vertical component of the resultant of these accelerations. The roll angle, ϕ_R, can be obtained from a pendulum inclinometer or the inner gimbal displacement of a vertical gyro. The angle read from the outer gimbal of the gyro, ϕ_{PG}, is not a strictly vertical reference but is tilted off-vertical an amount ϕ_R. The absolute vertical reference is given by ϕ_{PINC} and can be obtained directly from a dual axis pendulum inclinometer or from the gyro data as shown in Equation 8.

$$\sin\phi_{PINC} = \sin\phi_{PG} \cos\phi_R \qquad (8)$$

The total vertical angle, ϕ_V, can also be related by Equation 9.

$$\sin\phi_V = \sqrt{\sin^2\phi PINC + \sin^2\phi R} \qquad (9)$$

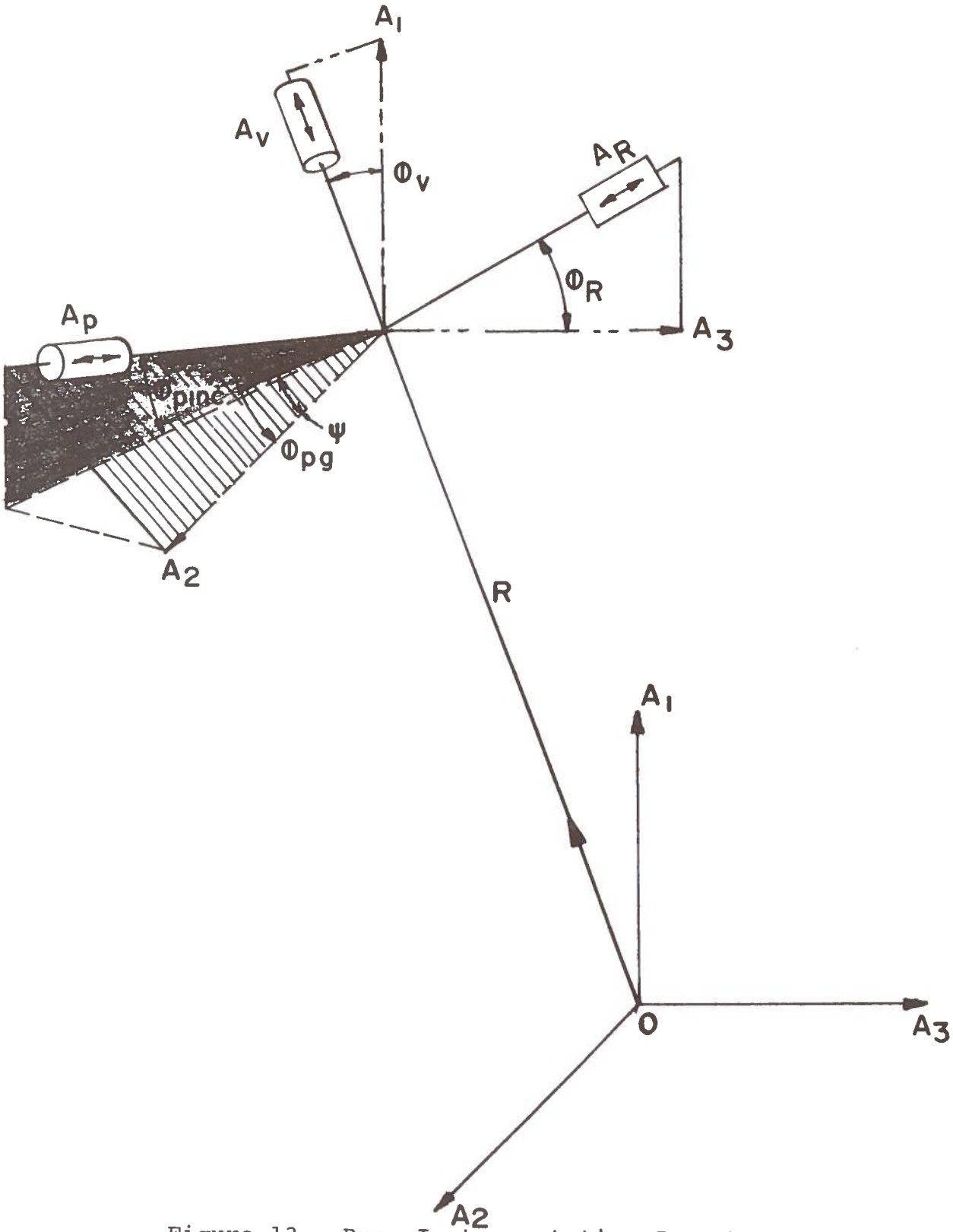

Figure 13. Buoy Instrumentation Geometry

From geometrical and dynamic considerations, it can be shown that the outputs of the five transducers selected for the prototype unit are as follows:

Pitch Inclinometer (10)

$$X = [\phi_{PINC}]_1 + \left[\text{Arctan } \frac{A_2\cos\psi - A_3\sin\psi}{A_1 + g}\right]_2 + \left[\text{Arctan } \frac{R\ddot{\phi}_{PG}\cos\phi_{PINC}}{A_1 + g}\right]_3$$

Roll Inclinometer (11)

$$Y = [\phi_R]_1 + \left[\text{Arctan } \frac{A_3}{A_1 + g}\right]_2 + \left[\text{Arctan } \frac{R\ddot{\phi}_{RG}\cos\phi_{PG}\cos\phi_{RG}}{A_1 + g}\right]_3$$

Pitch Accelerometer (12)

$$A_P = [\sin\phi_{PINC}]_1 + [A_1\sin\phi_{PINC} + A_2\cos\phi_{PG} - A_3\sin\phi_{PG}\sin\phi_R]_2 + [R\ddot{\phi}_{PG}]_3$$

Roll Accelerometer (13)

$$A_R = [\sin\phi_R]_1 + [A_1\sin\phi_R + A_3\cos\phi_R]_2 + [R\ddot{\phi}_{RG}\cos\phi_{PG}]_3$$

Vertical Accelerometer (14)

$$A_V = [\cos\phi_V - 1]_1 + [A_1\cos\phi_V - A_2\sin\phi_{PG} - A_3\sin\phi_R\cos\phi_{PG}]_2 - [R\dot{\phi}_V^2]_3$$

where $[\ ]_1$ quantities, refer to gravity induced components
$[\ ]_2$ to lateral acceleration components
$[\ ]_3$ to angular acceleration components

From equations 10 and 11, it is obvious that inclinometer errors are introduced due to the angular and lateral accelerations. The magnitude of these accelerations in the ocean environment will determine the utility of the inclinometer for angular data. If the errors are small (less than .5°) and therefore neglibible, the output of the inclinometer will represent the desired angles. If the errors are large, however, use of a more stable reference such as the vertical gyro is dictated.

Equations 12 through 14 indicate that if the instrumentation package is not placed at the center of rotation, tangential and normal acceleration components of the angular motion, in addition to the translational acceleration components, will be sensed by the accelerometers. Upon double integration of the vertical component of these accelerations, the vertical displacement of the package caused by these angular motions will be superposed on the vertical displacement caused by translational motion of the center of rotation. Correction for this term can be accomplished by multiplying the length of the radius arm, R, by $[1-\cos\phi_V]$ and subtracting this value from the total integrated displacement. At present, R is found by experiment and assumed to be constant. Assuming the package is located at the center of rotation or the final displacement is corrected by the above method, the total vertical acceleration, A_1, is given by equation 15.

$$A_1 = \frac{A_V + A_P\tan\phi_{PG} + A_R\tan\phi_R\left(\frac{1}{\cos\phi_R}\right) + 1}{\cos\phi_V + \tan\phi_{PG}\sin\phi_{PINC} + \tan\phi_R\sin\phi_R\left(\frac{1}{\cos\phi_{PG}}\right)} - 1 \qquad (15)$$

Using the five measurements above and the tension load cell, all of the stability parameter measurements specified can be derived. Specifically,

a. Double displacement - two successive integrations of A_1 with respect to time.

b. Heave rate - a single integration of A_1 with respect to time.

c. & d. Neutral angles - time average of angular data for a specified interval.

e. & f. Angular excursions - raw output of angle measuring device.

g. & h. Angular rates - single differentiation of angular data.

i. Mooring line tension - raw output of strain gage tension link.

Further analysis of the above data also yields A_2 and A_3, the lateral accelerations and $\ddot{\phi}$, the angular accelerations. An alternate method used to measure the angular acceleration was also included in the prototype unit. By locating two accelerometers a known distance apart and oriented in the same direction, the difference between the outputs of the

two instruments divided by the separation distance yields the angular acceleration directly.

A total of fourteen transducers was included in the prototype package to determine the relative magnitudes of the system equation components. Data from these transducers will be discussed in the conclusions of the report with explanatory samples included for reference.

4.0 DATA TRANSMISSION AND REMOTE CONTROL

TRANSDUCER CONSIDERATIONS

Consider the problem of how to read-out the data from a group of the above sensors properly located on a buoy. Since it is desired to do this both remotely and in real time it is apparent that some form of electrical, and preferably wireless transmission is required. The answer of course is to use the modern day techniques of radio telemetry. However, before broaching this subject one should first consider the read-out format of individual sensors. Since an electrical transmission system was apparent, it was obvious that instruments with an electrical read-out capability be utilized. After reviewing the problem it was decided that in most cases a simple potentiometric pickup would be sufficient, thus all of the inclinometers, gyroscopes, and all but one of the accelerometers used this type of read-out. The exception was the sensitive vertical accelerometer and the load cell. In the case of the sensitive vertical accelerometer a variable reluctance pick-up is used, whose position via internal circuitry is converted to an output voltage. The net effect is very similar to the potentiometric pick-up in that with the application of an input voltage, an output voltage is produced that is a direct analog of the mechanical state of the sensor. This is illustrated in figure 14. The load cell is necessarily different in order to satisfy the requirements of a large stress range (0 to 20,000 pounds) with limited deflection. In this case the load cell utilized a resistive strain gage in a bridge circuit as illustrated in figure 15.

In the case of the potentiometric and bridge circuits it is apparent that the output voltage is a direct function of the input voltage and therefore considerations of accuracy dictates that the input voltage be well regulated. In the final package this was accomplished using solid state regulators and will be discussed in a later section of this report.

Before discussing the design of the telemetry system it should be emphasized that telemetry is not a specific system of any one type. There are invariably many options available to the designer and the final choice must include such considerations as size, weight, environment, distance, prime power and type and amount of information to be transmitted.

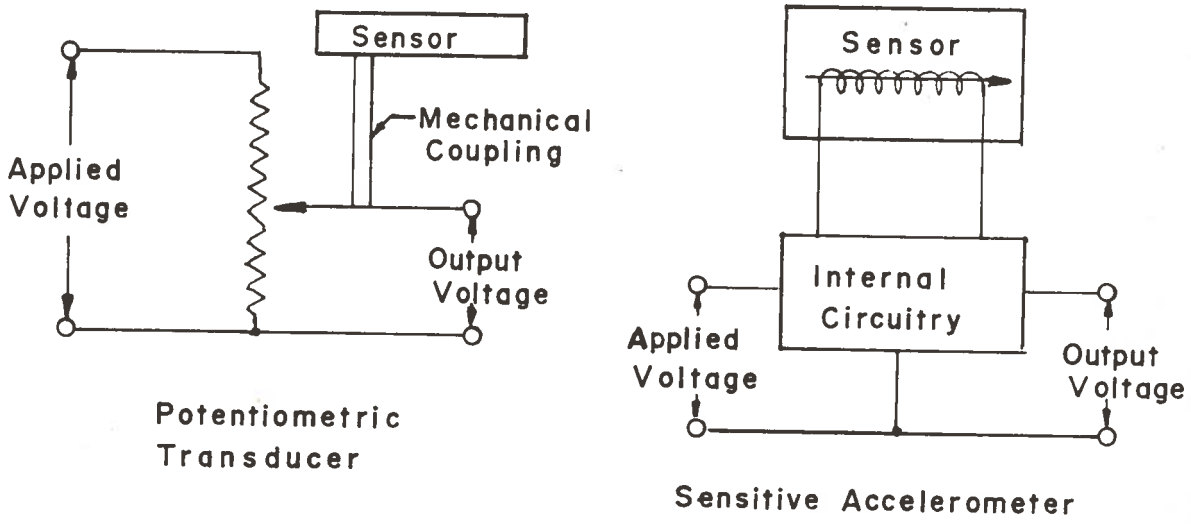

Figure 14. Inertial Transducer Schematics

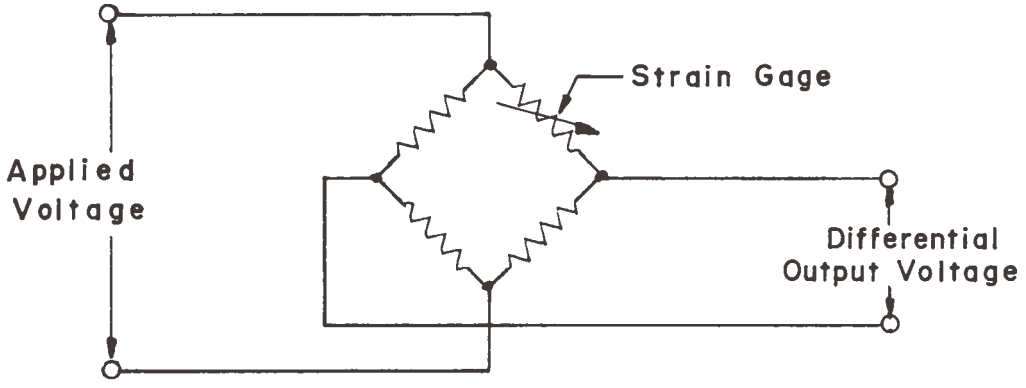

Figure 15. Load Cell Schematic

Beginning with the information to be transmitted two factors were apparent; namely, that at most no more than fourteen data inputs would be required, and in all cases the rate of change of data would be relatively slow. Furthermore it was concluded that at any one time only six data inputs need be recorded on a simultaneous basis.

Buoy Telemetry System

With these considerations established it was decided that a frequency-division multiplexing system would be sufficient using the first six IRIG* subcarrier bands. To understand how such a system works, first refer to figure 16 which simply illustrates the data transmission system. With this system the analog voltage developed at the sensor is used to control the frequency of a subcarrier oscillator which in turn is used to modulate the telemetry transmitter. It is possible to use a total of 18 subcarrier-oscillator channels to monitor 18 variables. It is also possible to increase the number of variables by sequential sampling in any or all of the subcarrier channels (time-division multiplexing); however this report will only discuss the system used.

Table 4 lists the frequencies of the first six IRIG subcarrier bands used in this program. In assigning the variables to be monitored to the subcarrier bands, band number 6 was assigned exclusively for the load cell located in the mooring line of the buoy.

Table 4. Telemetry Frequencies of Prototype

SUBCARRIER BANDS					
Band	Center Frequency (Hz)	Lower Limit (Hz)	Upper Limit (Hz)	Maximum Deviation (percent)	Frequency Response (Hz)
1	400	370	430	±7.5	6.0
2	560	518	602	±7.5	8.4
3	730	675	785	±7.5	11.
4	960	888	1,032	±7.5	14.
5	1,300	1,202	1,398	±7.5	20.
6	1,700	1,572	1,828	±7.5	25.

*IRIG, Inter Range Instrumentation Group

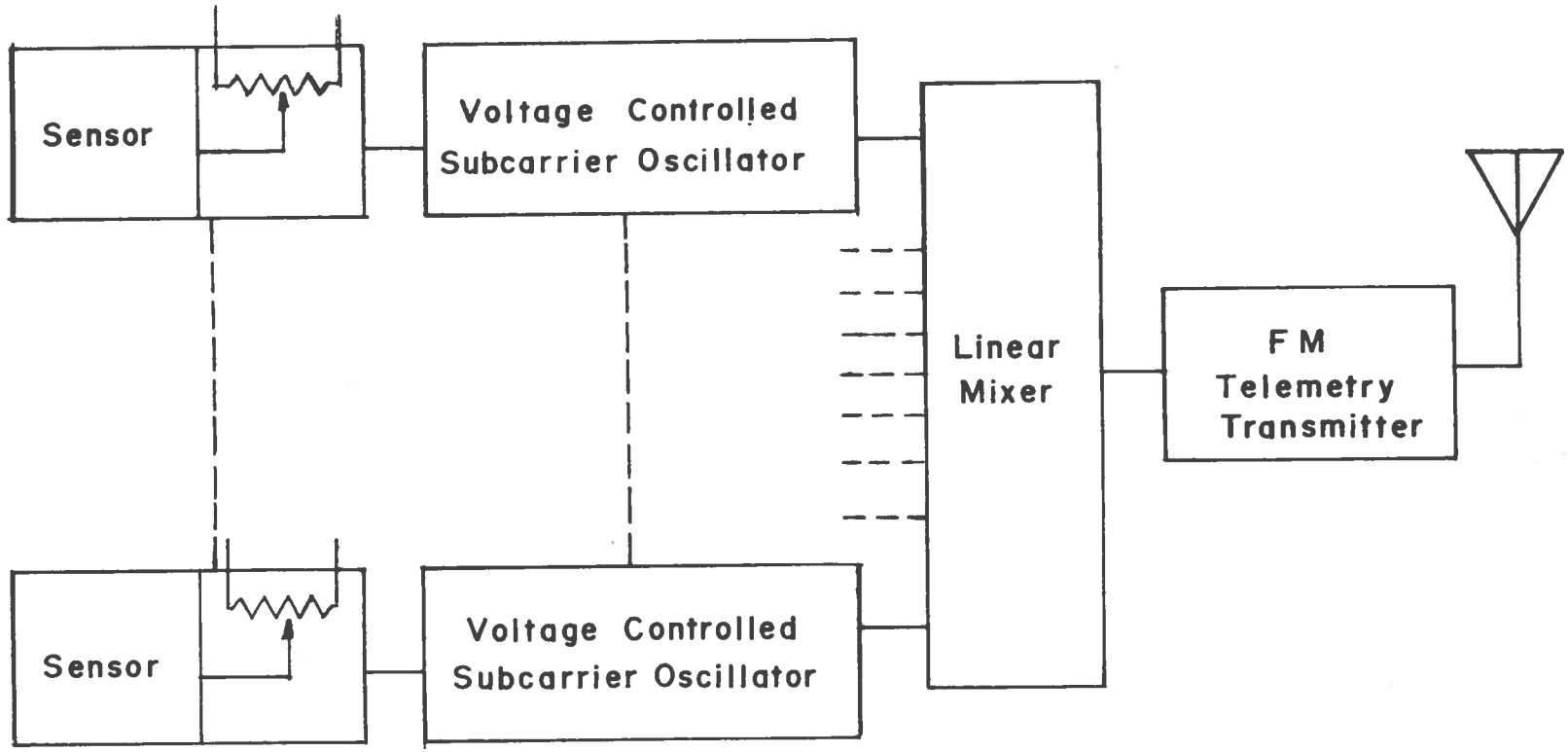

Figure 16. FM-FM Frequency Division Multiplexing System

This was done primarily because the highest data rate was expected to be from the load cell. Due to the resistance bridge circuitry of the load cell it was necessary to use a low level voltage controlled oscillator (VCO) with a differential input. This VCO could be tuned over its entire range with a differential voltage varying from 0 to 20 millivolts. The first five VCO's were of the high level type with a single ended input. These oscillators were controlled by an input voltage that was adjusted to vary from 0 to 5 volts. Referring again to the table it is estimated that even though the first six channels were selected, the frequency response capability of the system probably exceeds the rates to be measured by at least an order of magnitude.

With the load cell data assigned to channel 6 the problem then was to provide switching between the first five channels and thirteen possible inputs. This was done with a standard stepping switch which also permitted the additional capability of monitoring the input voltage and zero-balancing the system. These features will be discussed later in this report. It should be mentioned that the switching functions could be reduced by using additional subcarriers. While this was not done for reasons of economy, the capability to add four additional channels was provided in the design of the prototype equipment. Essentially this consists of adding an additional VCO to the instrument package and a subcarrier discriminator to the receive station for each extra channel.

The telemetry rf frequency used in the prototype was 216.3 MHz which is in the standard telemetry band of 216 to 235 MHz. A total of five frequencies was allocated in the event the program is extended. These are listed as follows.

216.3 MHz, 217.2 MHz, 217.9 MHz, 218.9 MHz, 219.6 MHz

The spacings between these frequencies are sufficient to permit simultaneous operation of five separate systems in relative proximity.

RECEIVING SYSTEM

As discussed in the previous section the telemetry system in the instrument package transmits an fm signal modulated by a single complex composite signal. The function of the receive system is first to select the desired signal (216.3 MHz in this case), amplify it, and demodulate the rf carrier. This output is now a reproduction of the original composite signal which consists of the mixed subcarrier-oscillator frequencies. At this stage of recovery, this signal may be either stored on a magnetic tape for future

processing or routed directly to the demodulation equipment. The advantage of recording becomes particularly apparent if more than one system is operational since only one set of demodulation equipment is required. Refer now to figure 17 which depicts the entire ground receive system. Thus far the telemetry signal has been traced to the output of the fm receiver where it exists in a complex composite form. The task now is to separate the individual modulating frequencies. This is done by feeding this signal in parallel fashion to a group of band pass filters designed to pass only the complete range of frequencies of each individual subcarrier channel. The next step in the process is to generate signals which change in accordance with the variations in frequency of the subcarrier channels. This is the function of the discriminator. Since the output of the discriminator should be a reproduction of the original sensor signal it is important that the discrimination process introduce no distortion. Modern day discriminators such as the one designed for this application use pulse-averaging techniques. The signal after filtering is routed through a limiter to a Schmitt trigger which produces a constant-pulse-width square wave. This square-wave signal in turn is fed to a detector whose output is directly proportional to the average value of the square-wave signal which is indeed the signal we wished to recover.

Because many different frequencies were used in the processing, all higher than the output signal, it is reasonable to expect some leakage to be present at the output of the discriminator. This effect however is completely eliminated by a low pass filter. In the present system, three-pole active filters are used with an 18 db per octave characteristic . With final reference to figure 17 the band pass filter, subcarrier discriminator and low pass filter functions are incorporated into a single package, one for each subcarrier channel, and will henceforth be referred to as the "discriminator".

THE COMMAND SYSTEM

Thus far the discussion has been restricted to the data transmission aspects of the telemetry system. The discussion will now be directed to the command aspects of the system; i.e., how the equipment is activated, and how the stepping switch is controlled.

In designing the buoy package, two restraints were evident. First only a limited source of prime power would be available, and second, long periods of time could elapse between interesting sea conditions where data would be

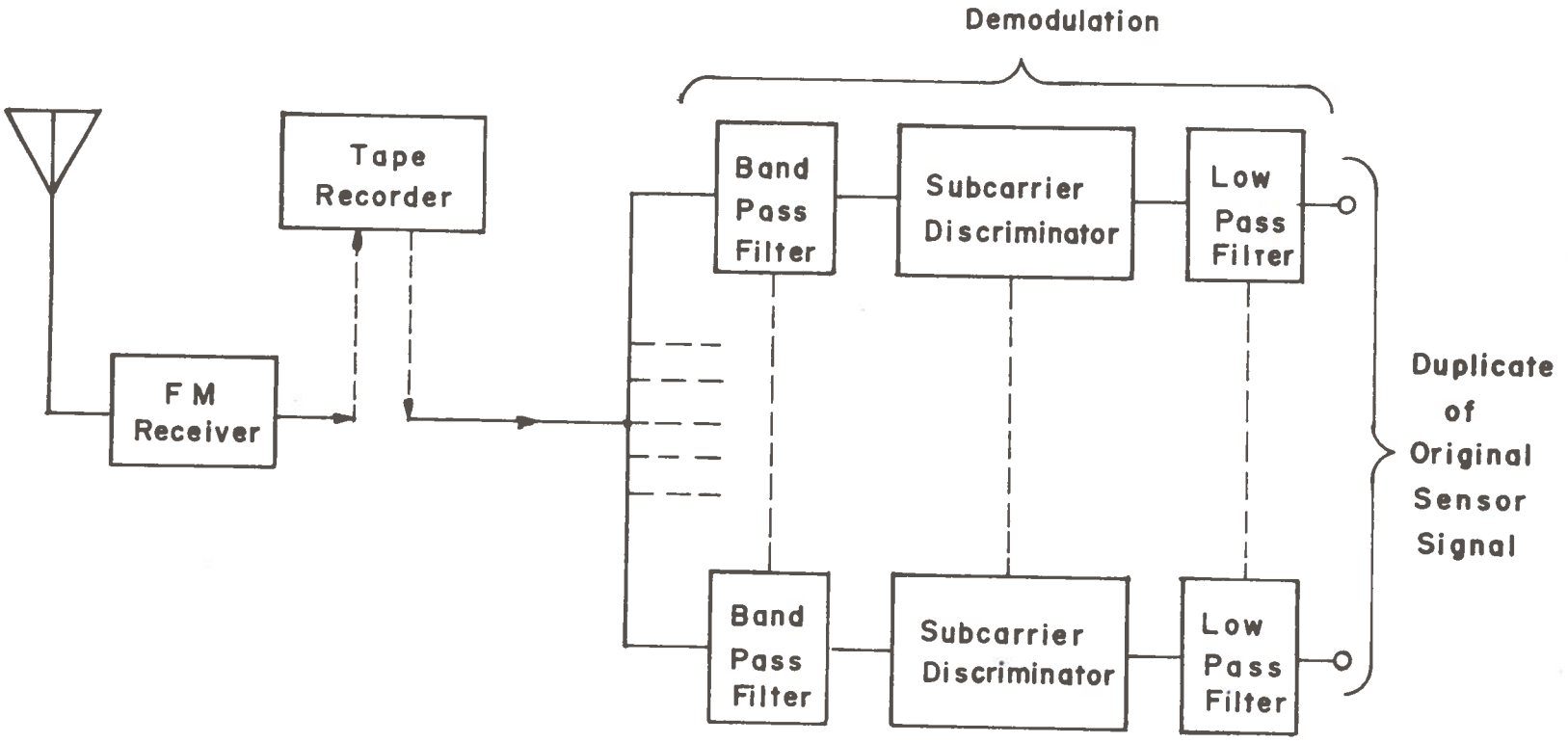

Figure 17. Ground Receive System

desired. In view of these considerations it was clear every effort would have to be made to conserve prime power which in this case was a battery. The answer of course is a command system such as shown in figure 18.

The input commands were simply four toggle switches on the signal encoder which remotely controlled four relay closures in the signal decoder. The rf link operates at a frequency of 416.85 MHz and like the data link is an fm system. In this system an input command results in the generation of an audio tone that is used to modulate the transmitter. At the receiving end this tone is detected and used to activate the relay circuitry. With the use of tuned circuits there is little likelihood of false commands or interference between commands. An important feature of the receiver and decoder is the low value of quiescent current drain which was measured at 110 milliamperes (28V battery source). While this is the minimum value of current drain by the buoy package it is also the prime factor insofar as battery life is concerned. While it is true that the fully activated package will draw many times this value of current, the duty cycle of data transmission is very low on a daily or overall basis. Current versus time profiles will be presented in a following section of this report.

Early in the program the following frequency allocations were obtained for the command link in the event that additional systems would be constructed.

416.85 MHz, 419.125 MHz, 419.6 MHz, 419.8 MHz, 419.975 MHz

It should be noted that these frequencies are not harmonically related to the data frequencies in order to avoid any possible interference. With improper frequency spacing, difficulty could arise at the buoy due to the necessarily close physical location of command and data antennas.

THE ELECTRONIC SYSTEM – JUNCTION BOX

In the foregoing sections of this report the discussions of the electronic systems have been essentially on a qualitative basis with the aim of establishing the overall operation of the complete system. This section will deal in more detail with the electrical design aspects of the system.

The basic building blocks of the telemetry used in the instrument package were supplied by Dorsett Electronics, Inc. and are as follows:

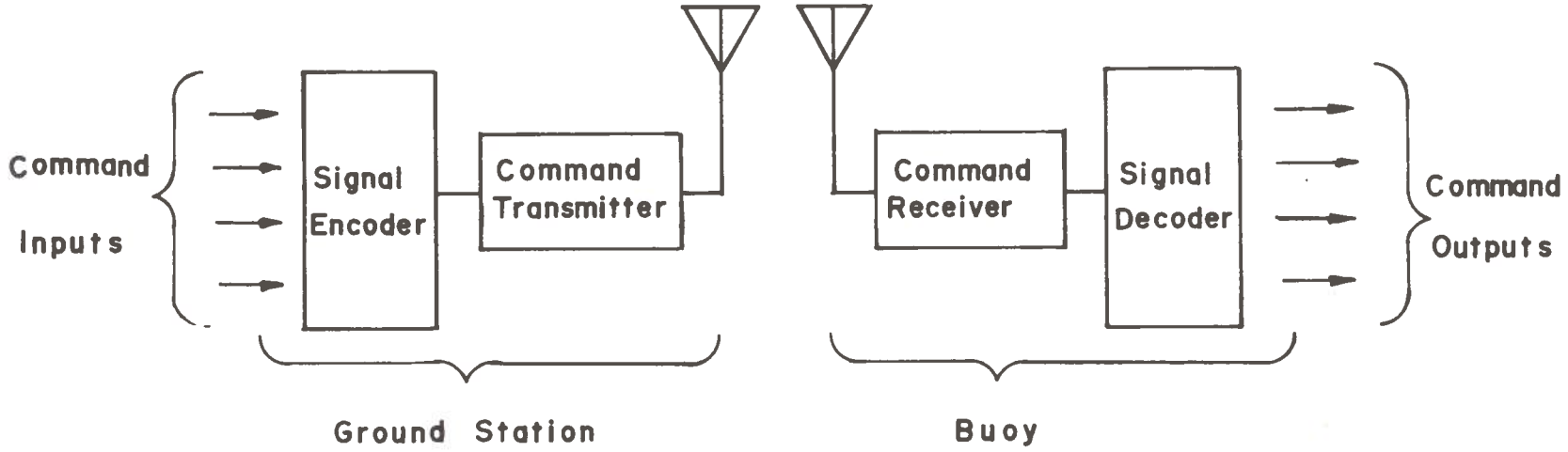

Figure 18. Command System

Command Receiver	Model RC-184-3
Signal Decoder	Model SD-284-1
VCO/Mixer Chassis	Model TMS-304-212
VCO(Channels 1-5)	Model O-18K-1
VCO(Channel 6)	Model MVO-18K-1
Mixer Amplifier	Model MA-18K-1
Telemetry Transmitter	Model TR-501A

These units which are evident in figure 19 represent the present day state-of-the-art where each unit is completely self-contained and designed to operate in a reliable manner over a wide range of temperature, shock, and line voltage. In the following discussion these items will be treated as "black boxes" with the detailed discussion being confined to the protective switching and regulatory circuitry. With the exception of interconnecting cables, all of this circuitry is located in what is referred to as the "junction box". Figure 20 clearly shows the junction box. Figure 21 is a schematic diagram of the junction box which also includes the wiring of the sensors.

To describe the operation of the junction box, first begin at connector J4 (figure 21) where the prime power is introduced. The negative connection on pin #1 is shown to be grounded to the chassis. In this schematic the chassis is used as the ground for convenience while in the actual box additional ground wiring is routed to assure both good connections and the elemination of any ground loop effects. The positive lead which is routed through pin #3 is immediately fused at F1. At this point diode CR-1 is placed directly across the line in a reverse connection. In normal operation this diode is effectively out of the circuit, however if the polarity of the prime source (battery) had been inadvertently reversed the diode would have conducted causing fuse F1 to blow thus protecting the rest of the equipment. This crow-bar arrangement was used rather than a series diode for regulation purposes. If the positive line, which is normally at 28 volts, is traced from the diode it will lead to connectors J3, J6 and a set of relay contacts. Connector J6 is simply a test or access connector in which many points in the circuit are terminated for convenient auxiliary monitoring or testing. Since the use of J6 does not contribute to the functioning of the box it will no longer be discussed. Connector J3 however provides the connection to the command

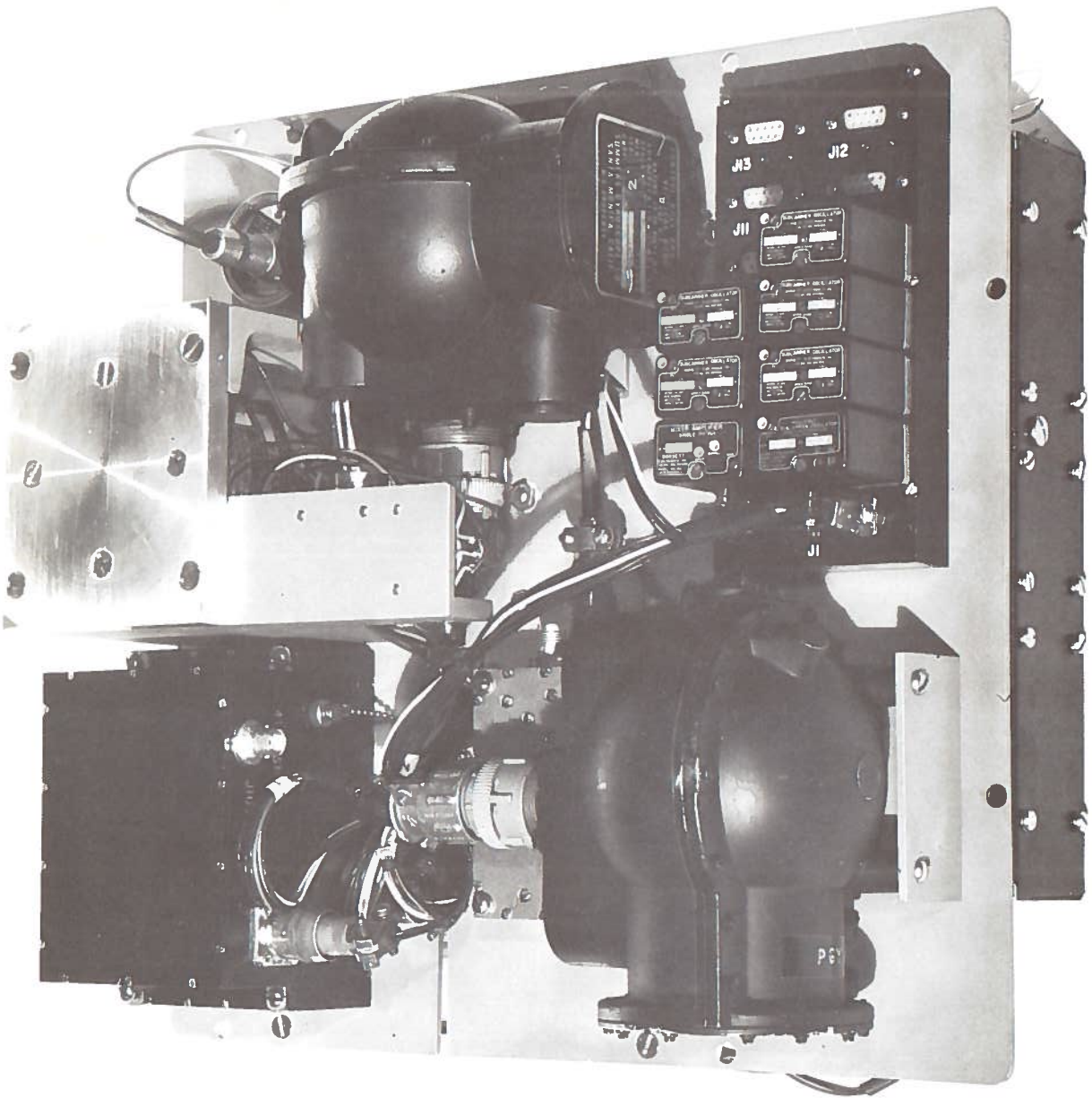

Figure 19. Photograph of Underside of Instrumentation

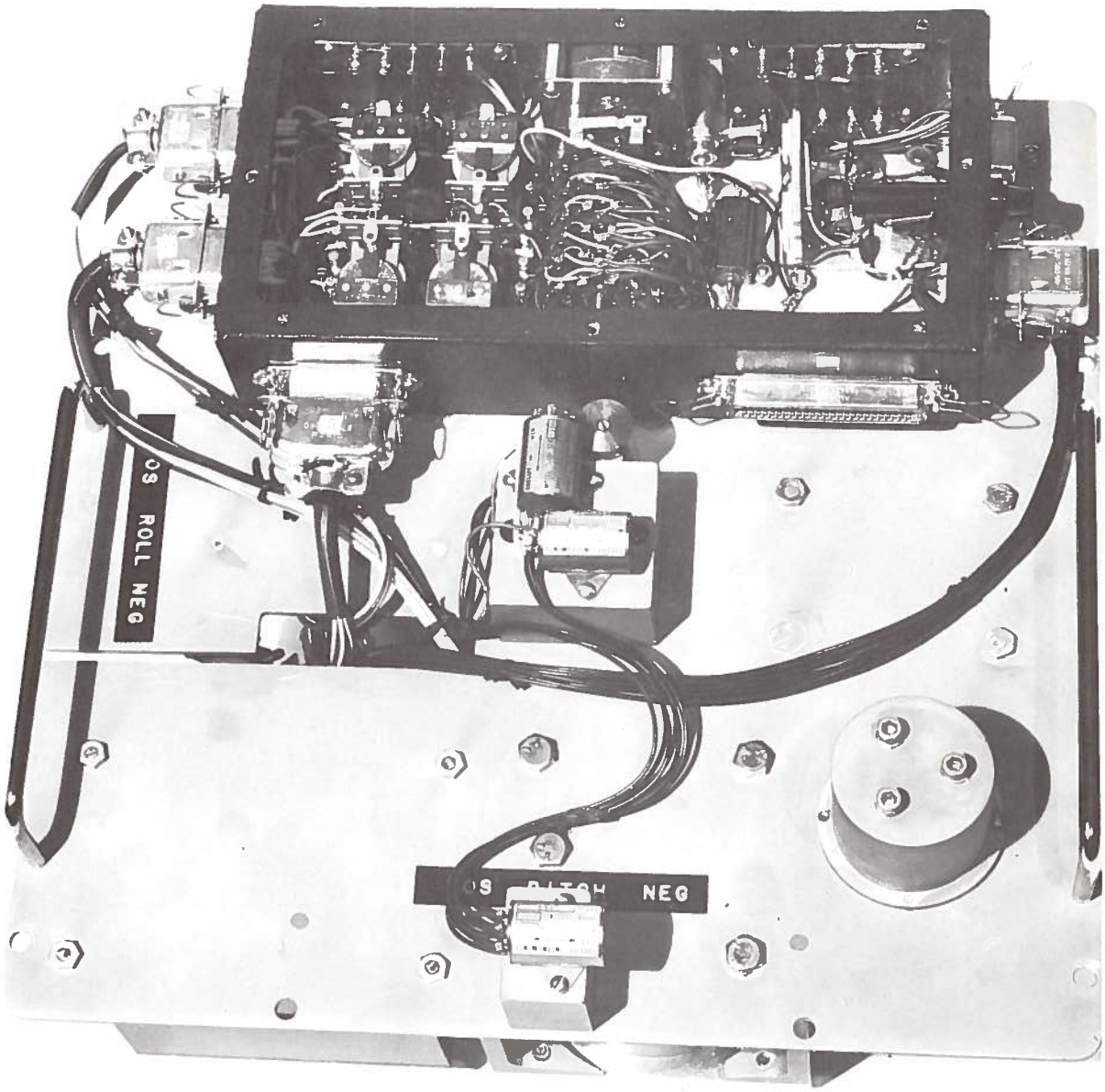

Figure 20. Photograph of Topside of Instrumentation

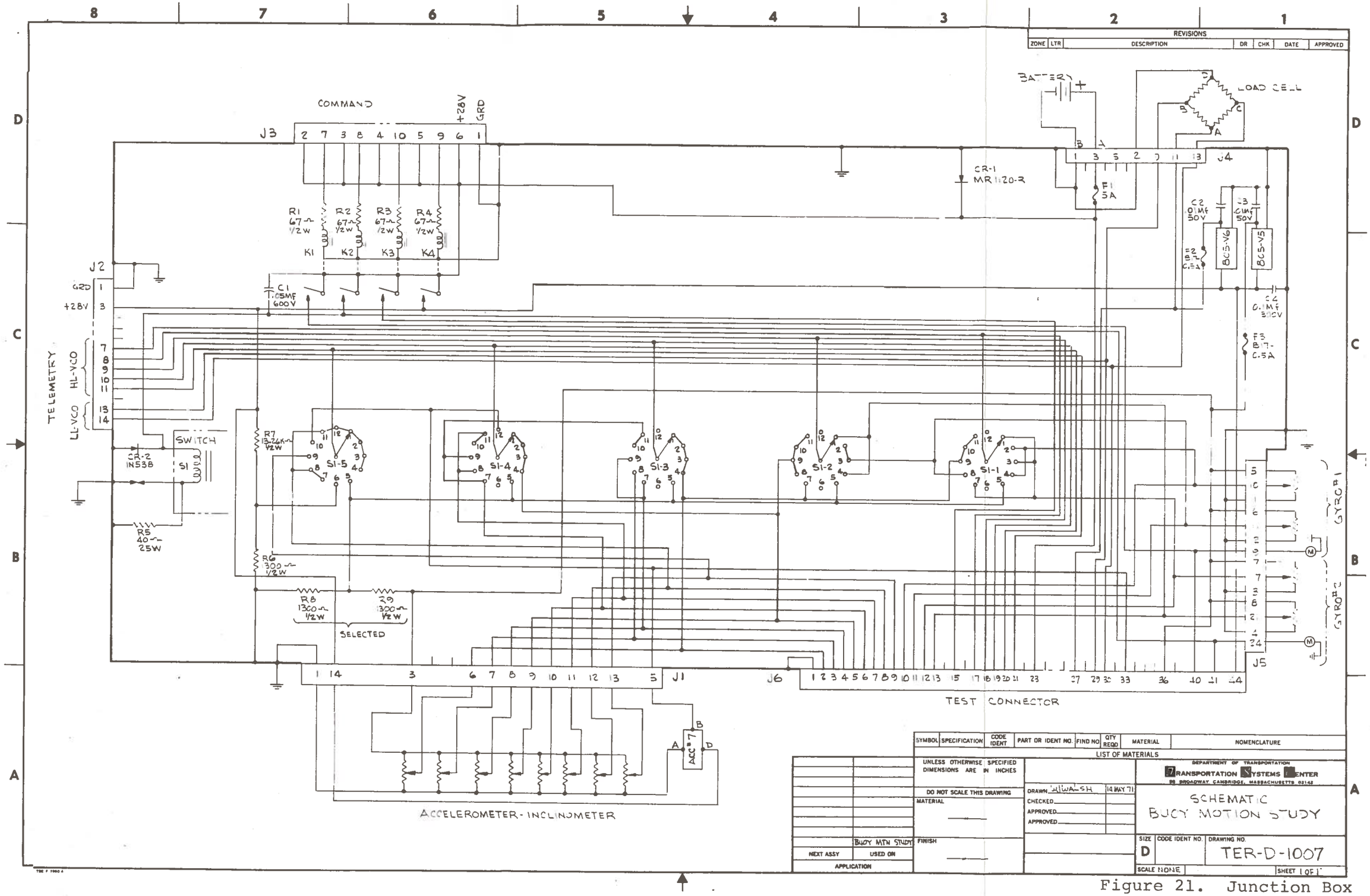

Figure 21. Junction Box Schematic

receiver and signal decoder. The interconnecting cable is branched so as to provide an interconnection between these two units as well as to the junction box. Refer now to figure 22 which is a partial schematic showing only the command circuitry. Thus far the +28 Vdc line has been traced from J4 to J3 and the relay contacts. It should be noted that the system is activated as soon as the battery is connected. In the quiescent state this system draws 110 milliamperes. Command signals are first processed by the command receiver where the modulating tones are detected and routed along the signal line to the signal decoder. In the signal decoder these tones will activate only those circuits which are compatible on a tone frequency basis. Activation of a circuit results in the closure of a relay contact to the +28 Vdc line. This voltage which is now routed to the junction box is used to activate a heavy duty relay (K1 through K4) which in turn is used to power other circuitry. It is seen that four commands are provided. The lettering and numbering is that of the actual connectors and may be used for reference. The four resistors shown are used for voltage correction at the relay coils. Where 28 volts is a standard in telemetry, 24 volts is common to many relays.

The functions that are activated by the commands are listed below and also are illustrated in figure 22.

(1) K1 Gyro #2 Motor

(2) K2 Stepping Switch

(3) K3 Gyro #1 Motor

(4) K4 Telemetry

With reference back to figure 21 it is seen that command circuits (1) and (3) are simply lines to the gyro motors via J5. Separate commands were assigned to these motors primarily because of their relatively large current drain. At start each motor draws about 1 ampere which, over a period of approximately two minutes, falls to about 0.5 ampere as the motor speed reaches its maximum value. Once full speed is obtained several more minutes may be consumed for the instrument to erect to the vertical and the collection of data can proceed.

Command step (4) which turns on the entire telemetry system can best be described by referring to a partial schematic as shown in figure 23. This circuit draws just under 0.7 amperes and is a constant load with the largest part of this

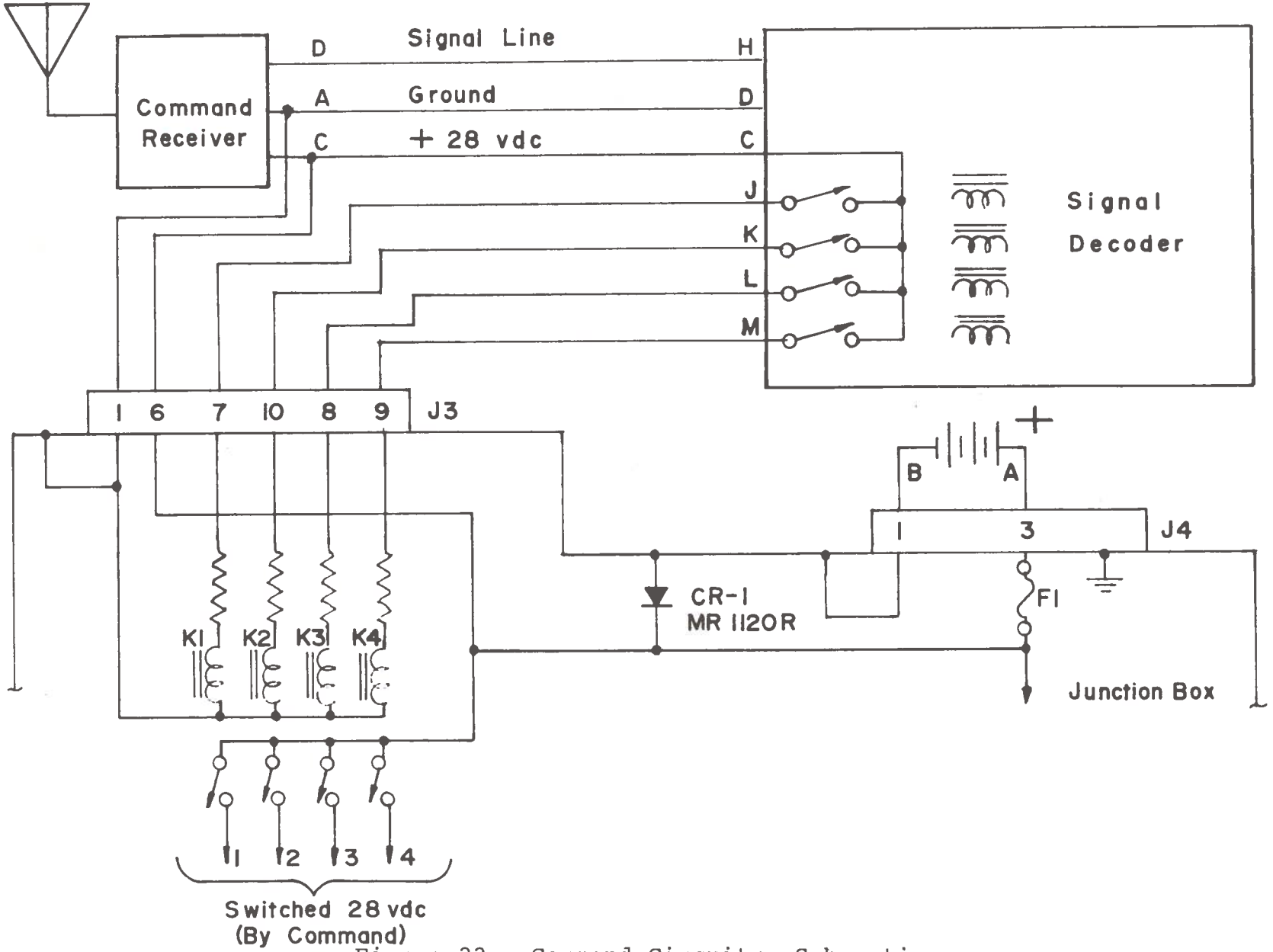

Figure 22. Command Circuitry Schematic

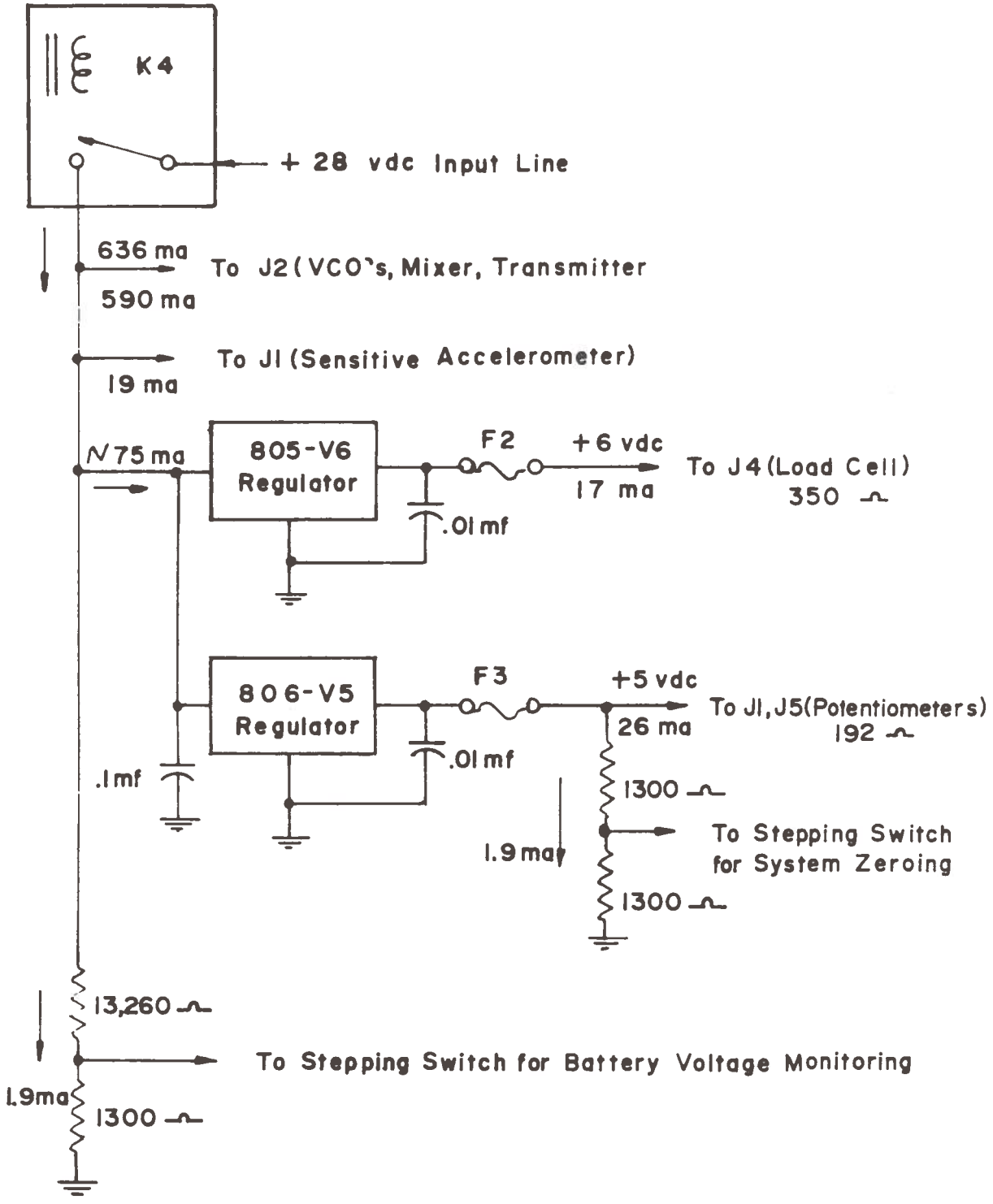

Figure 23. Command Circuit 4 Schematic

drain, 0.475 amperes, being accounted for by the fm telemetry transmitter. In the case of the potentiometric and bridge voltages, regulation is used since the readout is a direct function of the applied voltage. These regulators are fully sealed self-contained hybrid cermet thick film units with a 0.5 ampere load capability. With an input voltage change of 10 percent the regulation is typically $\pm$ 0.07%. When the input voltage was varied between 22 and 32 volts the total output change was less than 40 millivolts. Because of this excellent regulation two resistive dividers were used for system zeroing and battery voltage monitoring. The first divider, consisting of two selected resistors of about 1300 ohms each, is used with one position of the stepping switch to apply a fixed 2.5 volts to all of the VCO's. Since these units are now set at center frequency the ground based discriminators may be adjusted for zero output. This feature permits correction of any long term drifting. The second divider which is across the input line was initially adjusted for a 2.5 volt output with a 28 volt input. By applying this voltage to a VCO via the stepping switch and comparing the readings against those of the regulated 2.5 volts a direct monitoring of the input voltage was obtained. With this procedure an input voltage calibration curve was prepared by using an adjustable supply and varying the voltage between 22 and 32 volts.

With solid state circuitry used throughout the instrument package, no warmup was required for data transmission, thus in the interest of battery conservation the telemetry could be activated after the gyros were erected.

The final control circuitry to be discussed is that activated by command step (2) and involves the stepping switch. Figure 24 is a partial schematic depicting this circuitry. To begin first consider only that portion of the circuitry required to "step" the switch. The solenoids used in these switches are designed for high output, but only at intermittent duty. To protect the coil from over-heating when energized continuously, interrupter contacts are used to connect a resistor in series with the coil at the completion of the solenoid stroke. This reduces the current to a point high enough to keep the solenoid energized, yet low enough to prevent overheating. When de-energized, a built-in spring then returns the solenoid to its original position but the shaft switch remains in advanced position. Aside from protecting the device this feature also serves to conserve prime power should the coil inadvertently be left in the energized state. To fully explain this, it should be emphasized that in proper use the command signal should be transmitted just long enough to step the switch and then turned off. This not only reduces the con-

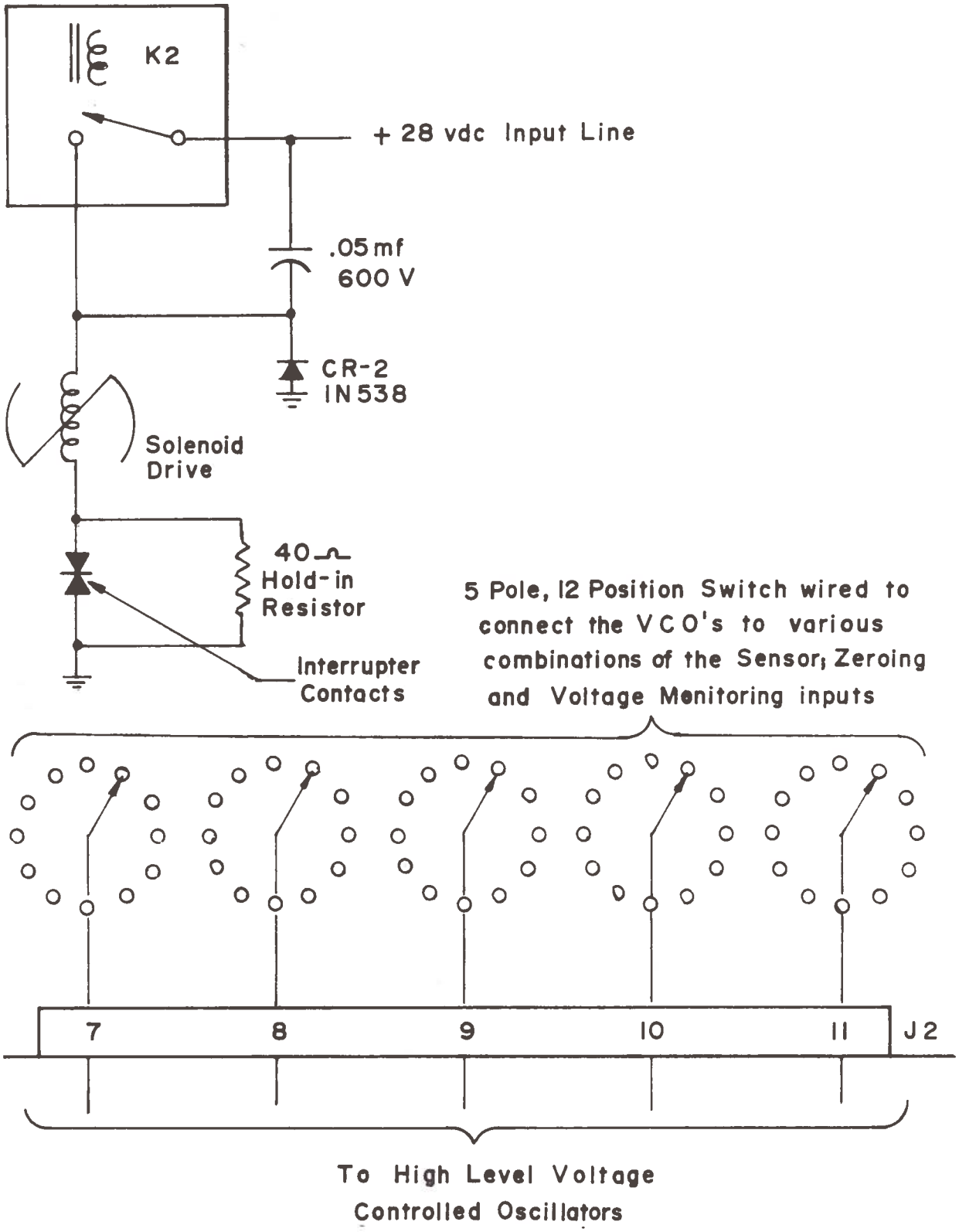

Figure 24. Stepping Switch and Control Circuitry Schematic

sumption of prime power for this function to a completely negligible value, but also prevents unwanted stepping of the switch which could be caused by any momentary interruption of the transmitted signal. If however the system is left in the energized state the current drain is determined by dividing the line volt- by the sum of the coil and hold-in resistances and is just under 0.6 amperes. During stepping the current is approximately 3 amperes however this lasts for only a small fraction of a second.

In looking at figure 24 it is also seen that a diode and capacitor are included in the stepping circuitry. The function of these components is to suppress arcing at the contacts of the control relay K2. This is necessary because the solenoid drive coil is an inductive load and as such can generate high reverse voltages whenever the circuit is interrupted.

The prime function of the stepping is most simply illustrated in figure 24. Each of the five rotary arms are connected directly to a high level VCO through connector J2. The rest of the connections are wired to provide four basic functions. The first and perhaps most important is to monitor the outputs of various combinations of the sensors. With twelve potentiometric inputs along with that of the sensitive accelerometer the task of tracing this wiring on figure 8 would be tedious and contribute little if anything in terms of knowledge. Instead reference is made to table 5 which lists the inputs for a particular position of the switch.

The second basic function of the switch is to provide a means of zeroing the overall system. This has been discussed earlier with reference to figure 21. On figure 21 this function is achieved with the switch in the number five position in which all of the VCO's are connected to a regulated source of 2.5 volts which sets each of them at center frequency.

The next switch function is that of measuring the prime input voltage. With the switch in position six it is readily seen that only one VCO is used, and that the input voltage is monitored with a simple resistive divider. By comparing the readings in this channel between positions five and six a quantitative measure of the input voltage is readily obtained.

The last switch function which is one of indexing is inherent in the wiring of the switch. In stepping through positions five, six, and twelve it is a simple matter to then deduce the state of the switch. Furthermore as has been pointed out earlier, if the command signal is turned off and left off the switch will reliably remain in its last

Table 5. Stepping Switch Position Designations

POSITION	DATA USE	VCO INPUTS 1	2	3	4	5
1	INCS with GYRO #2	PGYV2	RGYC2	PINC	RINC	AVT4
2	INCS WITH GYRO #1	PGYC1	RGYV1	PINC	RINC	AVT4
3	INCS WITH VERT AXIS GYROS	PGYV2	RGYV1	PINC	RINC	AVT4
4	INCS WITH CASE AXIS GYROS	PGYC1	RGYC2	PINC	RINC	AVT4
5	TRANSDUCER VOLTAGE	V_t	V_t	V_t	V_t	V_t
6	BATTERY VOLTAGE	-	-	-	-	V_B
7	PITCH ROT. EFFECT ON LAT. ACCELEROMETERS AND INCLINOMETERS	PGYV2	PINC	APL6	APT3	AVT4
8	ROLL ROT. EFFECT ON LAT. ACCELEROMETERS AND INCLINOMETERS	RGYV1	RINC	ARL5	ART2	AVT4
9	YAW ROT. EFFECT ON LAT. ACCELEROMETERS AND INCLINOMETERS	PINC	RINC	APL6	APT3	AYPT1
10	HEAVE DATA, SENSITIVE ACC.	PINC	RINC	APT3	ART2	AV7
11	HEAVE DATA, POTENTIOMETRIC ACC.	PINC	RINC	APT3	ART2	AVT4
12	VERTICAL ACC. COMPARISON	-	-	-	AV7	AVT4

set position. With the tone coding in an FM system there is an almost zero chance of accidental triggering.

In studying figure 21 it should be noticed that the low level VCO is never switched but instead permanently connected to the load cell. This is necessary because of the differential voltage developed by the load cell which is incompatible with the input requirements of the other VCO's. The dc common mode rejection of the low level VCO is 120db minimum for levels up to ± 50 volts.

THE GROUND STATION

The functions of the ground station are described under the previous sections of this report entitled ground receive system and command system. Let us now refer to figure 25 which is a photograph that shows most of the ground based equipment. The large rack is a multichannel strip chart recorder used to record the analog readouts of the subcarrier discriminators while the small rack shown on the left contains of the telemetry equipment. Figure 26 is a block diagram of this rack. With reference to this figure the top rack is the FM receiver which is a completely self-contained unit. The next rack down contains the signal encoder, command transmitter and off-set voltage controls. The off-set voltages simply add appropriate voltages in series with channels 4 and 5 when they are used to monitor the vertical accelerometers. In this way the 1G force of gravity is biased out of the readings and the strip chart readings are centered about the zero line. The third rack down contains a regulated 28Vdc power supply for the signal encoder and command transmitter as well as batteries for the off-set voltages. Because the off-set voltages are applied in high impedance circuits the battery drain is minimal to where battery life is essentially shelf life. Figure 27 is a schematic of the off-set voltage circuitry. The fourth rack down contains the subcarrier discriminators. Here again this is a self-contained unit with a built-in power supply. Due to rear apron access terminals the input and output lines were routed within the cabinet to bulkhead terminals on the second rack. These are evident in the photograph of figure 25. Although little heat is generated within the cabinet a blower is built into the base of the cabinet to assure long life operation.

ANTENNAS

The buoy antennas are shown in figure 25 and the ground station antennas in figure 28. Because the buoy is free to rotate in the water vertical polarization is used. The buoy

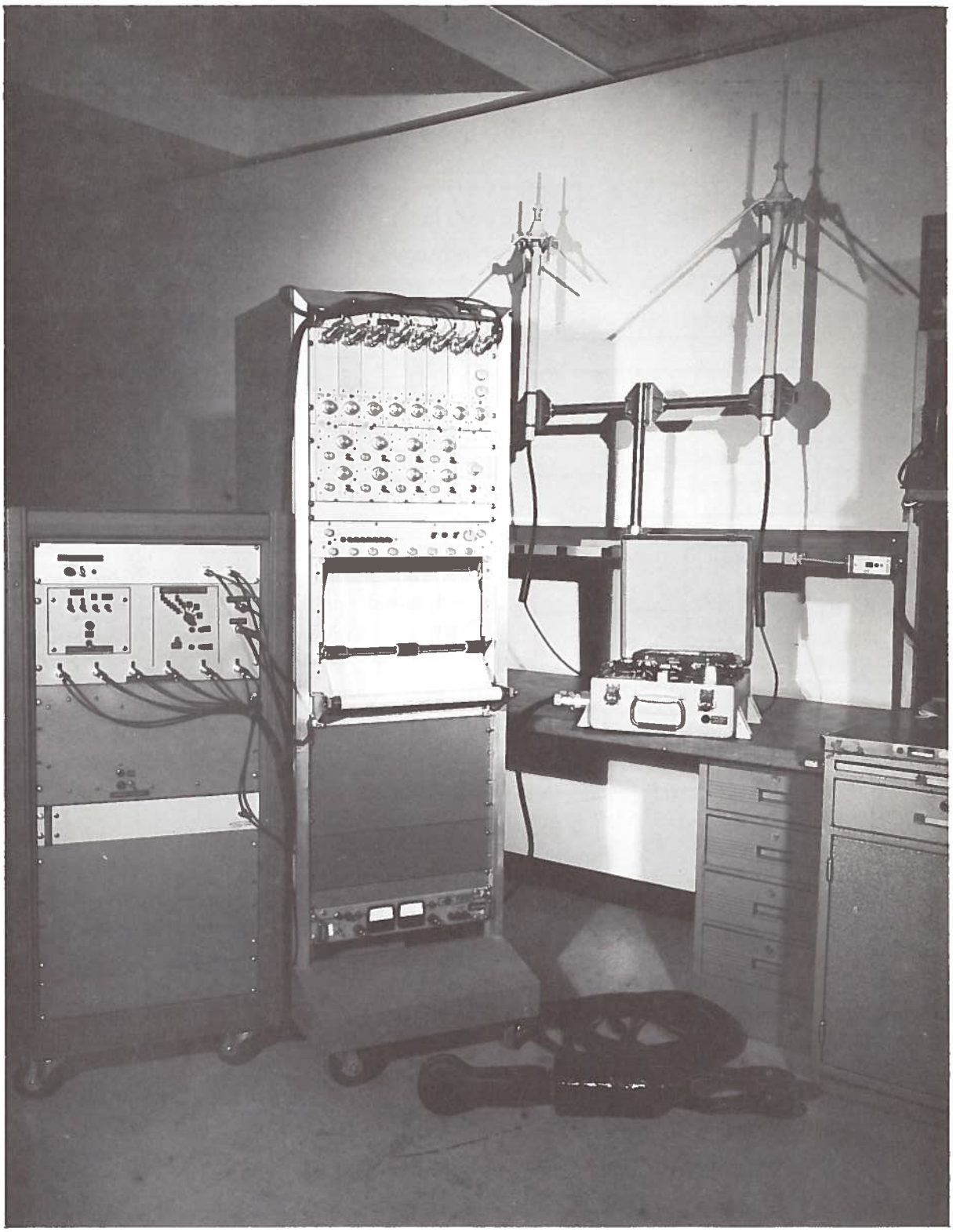

Figure 25. Lab Set-Up of System

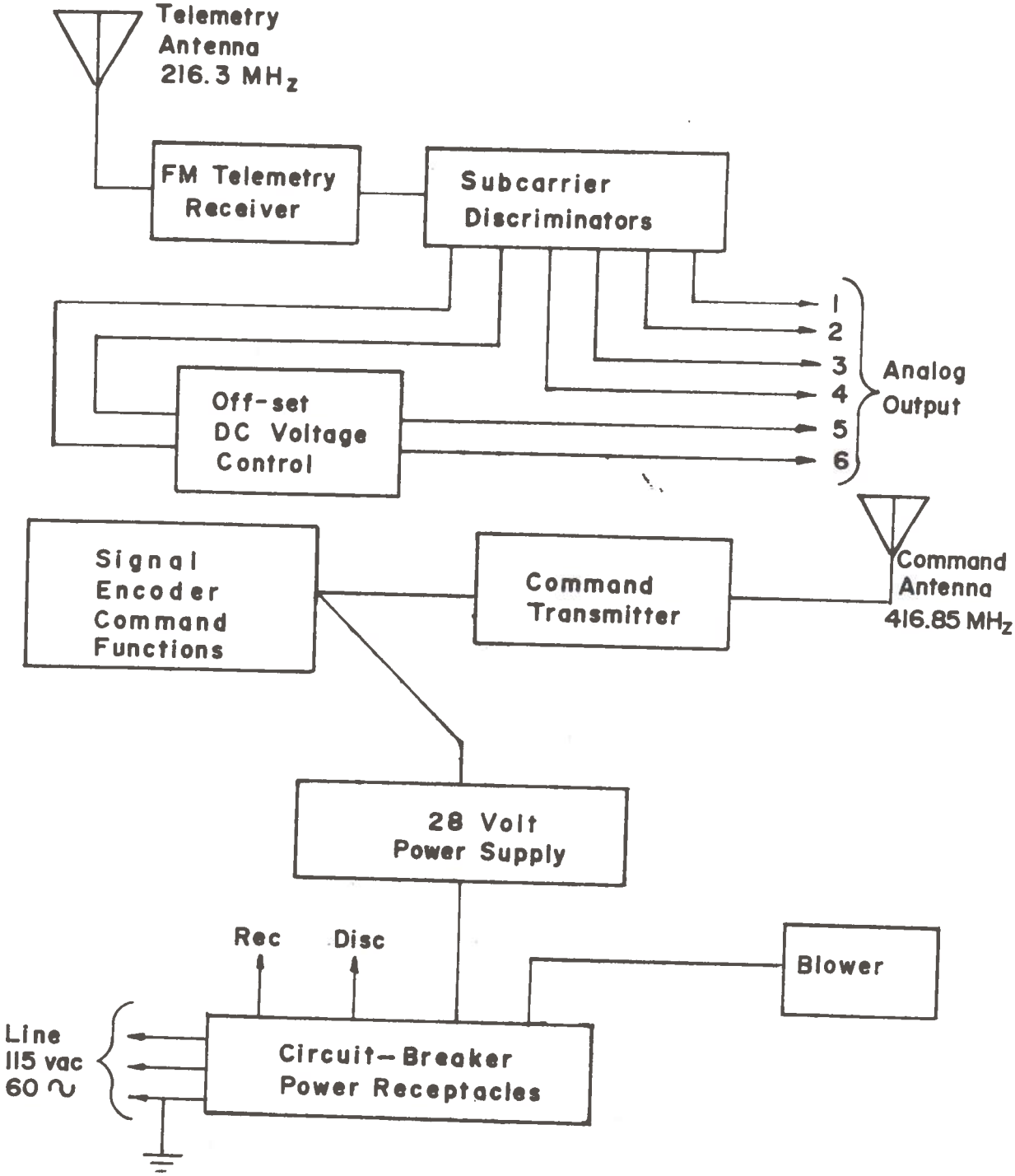

Figure 26. Ground Station

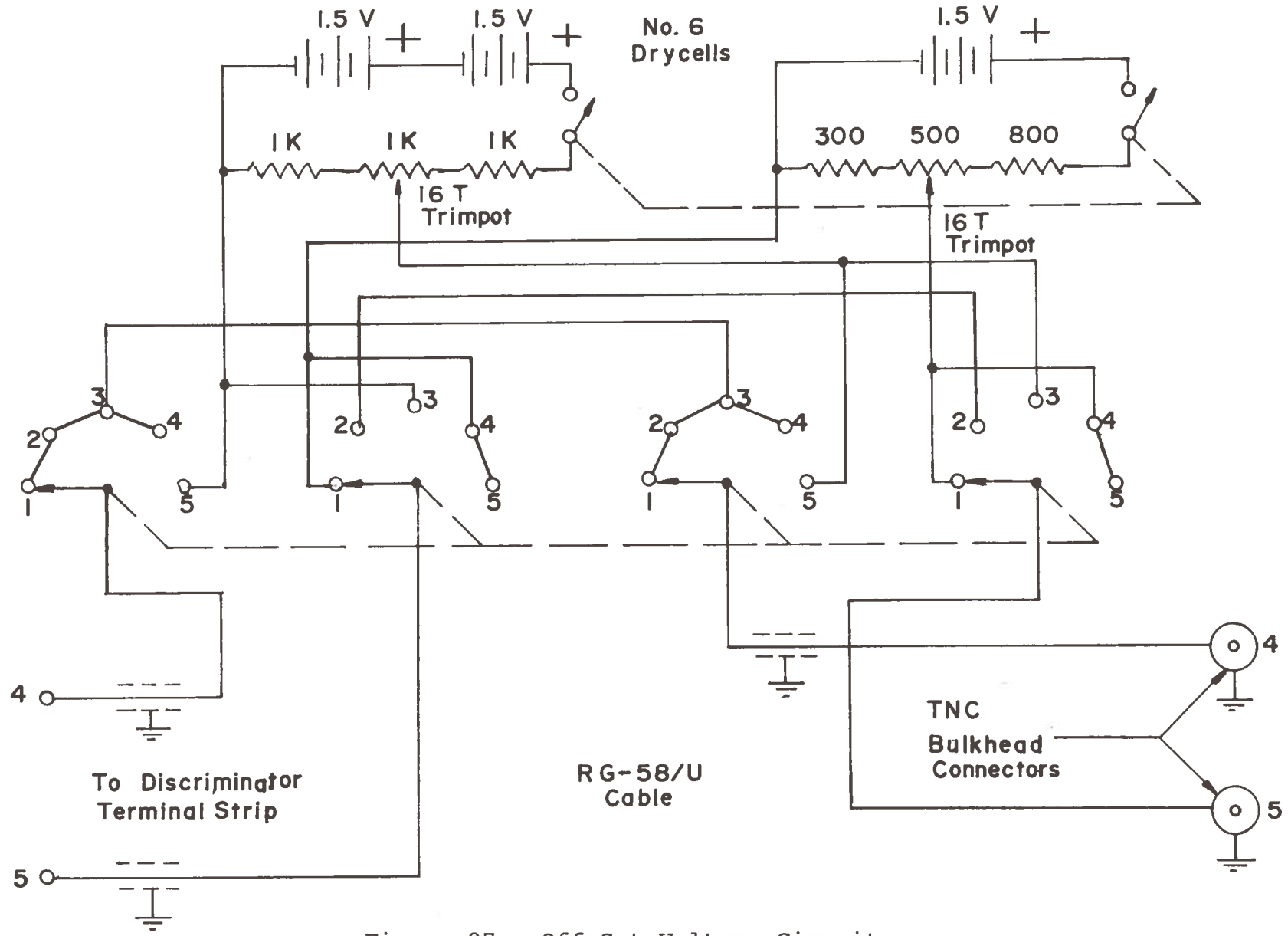

Figure 27. Off-Set Voltage Circuitry

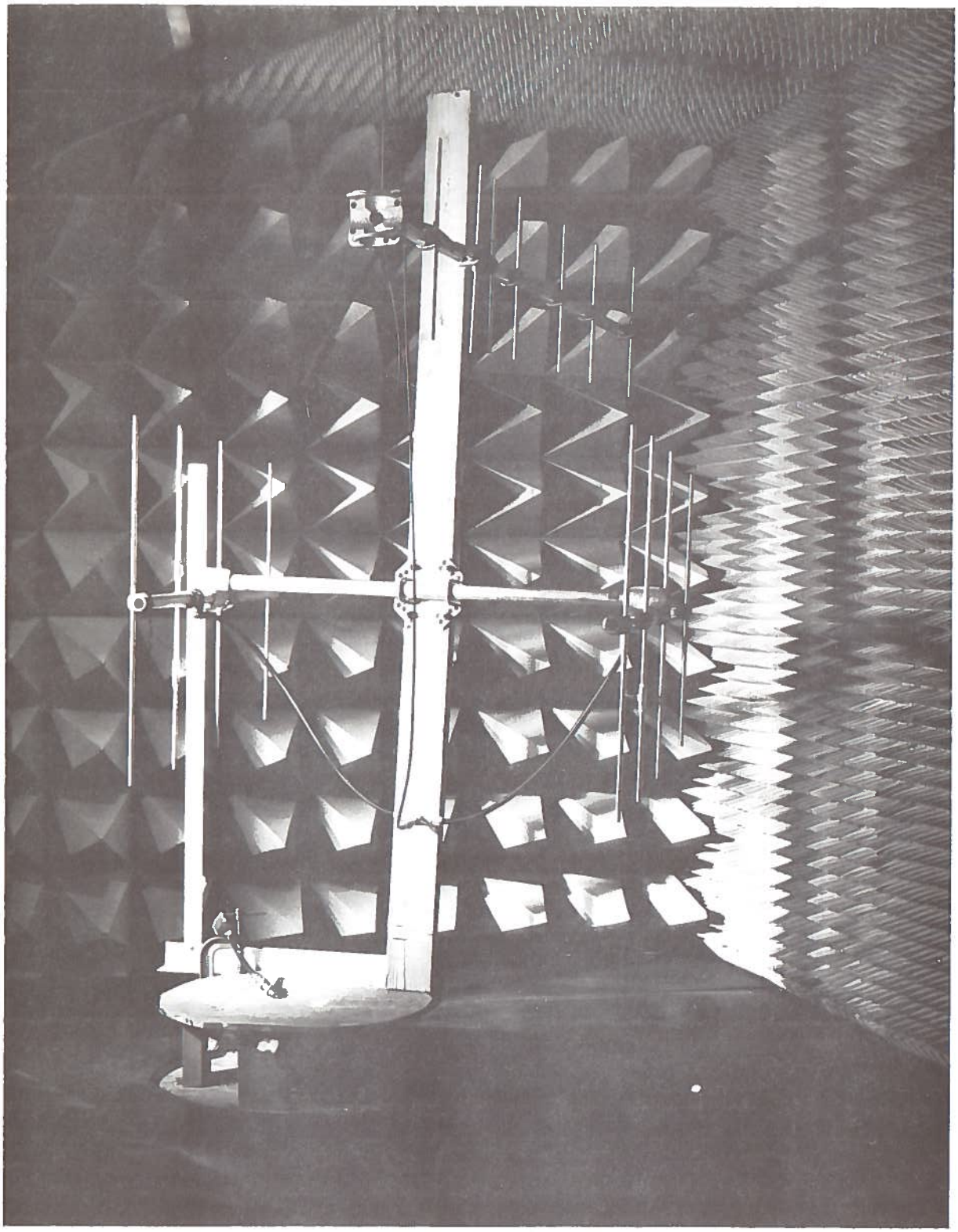

Figure 28. Ground Station Antennas

antennas thus have an omnidirectional field pattern in the horizontal plane and about a 90° beamwidth in the vertical plane. The vertical pattern is considered sufficient to assure communications under all conditions of buoy motion.

The ground based antennas are directional since their mounting and orientation is to be fixed. The receive antenna is a dual yagi with a 9.3dB unidirectional gain and a horizontal beamwidth of approximately 35°. The command antenna is a single yagi with a 10dB unidirectional gain and a horizontal field pattern of approximately 50°. It has been estimated that these beamwidths are sufficient for any multiple buoy tests that may be conducted. This is based on five buoys deployed along straight line in 60 feet of water with 180 feet of anchor chain tethering each buoy, where the ground antennas would be located one half mile away normal to the buoy line. Since buoys may also be deployed closer to or further away from the ground station it is obvious that many more buoys would fall within the antenna coverage. Estimates of path loss indicate that for the equipment used the coverage should be at least good out to line of sight. In the only test performed the equipment was separated by approximately one tenth of a mile with the antennas non-ideally deployed. The ground station antennas were located within a steel reinforced building amid various pieces of laboratory equipment while the buoy antennas were located near ground level. Even under these non-ideal conditions the received signal could be attenuated nearly 40dB before any degradation was discernible.

All the antennas used were wind rated for at least 100 mile per hour winds while the buoy antennas were treated with a chromate film and covered with an epoxy finish to protect against the sea environment.

5.0 BATTERY LIFE CONSIDERATION

The purpose of this section is to estimate the life of the batteries based upon an expected current profile and the stated ampere hour capacity of the batteries. Figure 29 is a current profile which might be encountered in a typical data run. Before and after any data run the equipment is in the quiescent state in which the command receiver and signal decoder draw 110 milliamperes. This quiescent level of current occurs as long as the battery line is connected to the equipment. At the start of a data run a gyro would be activated as shown in figure 29. At start, the gyro motor will draw about one ampere which will fall to a final value of 1/2 ampere in about two minutes. It should be noted that the increase in current at time t=0 is more than one ampere. This is due to the fact that the drain of the command circuitry also increases as command functions are initiated. In the illustration the total command drain was used at the outset and the gyro motor fall-offs were taken as linear. While this is probably more severe than what actually happens, it does simplify the analysis. The second gyro is shown activated after the first one is up to speed. When both gyros are up to speed the telemetry is then turned on. The typical data run period was taken as 20 minutes with 14 commands to the stepping switch. The problem now is to compute the area under the profile curve, which is a straight forward procedure. An expanded view of the estimated stepping switch spikes are also shown in figure 29. This estimate is based on a switching rate of ten per second with equal time division between activation and return of the mechanism, and a total switch hold time of one second. For the curve of figure 29 the result of the integration is .719 ampere hours. It is interesting to note that the switching spikes accounted for .0028 ampere hours, which by comparison is essentially negligible. An interesting ampere product however is obtained by integrating the quiescent current over the remainder of a 24 hour period. The result is 2.603 ampere hours which is significantly higher than that required for the full data run. The total which is 3.322 ampere hours, based on one run per day, is certainly small considering a battery capacity of 3000 ampere hours. The batteries used in the experiment were of the lead acid type where the capacity is based on an 8 hour discharge rate. There is reason to believe that for this experiment, one would have to consider the self-discharge rate of the battery itself to determine how long the experiment could be run. In view of the circumstances there appears to be no reason why the experiment cannot be run for at least six months with many data runs taken each day.

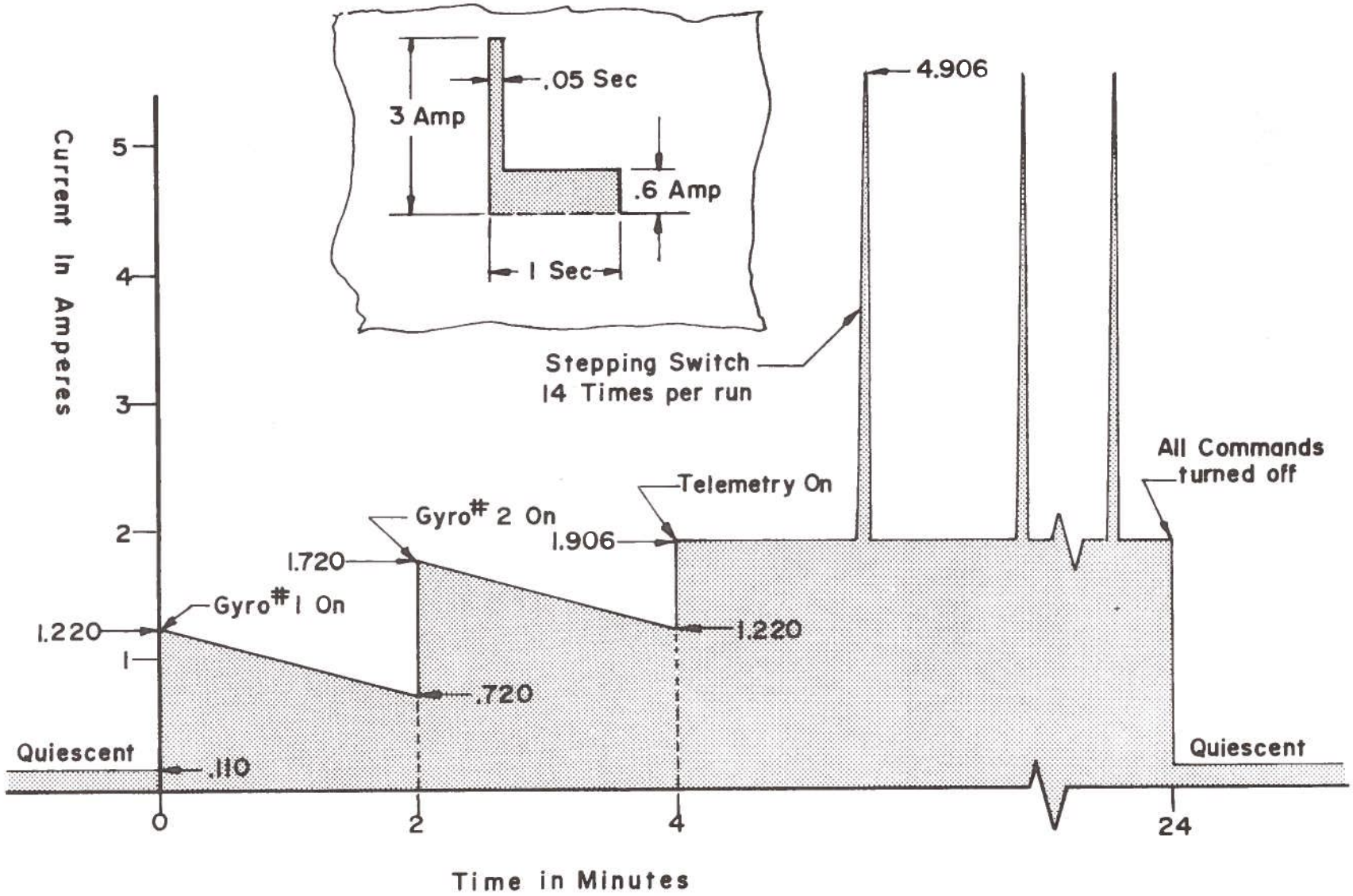

Figure 29. Current Profile

6.0 MECHANICAL CONFIGURATION OF PROTOTYPE

Figure 30 is a detailed drawing of the package assembly while figures 19 and 20 are photographs of this assembly. All components were secured to a 1/8" thick 6061.T6 aluminum plate, by tapping the plate with the appropriate thread size. Jam nuts were used to lock the mounting screws to the plate and a bead of epoxy was placed on all screw fasteners as an extra safeguard against loosening.

The top surface of the plate contains the junction box with connectors (Amphenol 57 Series), handles, and the following accelerometers:

AYPT1 - Mounted in the pitch plane and used to specify yaw motions.

ART2 - Mounted in the roll plane.
APT3 - Mounted in the pitch plane.
AVT4 - Mounted parallel to the buoy centerline.

AV7 - Variable reluctance type mounted parallel to the buoy centerline.

Mounted to the lower surface of the plate are the telemetry components and remaining transducers below:

ARL5, APL6 - Used to form accelerometer couples with corresponding units mounted on the top surface.

PINC, RINC - Pitch and roll axes of the dual inclinometer

PGYC1, RGYV1, RGYC2, PGYV2 - Pitch and roll axes of the two vertical gyros. "C" corresponds to the axes that align to case, while "V" refers to the vertically erected axes.

To facilitate adjustments and testing, the plate assembly will support itself in several different positions and no additional fixture is required. The plate assembly mounts in the aluminum case as shown in figure 31. The case contains an integral flange with captive nuts that secure the plate to the flange. Attached to the case are a spring-loading carrying handle and welded aluminum brackets used to mount the case to the buoy.

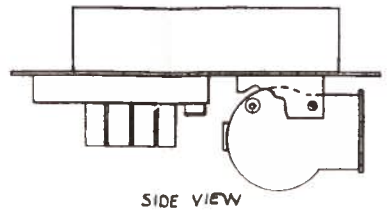

CONN	FUNCTION
J1	ACCELEROMETERS & INCLINOMETERS
J2	TELEMETRY
J3	COMMAND
J4	BATTERY & LOAD CELL
J5	GYROS
J6	TEST RECEPTACLE

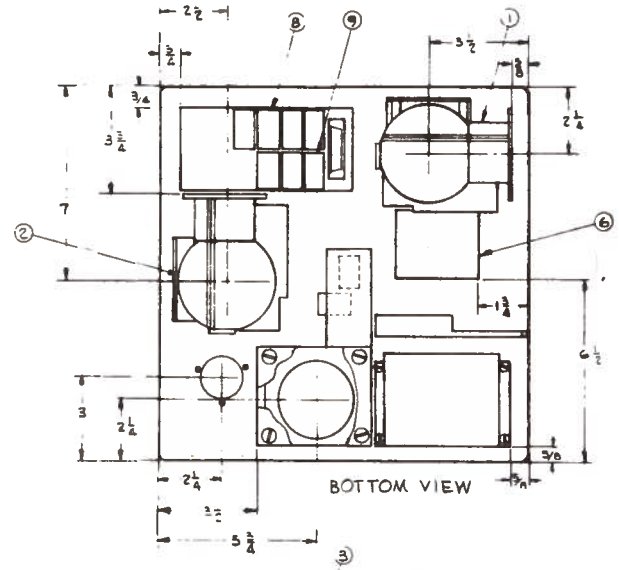

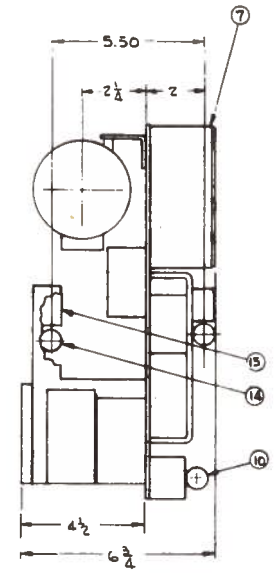

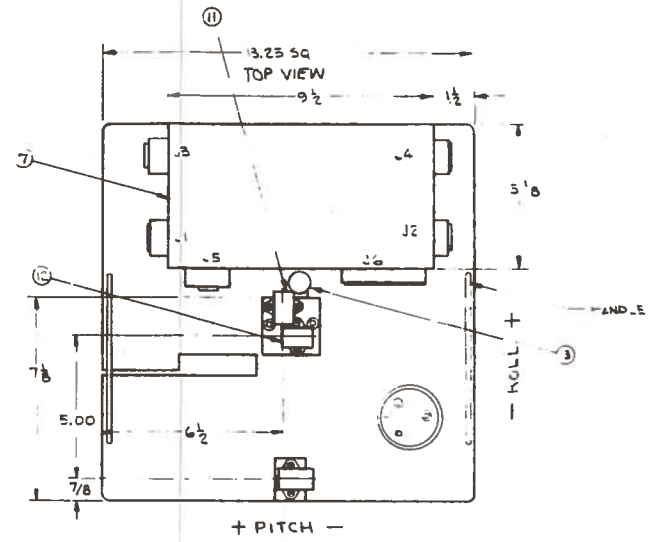

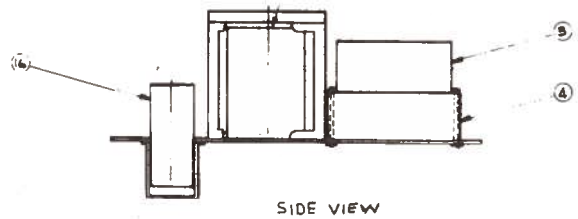

16	1	ACCELEROMETER AVT
15	1	APL6
14	1	ARL5
13	1	AVT4
12	1	APT3
11	1	ART2
10	1	ACCELEROMETER AVPT1
9	1	MIXER OSCILLATOR
8	1	VOLTAGE CONTROL OSC
7	1	JUNCTION BOX
6	1	TRANSMITTER
5	1	DECODER
4	1	RECEIVER
3	1	INCLINOMETER
2	1	GYRO
1	1	GYRO

SYMBOL	SPECIFICATION	CODE IDENT	PART OR IDENT NO	TYPE NO	QTY REQD	MATERIAL

LIST OF MATERIALS

UNLESS OTHERWISE SPECIFIED DIMENSIONS ARE IN INCHES

DO NOT SCALE THIS DRAWING

MATERIAL

FINISH

NEXT ASSY | USED ON | APPLICATION

DEPARTMENT OF TRANSPORTATION — TRANSPORTATION SYSTEM CENTER

DRAWN | CHECKED | APPROVED | APPROVED

SIZE F | CODE IDENT NO | DRAWING NO

SCALE | SHEET

REVISIONS

ZONE	LTR	DESCRIPTION	DR	CHK	DATE	APPROVED

Figure 30. Detailed Drawing of Mechanical Assemble

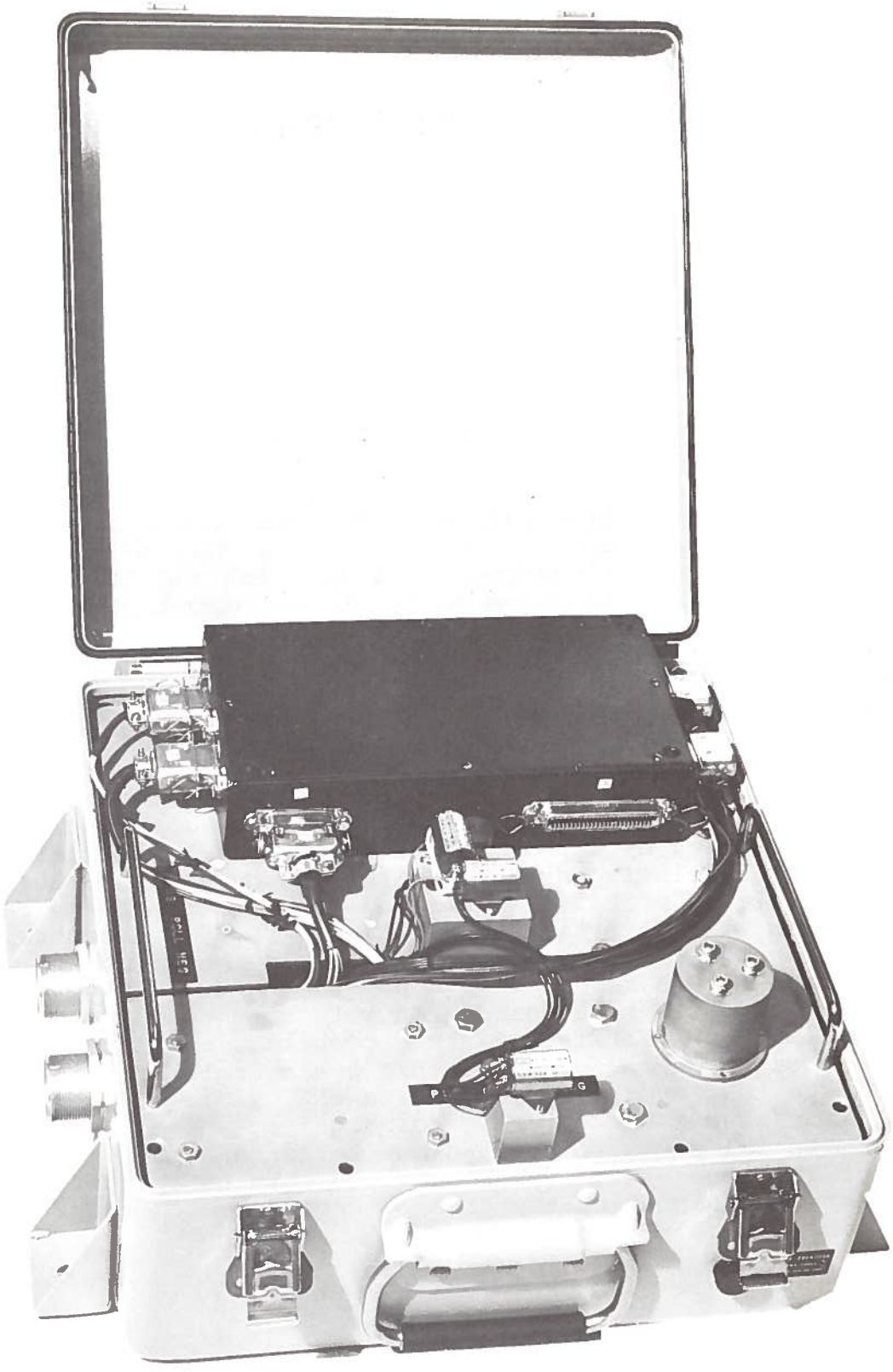

Figure 31. Instrument Package in Case

7.0 ENVIRONMENTAL CONSIDERATIONS

The environmental conditions experienced by an ocean buoy dictated that special attention be focused on the protection of systems components. All of the components with the exception of the load cell and telemetry antennas were housed in an instrument case manufactured by MM Electronics Endlosures, Inc. This case was fabricated from .090 inch aluminum and painted inside and out with a zinc chromate primer and two coats of grey epoxy base paint. All external hardware, such as the cam-type latches, separable hinges, and handles were stainless steel.

The case confirms with MIL-STD-108E (Table 111) for a water tight enclosure. This test states that no leakage will occur during a one hour test in which the case is submerged at a depth of three feet. It was noted, however, that air leakage did occur if a differential pressure existed in the case. For example the temperature change from day to night can induce a differential pressure and air would be drawn into the case to equalize the pressure. The quantity of air "breathed" and hence the moisture is proportional to the free volume of air within the case. To minimize this volume, blocks of plastic foam were formed with a hot wire cutting tool and custom fit into the case. Also included in the case was a quantity of silica gel desiccant calculated to keep the relative humidity within the case below 30% for a temperature 70° F. All external connections to the case were made with watertight Amphenol Series 89 connectors. Following these additions to the case, submergence and water spray tests were repeated with no leakage detected. Although the prototype test was conducted with this configuration and no leakage or electrical failure occurred, subsequent discussion with personnel at the MIT Ocean Engineering Department indicate that another problem area may exist. If, on a hot day, the case is momentarily submerged by a cool wave, the differential pressure created may be large enough to draw water into the case. This event would be catastrophic and further evaluation of the case is necessary to determine the possibility of this occurence.

8.0 INSTRUMENT CALIBRATION AND SALE FACTORS

The output of the package instrumentation in many cases is a function of battery voltage, therefore the affected components were calibrated in the lab with various voltage inputs. As stated earlier, the battery voltage can be ascertained using stepping switch positions 5 and 6 which incorporate resistance dividers. The difference between the voltages at these positions is plotted as a function of battery voltage in figure 32. Knowledge of the battery voltage is then used to determine the regulated voltages applied to the potentiometric transducers and the load cell. These voltages as a function of battery voltage are plotted in figures 33 and 34.

To determine the gain factors of the VCO-discriminator combinations, a regulated 0-5VDC signal was used to modulate the VCO's while recording the output of the discriminators. This test was done using simulated battery voltages of 23.0, 28.0, and 32.0 with differences less than 0.4% of the values shown in Table 6.

Certified calibration of the individual transducers was furnished from the manufacturer with the exception of the vertical gyros and the variable reluctance accelerometer (AV7) both purchased from a surplus house. The gyros to be used as "smoothers" were roughly calibrated in house while AV7 was more carefully calibrated using the acceleration of gravity. The accelerometer was adjusted to maximum sensitivity and a test made varying the input voltage. Results of this test are plotted in figure 35. Also plotted in this figure is the voltage that refers to the gravity component which must be "bucked" in the gravity bias unit described earlier. Using manufacturer's data and experimental values, the following conversions factors can be surmised:

GYRO

Vertical axis	22.5 deg/volt
Case Axis	30.0 deg/volt

Inclinometer

Pitch	$\frac{90°}{(.972\ V_t)}$ deg/volt
Roll	$\frac{90°}{(.976\ V_t)}$ deg/volt

V_t = Transducer Voltage from figure 34

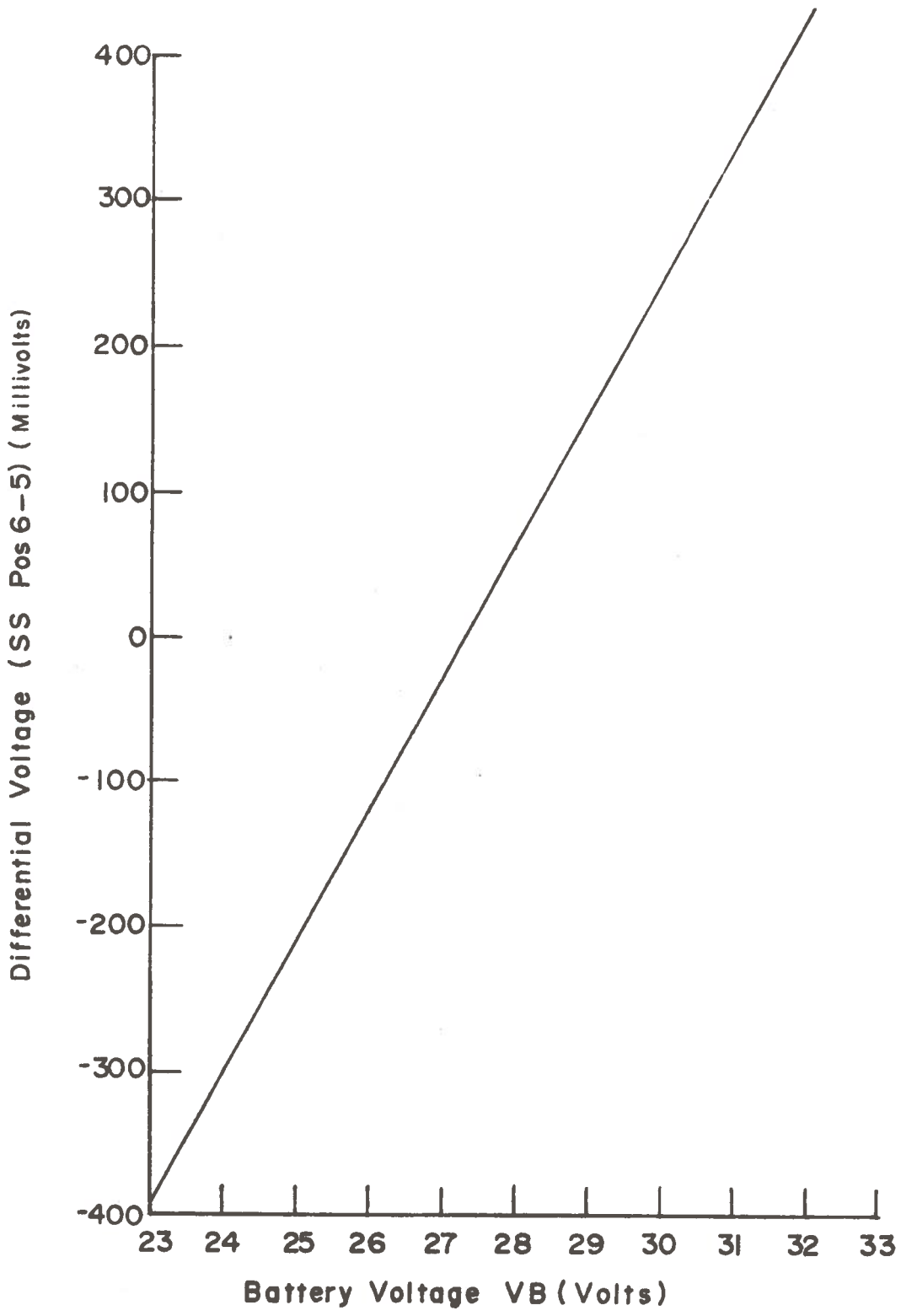

Figure 32. Battery Voltage Determination

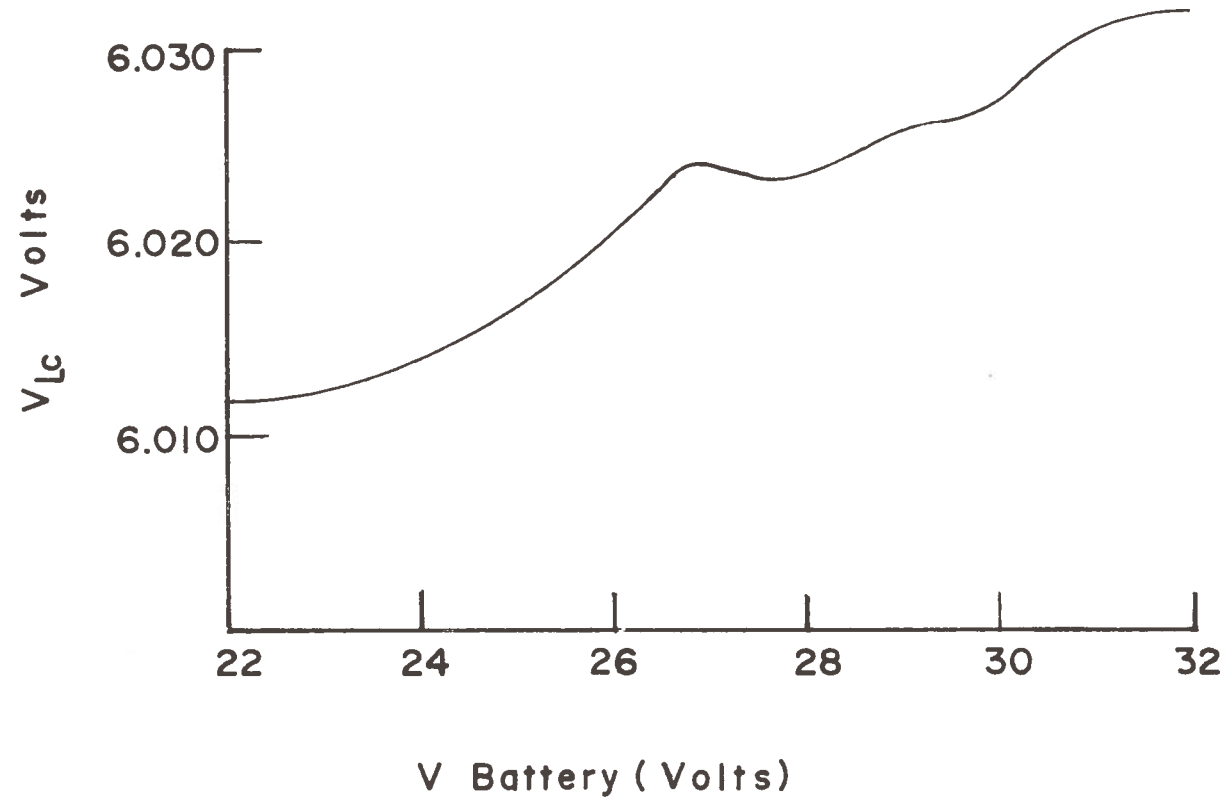

Figure 33. Load Cell Voltage

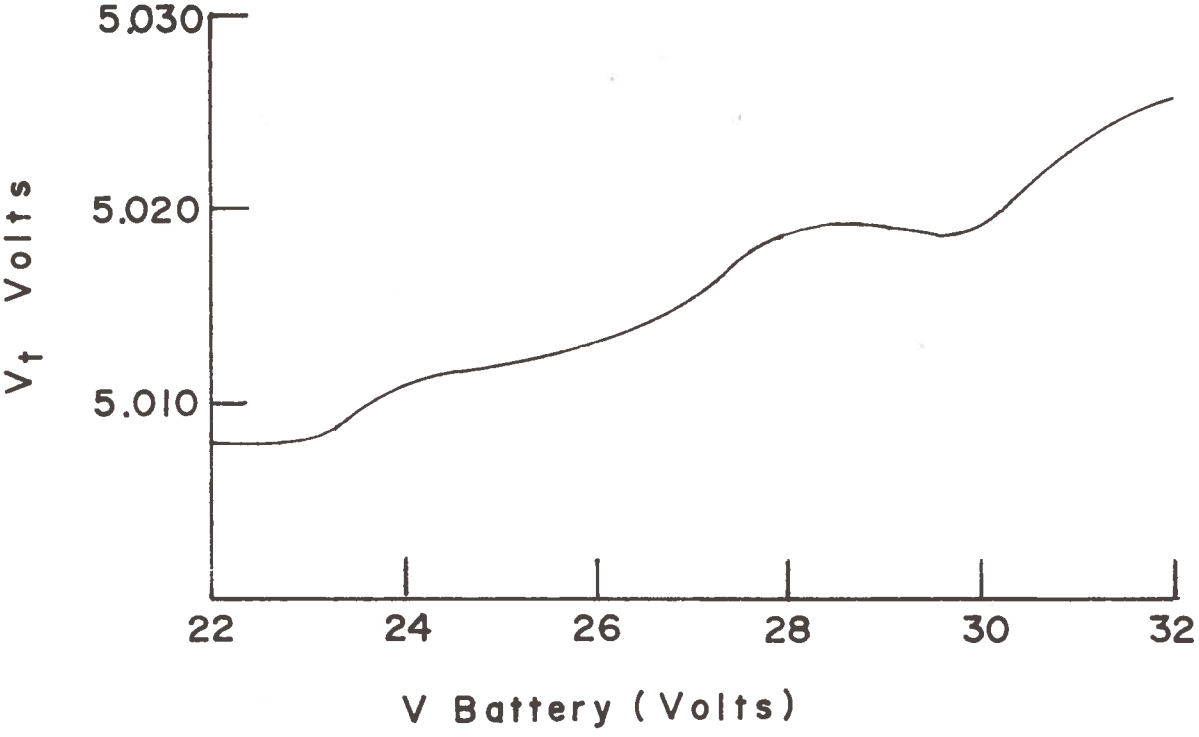

Figure 34. Transducer Voltage

Table 6. Telemetry Gain Factors

GAIN FACTORS (OUTPUT/INPUT)

VCO-DISCRIMINATOR COMBINATIONS

CONSTANT IN 23-32 VDC RANGE

1.	400 hz	0.978
2.	560 hz	1.006
3.	730 hz	1.016
4.	960 hz	1.013
5.	1300 hz	0.998
6.	1700 hz	1.0

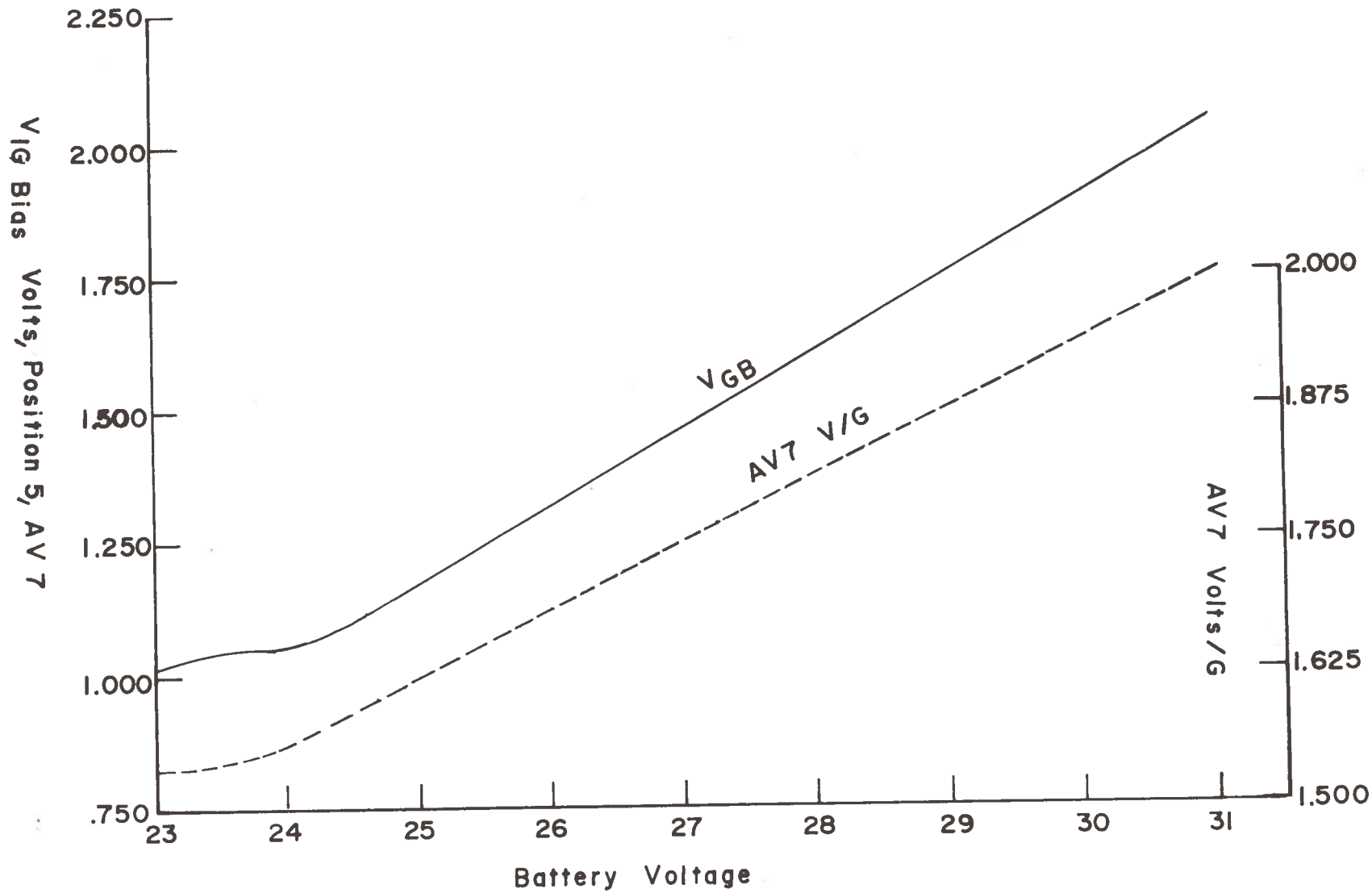

Figure 35. Accelerometer AV7 Sensitivity

Accelerometer

AYPT1	$\frac{1}{(.103\ V_t)}$	G/volt
ART2	$\frac{1}{(.102\ V_t)}$	
APT3	$\frac{1}{(.102\ V_t)}$	
AVT4	$\frac{1}{(.100\ V_t)}$	
ARL5	$\frac{1}{(.100\ V_t)}$	
APL6	$\frac{1}{(.098\ V_t)}$	
AV7	See Figure 35	

Load Cell

$$0\text{-}20{,}000 \text{ lbs.} \simeq V_{LC} \times SENS_{LC}$$

V_{LC} = Load cell voltage from figure 33

$SENS_{LC}$ = Load cell sensitivity

9.0 PROTOTYPE TESTING

TEST CONFIGURATIONS

The purpose of the prototype testing was several fold. In the first phase a series of tests were performed on the equipment in the laboratory under various environmental conditions to see if any malfunctions would occur. In the first of these tests the instrument package was operated in an oven at 120° F for three hours. In the second test the package was operated in a freezer at 0° F for three hours, and finally the system was run under ambient conditions for 24 hours. During the tests the ground based equipment was generally remote from the instrument package and its antennas. Large distances were simulated by placing attenuators in the antenna line while also monitoring rf power levels. No malfunctions occurred during any of this testing. The in-house testing was concluded with a series of tests in which the overall calibration of the system was established.

The second phase of testing was performed at the Coast Guard Station at Curtis Bay, Maryland using a standard 8x26 buoy. The purpose of these tests was to determine the types, sensitivities, and ranges of the instrumentation required to adequately measure the stability parameters as well as evaluate the command and data transmission systems. It should be emphasized that the ranges of the instruments used in the prototype package were "best guesses" based upon careful review of available existing data. Prior to testing, a prototype test plan was prepared which is included as Appendix B to this report.

In these tests the buoy was placed in the water by the Coast Guard at a dockside location. This buoy (figure 1) was outfitted with the load cell, instrument package, antennas and associated cabling. The ground station equipment was set up in an enclosure about one fifth of a mile away, from which visual sighting of the buoy was possible. A modified mooring system was constructed for these tests to impart heave motion to the buoy as well as vary the tension sensed by the load cell. This was accomplished by threading a wire rope attached to the load cell on the buoy, through a sinker on the bottom of the bay and returning the free end of the rope to the pier. Heave motion was generated by pulling on the rope with a tractor. Angular excursions were imparted by two men riding the buoy and simultaneously shifting their body weight while a third man on the shore pulled on a rope attached to the superstructure. These events were recorded on movie

film while strip chart recordings were made at the ground base station. Time synchronization between the two locations was achieved using portable radio transceivers.

Once the tests were underway two facts became quite obvious. First, it became apparent that the instrument package and telemetry system were operating in a satisfactory manner as expected, and secondly, that the dockside excursions of the buoy were not representative of conditions that were hoped would be simulated. The prime cause of the difficulty was that very little heave motion could be imparted to the buoy. This was mainly due to the size of the vehicle used to pull on the wire rope and the general footing which did not provide good traction. From the load cell data it was seen that the forces generated were about 3000 pounds on the average with an occasional pull of 5000 pounds. Unfortunately however, all of these forces were in impulse form lasting only a fraction of a second which by observation was a small part of the natural heave period of the buoy. Since the buoy waterline is around the cylindrical portion of the buoy, the force necessary for a given displacement is easy to calculate. Taking the diameter of the buoy as 8 feet and the density of water 62.5 lbs. per cubic foot it is evident that a force in excess of 3000 pounds is required to displace the buoy one foot. If a steady 3000 pound force could have been applied there is reason to believe that the desired result would not be realized but instead the entire buoy and sinker would be dragged sideways. The situation was further complicated by the shallowness of the water which meant there was very little line distance between the buoy and the sinker. The result of this was that the line tugs simply introduced severe perturbations into the roll and pitch measurements. The general conclusions derived from these tests will be discussed in another section of this report however in brief it is apparent that actual on-site testing should be given serious consideration in any future program.

The tests were divided into two groups. Group A data was generated with the instrument package located on the gong pad approximately six feet from the apparent center of rotation. Group B tests were performed with the package mounted on the lantern base nearly eighteen feet from the center of motion. Ten different combinations of data were recorded in each group with movie film documentation of each run. Selected representative data will be included in the following section. The calibration data for the prototype tests is shown in figure 36.

TEST A & B

DATE 6-10-71

TIME 10AM-4PM

V_{BATT} 31.1

V_{TRANS} 5.023

$V_{LOAD\ CELL}$ 6.031

AV7 .497 G/volt

V_{GB} 2.080 volts

TRANSDUCER SENSITIVITIES

AYPT1	1.924 G/volt	PGYC1	30°/volt
ART2	1.952 G/volt	RGYV1	22.5°/volt
APT3	1.952 G/volt	PGYV2	22.5°/volt
AVT4	1.991 G/volt	RGYC2	30°/volt
ARL5	1.991 G/volt	PINC	18.434°/volt
APL6	2.042 G/volt	RINC	18.358°/volt
AV7	.497 G/volt		

LOAD CELL

SENS 4912 lbs/volt

CHART ZERO ≈ 12.282 lbs

Figure 36. Calibration Data, Prototype Test

DATA ANALYSIS OF THE PROTOTYPE TEST

The purpose of the prototype test is to determine if the sensors furnish adequate data to define the stability of a buoy. Specific items to be checked include:

1. Sensor Range
2. Sensor Sensitivity
3. Magnitude of lateral accelerations
4. Magnitude of angular accelerations

As stated in the transducer discussion, it is the latter two items that determine if pendulum inclinometers are suitable for use as angle measuring devices.

HEAVE MOTION

The proposed method for measuring heave motion was to use the pitch and roll data to resolve three orthagonal accelerometer outputs into vertical and horizontal components. Integration of the time related vertical component will yield vertical velocity while a successive integration will yield vertical displacement. In the prototype tests the limiting factor in performing these tasks was the accuracy of the accelerometers. In short, the accuracy of the units selected is a function of the full scale range. The potentiometric accelerometers had a $\pm$ 5 G range with a maximum error limit of 1.5%, or .15 G. Maximum error on the variable reluctance unit was 0.03 G. Observation of the accelerometer test data indicate a maximum vertical acceleration of 0.30 G during a severe chain pull impulse and a 0.15 G maximum from normal bobbing action. Because of these unexpected low G values, 100% error could result with the potentiometric devices while 20% error is possible in the variable reluctance type.

Although it is possible that the error margins could render the data completely worthless, these maximum errors are not probable. For this reason, three runs of data from the A tests were graphically analyzed to determine the heave displacement. From the dynamics of the prototype test, it is apparent that no method was used to impart lateral acceleration to the buoy. Therefore Equation 14, the output of the vertical accelerometer can be revised as shown in Equation 16 eliminating A_2 and A_3.

$$A_V = [\cos\phi_V - 1] + [A_1\cos\phi_V] - [R\dot{\phi}_V^2]_3 \qquad (16)$$

By selecting a data run in which ϕ_R was nearly zero, and rearranging Equation 16 an expression for the vertical acceleration, A_1 is obtained.

$$A_1 = [A_V + (1-\cos\phi_p) + R\dot{\phi}_p^2]\frac{1}{\cos\phi_p} \qquad (17)$$

In the above"equation," $(1-\cos\phi_p)$ represents the gravity induced component while $(R\dot{\phi}_p^2)$ is the normal acceleration resulting from angular motion. Graphically compensating for the above terms and neglecting the $[1/\cos\phi_p]$ correction factor, a plot of the acceleration along the buoy centerline is obtained.

Integration of this data was accomplished by two methods. The first involved a step by step "count-the squares" process with the result being a continuous curve. A second method assumes the velocity curve to have a cosine distribution and utilizing averaging techniques calculates an average displacement for a given amount of time.

To illustrate, refer to figure 37 in which the motion of a body is described by simple harmonic relationships.

$$A = A_{PEAK}\sin\omega t$$

$$V = \int_0^t A\,dt = \frac{-A_{PEAK}}{\omega}\cos\omega t + C_1$$

$$D = \int_0^t V\,dt = -\frac{A_{PEAK}}{\omega^2}\sin\omega t + c_1 t + c_2$$

The dynamics of sea motion dictate that the average heave acceleration, velocity, and displacement approach zero as the integration time approaches infinity. Therefore, if the time integration period is sufficient, the values of c_1 and c_2 can be approximated by zero. From the above equations, it can be seen that if the sea motion was sinusoidal, knowledge of the peak acceleration would define the velocity and displacement distributions completely. Since this is not the case, an approximation is made.

Observation of a typical output of the vertical accelerometer indicates a periodic motion with perturbations in phase with the variable chain tension (see figure 38). To obtain an average value for the change in velocity (ΔV) per cycle, the output is integrated with a planimeter and the total absolute value of area (shaded in the figure) divided by the number of half-cycles. Assuming a cosine curve to describe the velocity in which the peak value is $\Delta V/2$, the average peak

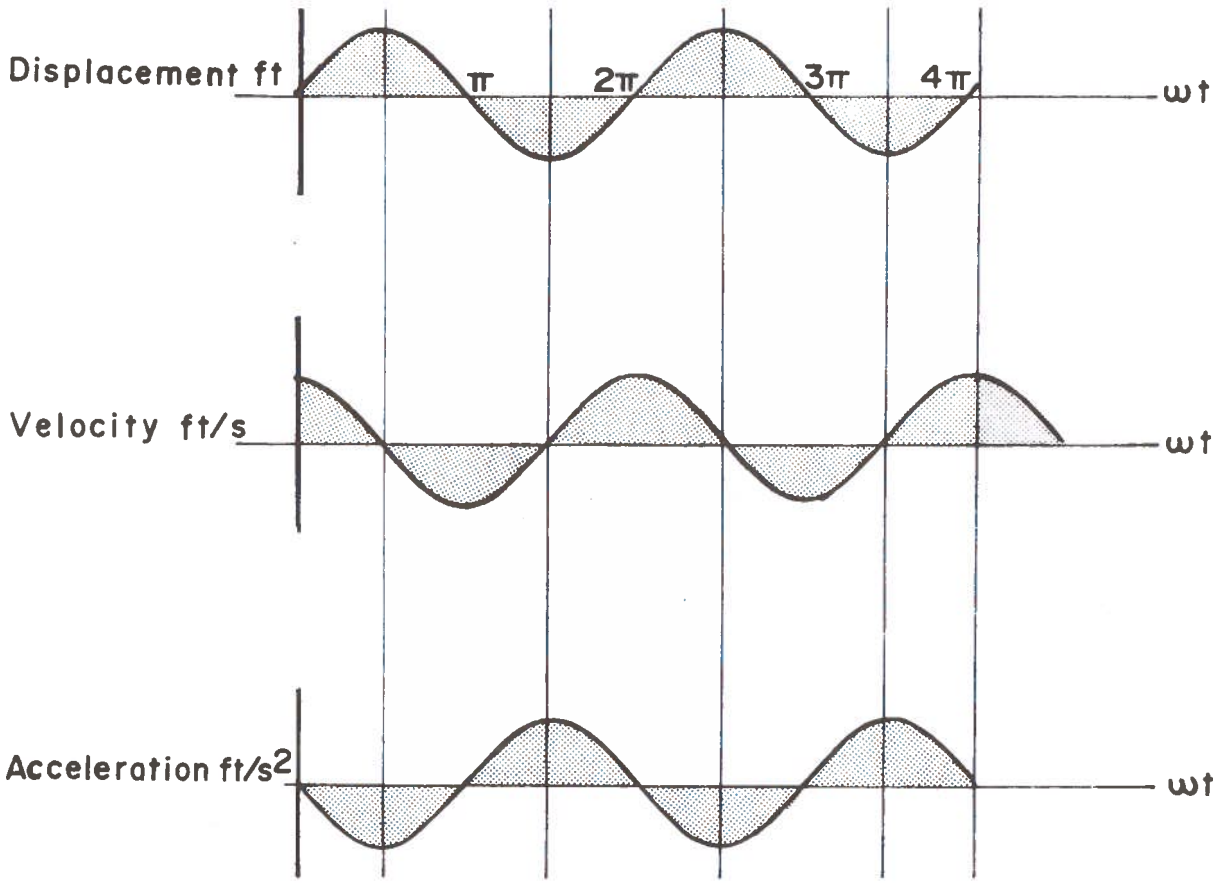

Figure 37. Simple Harmonic Motion.

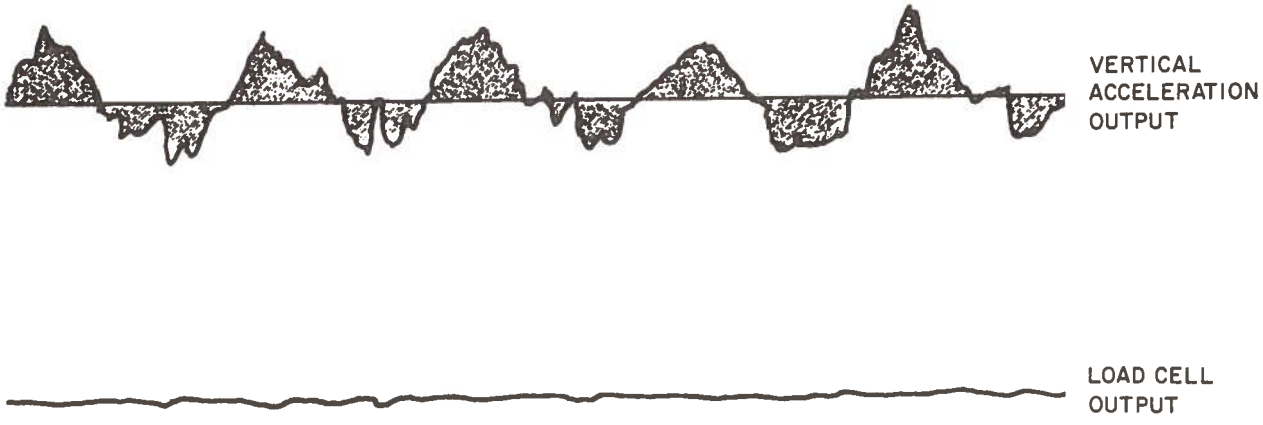

Figure 38. Integration Technique

displacement can be calculated by

$$\bar{D}_{PEAK} = .079\ \Delta V T \qquad T = \text{Period of acceleration} \qquad (18)$$

To compare the two methods of analysis, Test A 12-1 vertical acceleration data was graphically corrected for the component due to gravity. The angle of tilt was obtained from the movie film of the run and the term $[1-\cos\phi_V]$ was graphically added to the output. The normal component of acceleration assuming a 10° peak excursion and sinusoidal motion with $\omega = 1.05$ was 0.006G and was neglected in this analysis. Figure 39 shows the original accelerometer output and the corrected plot. Step by step double integration of this corrected plot is shown in figure 40. Limiting the discussion to the first two complete cycles in which sinusoidal motion is approximated, the average displacement is equal to 11.3 inches. Using the method of averaging and calculating the displacement using equation 18 with $\Delta V = .0515$ G-sec and T = 3 sec, the result is $\pm$ 4.7 inches or 9.4 inches total.

The displacements calculated from the accelerometer data represent motion along the buoy's axis of symmetry, which approximate the vertical displacement within 5% for ϕ_V less than 18 degrees. Those ascertained from the film are also

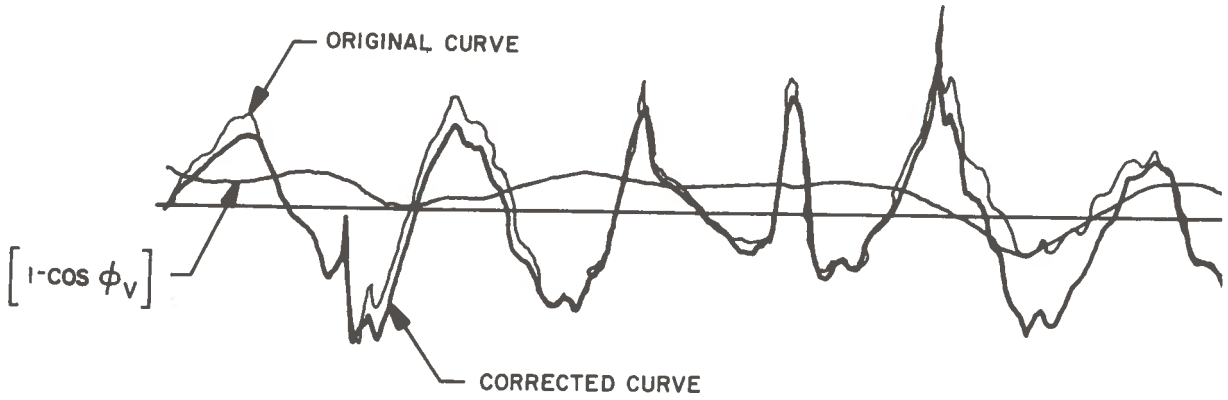

Figure 39. Test Data - A 12-1

vertical distances but in part, are caused by the rotation of the buoy. Assuming a moment arm of 6 feet from the center of rotation to the reference point and noting a 10° tilt angle, the vertical motion created by the tilt alone is equal to $72[1-\cos\phi_V]$ or 1.0 inch. Therefore, the vertical distance traveled by the buoy center of rotation in Test A 12-1 is 10.0 inches from the film, 11.3 inches for the step-by-step method, and 9.4 inches using the averaging method. Comparing these values and considering the error margins possible due to accelerometer inaccuracies, the correlation is encouraging.

Using the simplified data averaging technique, two additional data runs were analyzed in which the less sensitive potentiometric accelerometer output was corrected. Data from run A32 is reproduced in figure 41. It is seen that the pitch motions are $\pm$ 5° and in this analysis are neglected while the roll motions of $\pm$ 12° are graphically compensated for in the acceleration plot. The shaded portion of the acceleration plot is the result of these corrections. Determining the average area of a half cycle by dividing the total shaded area by the number of half cycles, a value for the average velocity change, ΔV, is obtained and is equal to .079 G-sec. Again using Equation 18, a total displacement of 14.1 inches is calculated. From the film, an average displacement of 10.1

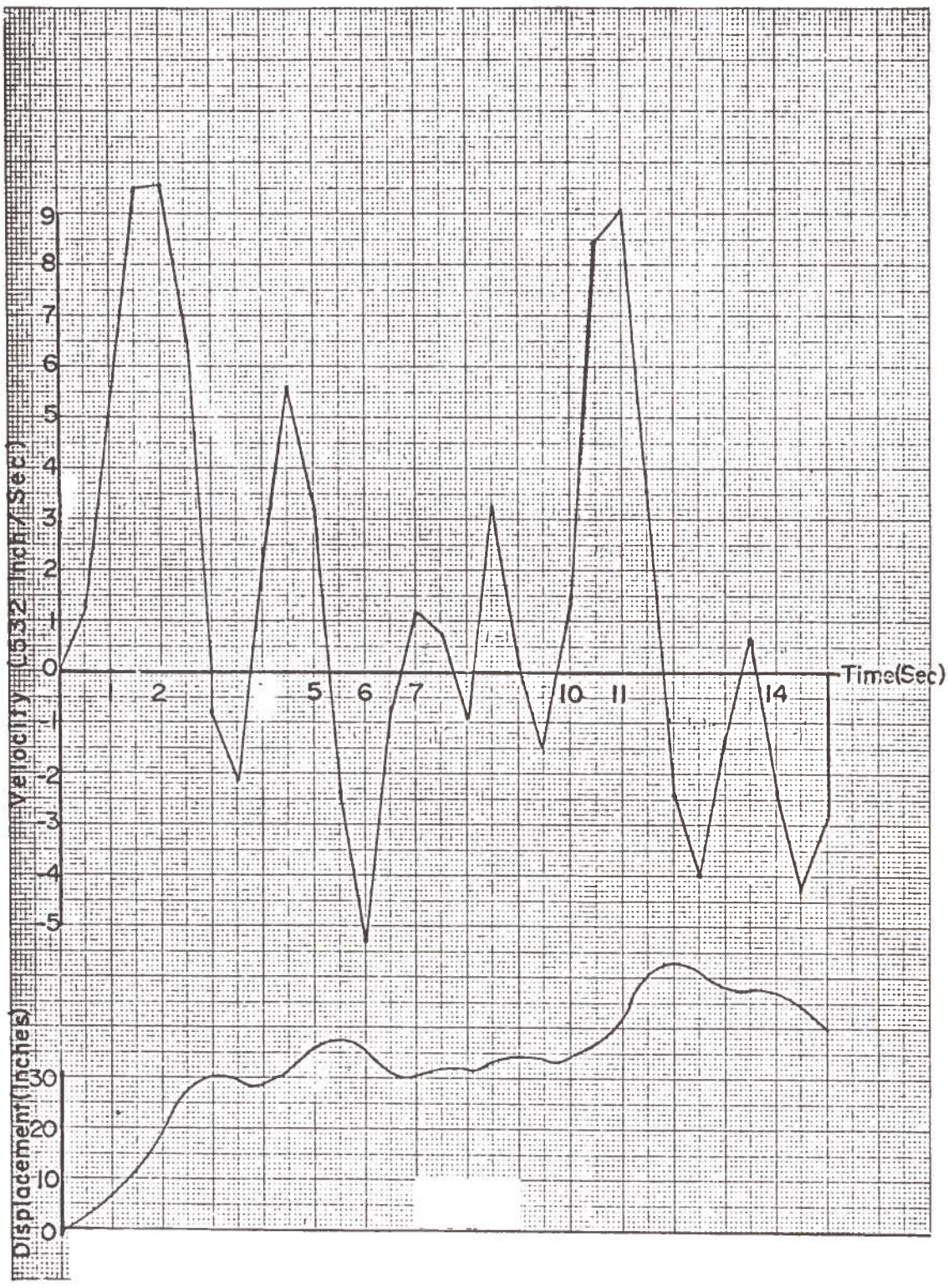

Figure 40. Step by Step Integration

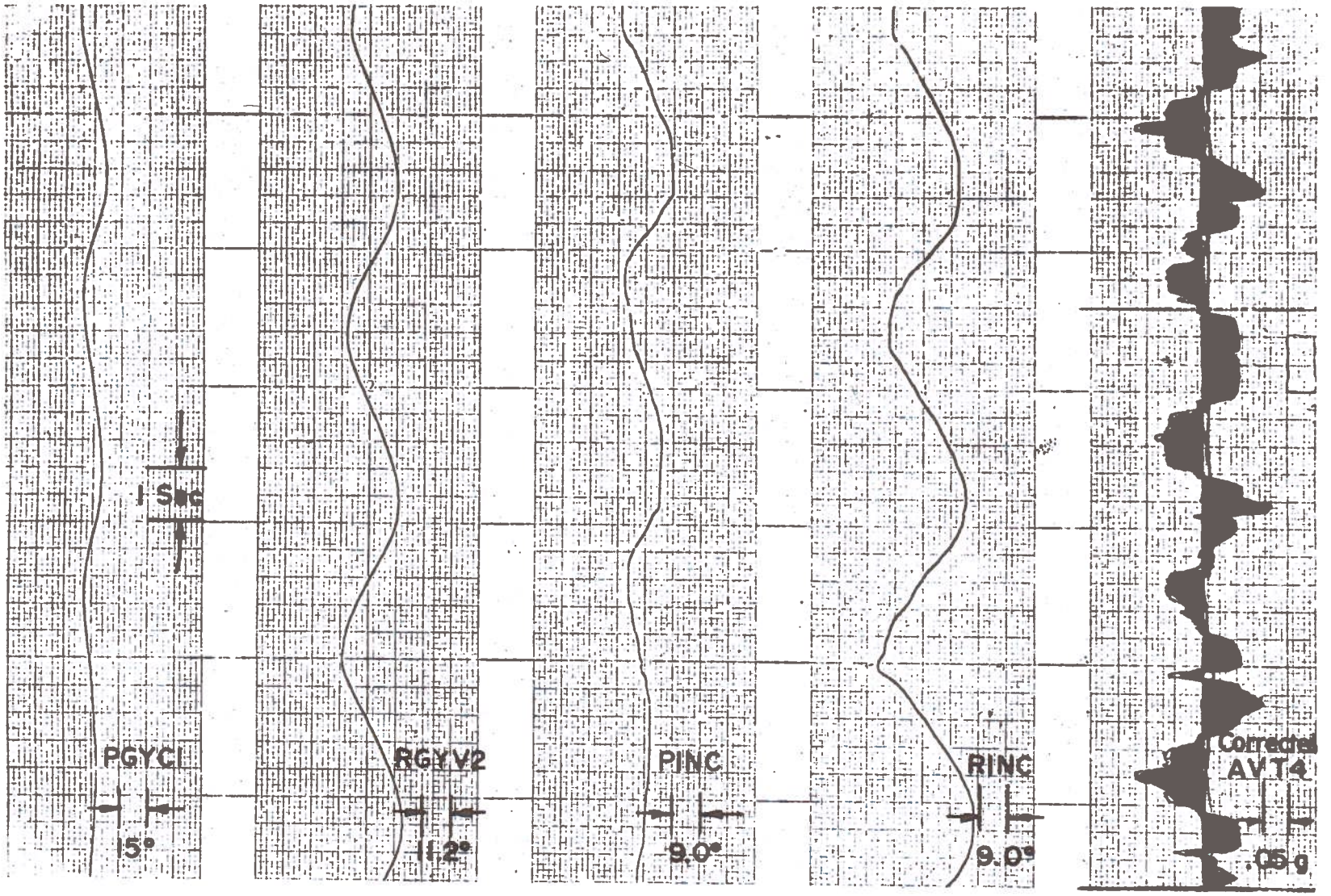

Figure 41. Test A 32 Data

inches is noted. In Test A41, the heave displacement from the film is 9.3 inches while the calculated value is 11.6 inches. This test data is shown in figure 42.

HEAVE RATE

The preceeding method also yields values for the average peak heave rate, $\Delta V/2$. For the three tests described, $\Delta V/2$ is given below.

TEST	$\Delta V/2$
A12-1	0.83 ft/sec
A3-2	1.27 ft/sec
A4-1	1.02 ft/sec

ANGULAR ACCELERATIONS AND NEUTRAL ANGLES

To determine the magnitude of angular accelerations two methods were proposed. The first utilized an accelerometer pair with known spacing which would yield the angular acceleration directly. This approach proved inadequate because of the previously stated accelerometer inaccuracies. The 5 inch separation distance with a moment arm of 72 inches from the center of rotation would result in a 7% difference in the two outputs. In reality, the angular accelerations were in the order of 0.30 radians-per-second. Lateral tangential components would therefore differ less than 0.004G. This small deviation is not detectable from the stripchart and is well below the accuracy limits of the accelerometers.

The alternate method is to assume the pitch and roll motions can be expressed by a sine function. Examination of the gyro data in figure 43 confirms this assumption. Therefore,

$$\phi = \phi_{PEAK} \sin\omega t \tag{19}$$

ω = Frequency of Angular Motions

ϕ_{PEAK} = Maximum Excursion

$$\dot{\phi} = \omega\phi_{PEAK} \cos\omega t \tag{20}$$

$$\ddot{\phi} = -\omega^2 \phi_{PEAK} \sin\omega t \tag{21}$$

From the analog data, the period of angular motion for the 8x26 test buoy was approximately 6 seconds or ω equal to 1.05 radians per second. The peak excursion was observed to be 18° resulting in an angular velocity peak of 0.330 radians per second and a peak acceleration of 0.345 radians per second per second. The error in the inclinometer output caused by

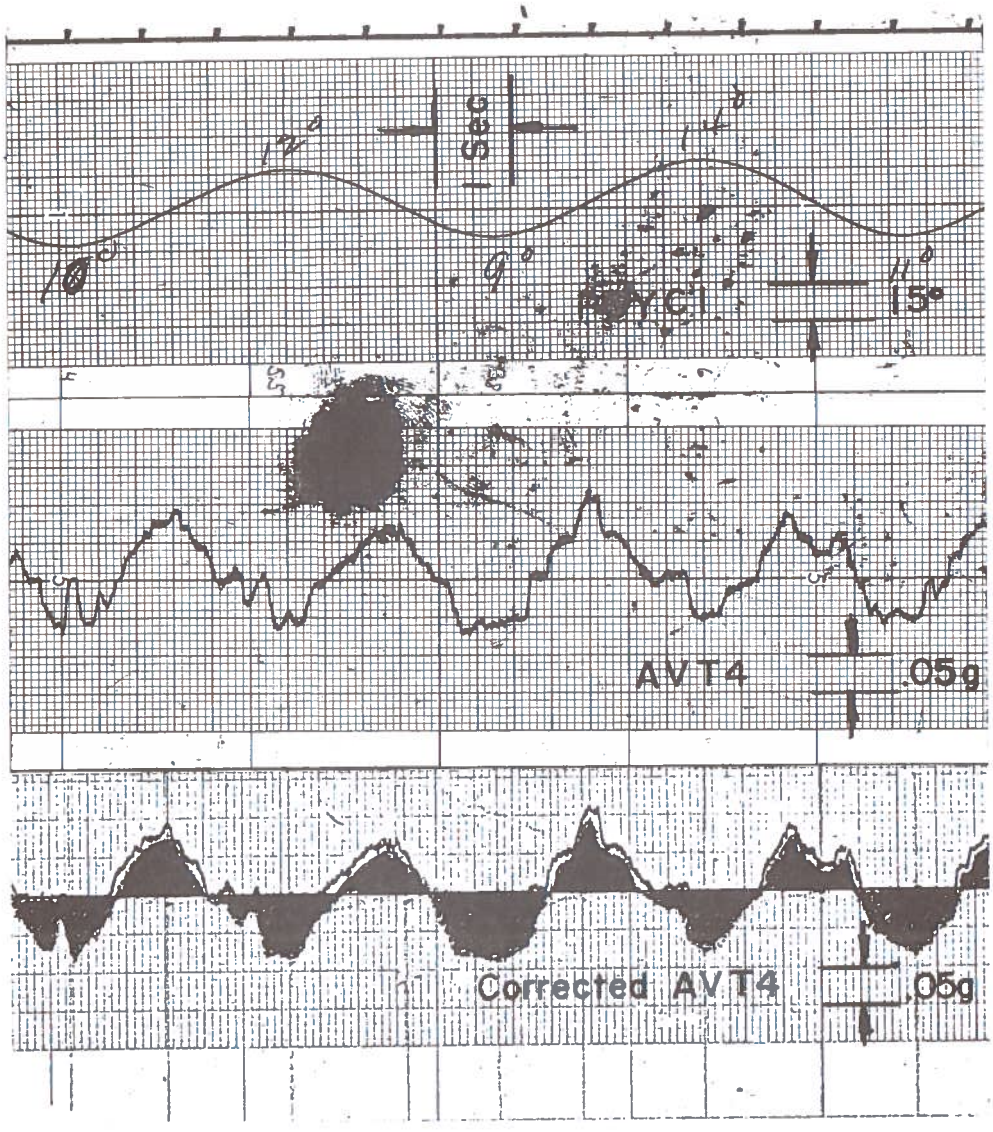

Figure 42. Test A41 Data

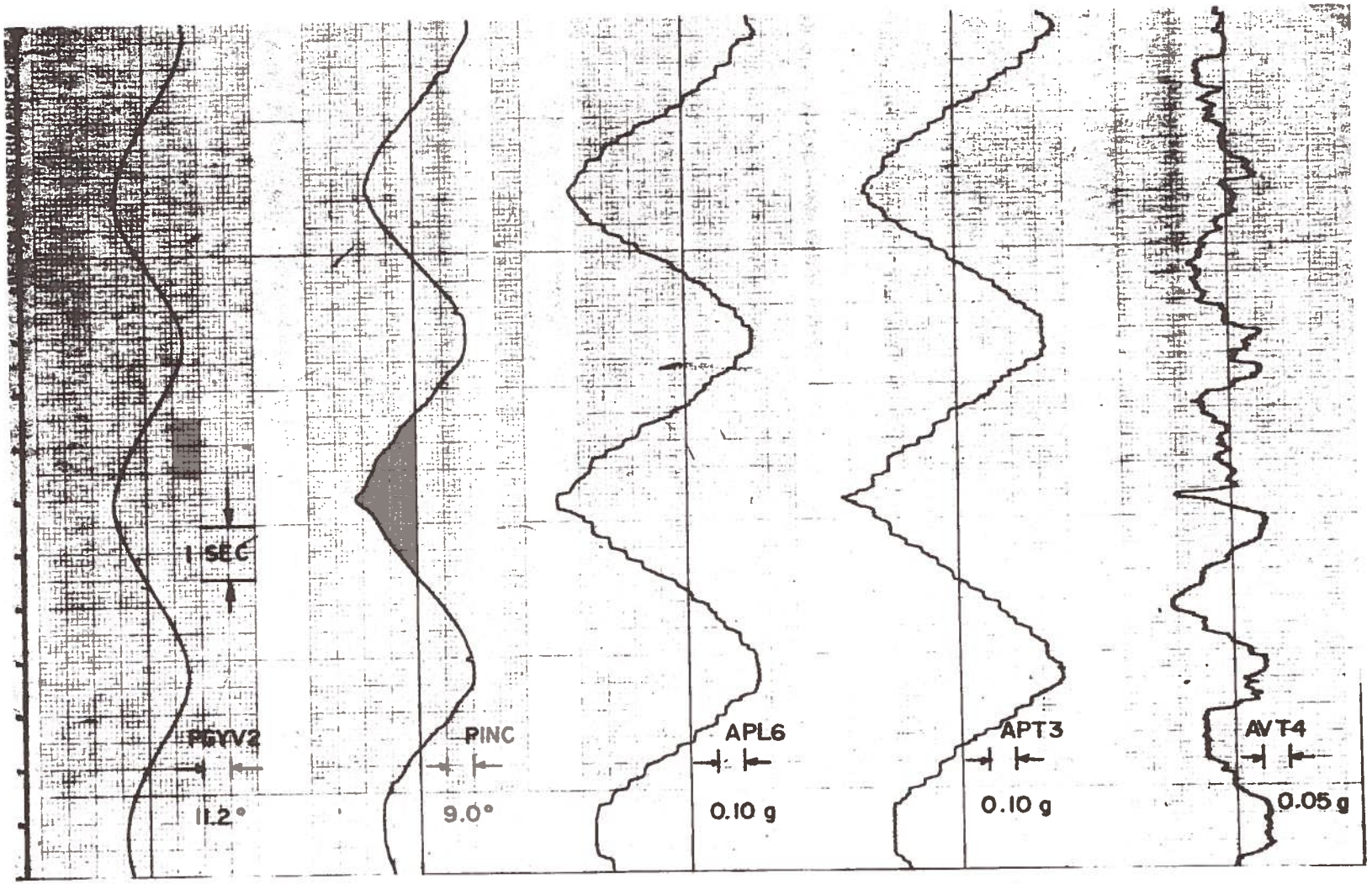

Figure 43. Prototype Test Data, A71

this acceleration is proportional to the radius arm length and is readily calculated. In the group A test package location, the error was 3.4° maximum while in the group B location, the error was 10.0° maximum.

It is obvious that the use of a pendulum inclinometer for absolute angular measurements is not feasible on a buoy. However, in the following discussion it will be shown that the inclinometer will furnish data about the average angle of tilt, that is, the neutral angle, within certain limitations.

Previously, it was stated that a pendulum points in the direction of the total acceleration vector for input frequencies below the natural frequency, f_N, of the pendulum. From table 3, the f_N of the inclinometer is 3 cycles-per-second and the angular motion input exhibited a frequency of 0.16 cycles per second while the heave motion frequency was 0.33 cycles-per-second. Referring to figure 6, the response of a second order system in these ranges is unity.

To determine the offset error that can occur in the averaging process, three cases are described.

CASE I

The buoy has attained a pitch angle, ϕ, created by a wind or steady current and the wave motion is causing motion directed along the buoy axis of symmetry. Let the acceleration be defined:

$$A = A_{PEAK}\sin\omega t$$

writing the vertical and lateral components of this acceleration and adding the gravity acceleration:

$$A_V = A_{PEAK}\sin\omega t \cos\phi + 1$$

$$A_L = A_{PEAK}\sin\omega t \sin\phi$$

Therefore

$$\theta_{ERROR} = \text{Arctan} \frac{A_{PEAK}\sin\omega t \sin\phi}{A_{PEAK}\sin\omega t \cos\phi + 1} \qquad (22)$$

At $\omega t = \pi/2$

$$\theta_1 = \text{Arctan} \frac{A_{PEAK}\sin\phi}{A_{PEAK}\cos\phi + 1}$$

At $\omega t = -\pi/2$

$$\theta_2 = \text{Arctan} \frac{-A_{PEAK}\sin\phi}{1-A_{PEAK}\cos\phi}$$

Letting $\theta_{OFFSET} = (\theta_1+\theta_2)/2$ values for θ_{OFFSET} are plotted versus the acceleration average and peak values for four values of ϕ. This plot is shown in figure 44 and illustrates that for ϕ less than 15° with acceleration peak values up to 0.29 g's, the offset angle is less than 0.5°.

CASE II

The buoy is pitching with $\theta°$ excursions about a neutral pitch angle at $\theta°$. Letting ϕ be the tilt angle of the buoy with respect to vertical and referring to figure 45, the following equations can be written:

$$\phi = \theta\sin\omega t + \theta$$

$$\dot{\phi} = \omega\theta\cos\omega t$$

$$\ddot{\phi} = -\omega^2\theta\sin\omega t$$

$$A_N = R\omega^2\theta^2\cos^2\omega t$$

$$A_T = -R\omega^2\theta\sin\omega t$$

The error in measurement is defined by equation 23,

$$\theta_{ERROR} = \text{Arctan} \frac{\beta\cos^2\omega t\sin\phi+\eta\sin\omega t\cos\phi}{\beta\cos^2\omega t\cos\phi-\eta\sin\omega t\sin\phi-1} \qquad (23)$$

$$\beta = R\omega^2\theta^2$$

$$\eta = R\omega^2\theta$$

Observing the pitch motion to have a 6 second period, the error is calculated at thirty-two discrete points for a single cycle of motion. The average of these errors is a reasonable approximation to the total offset angle. In figure 46, θ_{OFFSET} is plotted versus R for a sinusoidal pitch angle variation from 0° to 30°. The offset error is less than 0.125° for R values up to 15 feet with this motion.

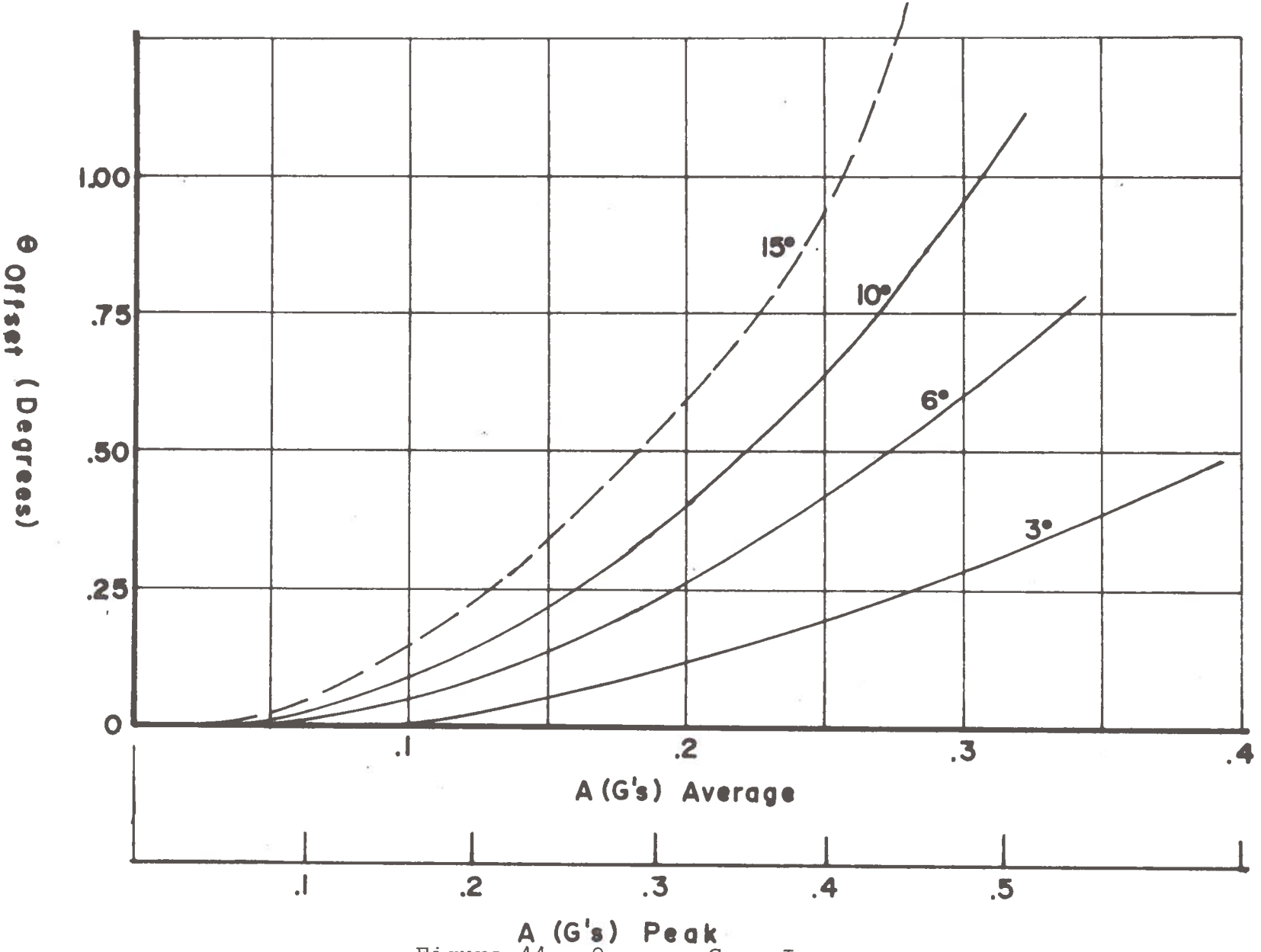

Figure 44. θ_{Offset} Case I

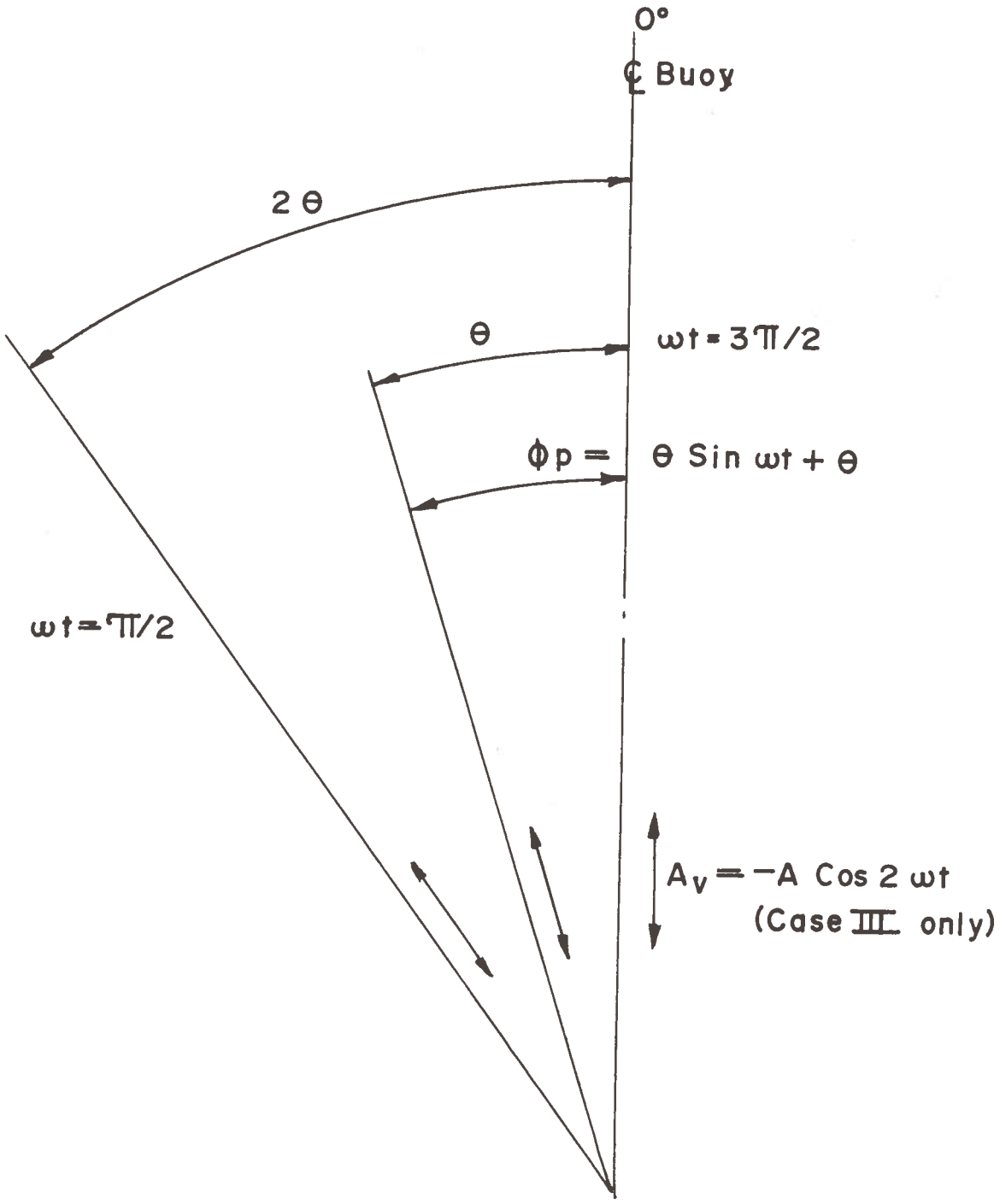

Figure 45. Buoy Motions Case II and Case III

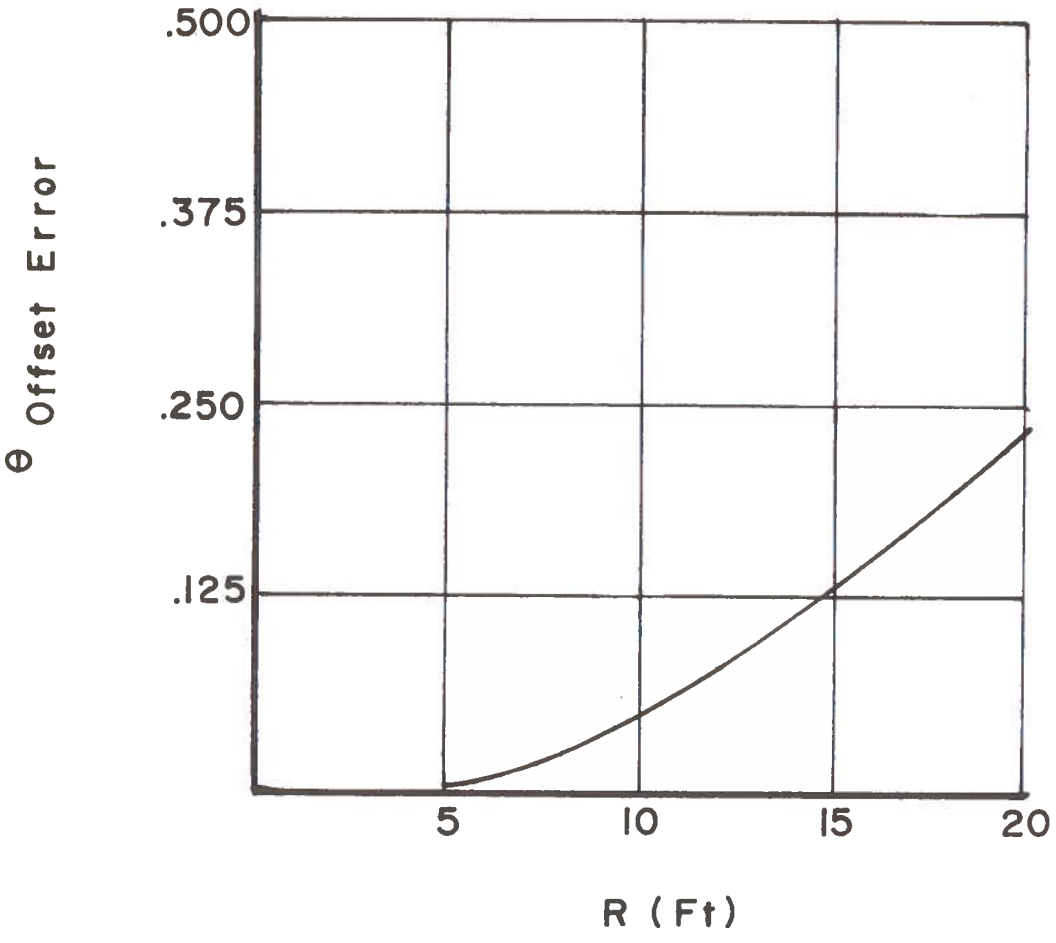

Figure 46. θ_{Offset} Case II

CASE III

Neglecting the components due to angular motions, consider the buoy pitching between 0° and 20°with accelerations along the axis of symmetry occurring at twice the pitching frequency as shown in figure 45.

$$\phi_p = \theta \sin\omega t + \theta$$

$$A_{BV} = -A_{PEAK} \cos 2\omega t$$

Using the average values shown in figure 47, the offset error can be written

$$\theta_{OFFSET} = 1/2 \left\{ 2\arctan \frac{.636A_p \sin\theta}{1-\cos\theta(.636A_p)} - \arctan \frac{.636A_p \sin(1.9\theta)}{1+\cos(1.9\theta).636A_p} - \arctan \frac{.636A_p \sin(.1\theta)}{1+\cos(.1\theta).636A_p} \right\} \quad (24)$$

Plotting this error versus the peak acceleration for values of θ equal to 5° and 10° in figure 48, it is shown that the offset error is less than 0.5° for a neutral pitch angle of 10° with 10° excursions for buoy axis accelerations up to 0.24 G. This error is larger than the error in Case I for a static pitch angle of 10° as would be expected due to the increased non-linearities associated with the varying pitch angle.

From the prototype tests, the peak buoy-axis accelerations were in the order of 0.15 G excluding momentary impulses from the tractor jerking and the angular excursions were more nearly centered about a zero angle. Both of these characteristics would indicate that the offset error upon averaging the inclinometer data would be well below the 0.5° limit. The actual linearity of the instrument was 0.4% or 0.36° which is also allowable.

The inclinometer data from the Series A tests was graphically averaged and the results are tabulated in Table 7. It was extremely difficult to correlate this data with the movie film because the pitch and roll planes were often not perpendicular to the camera lens but qualitative remarks can be made for each test.

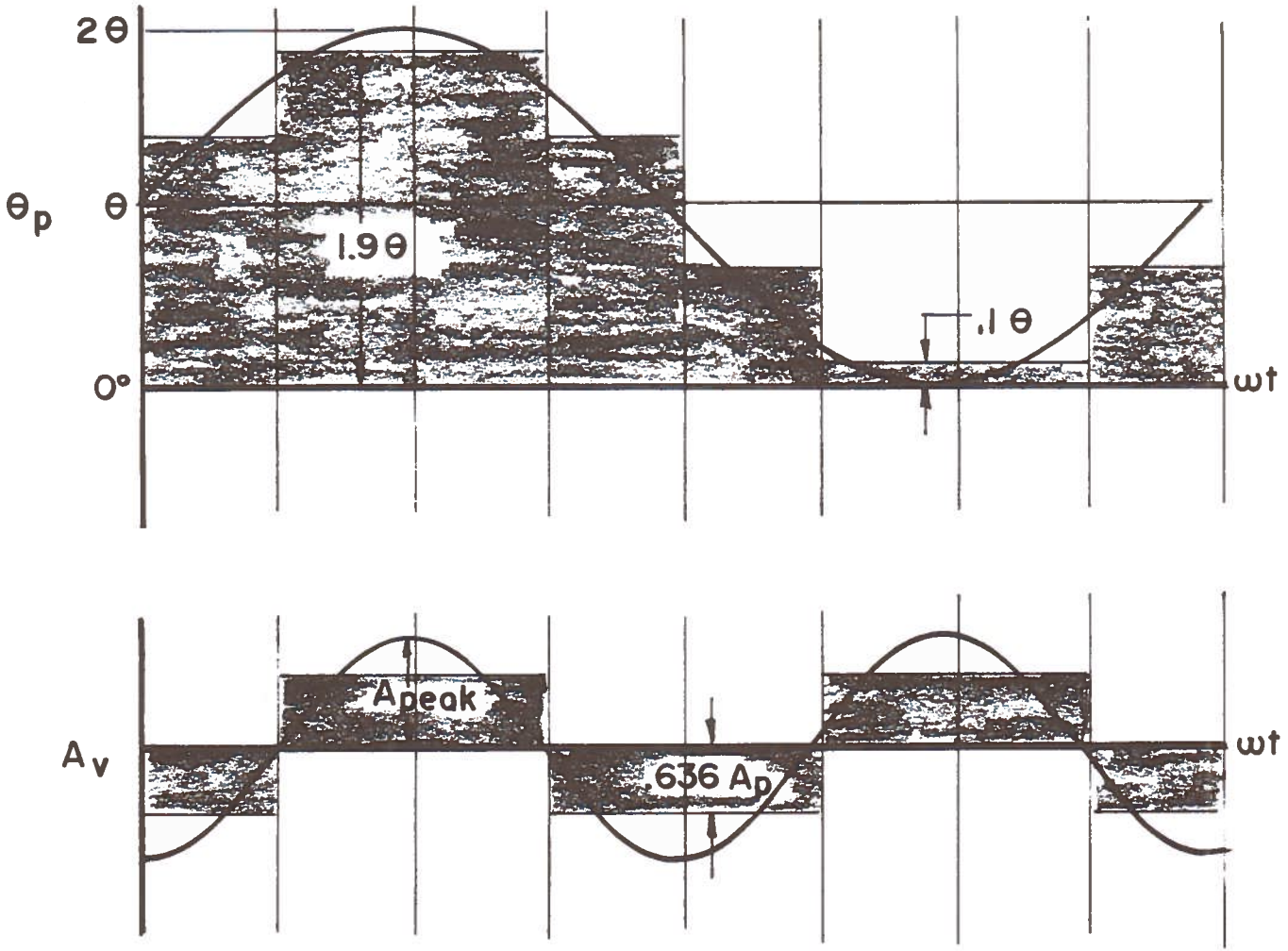

Figure 47. Case III Motions

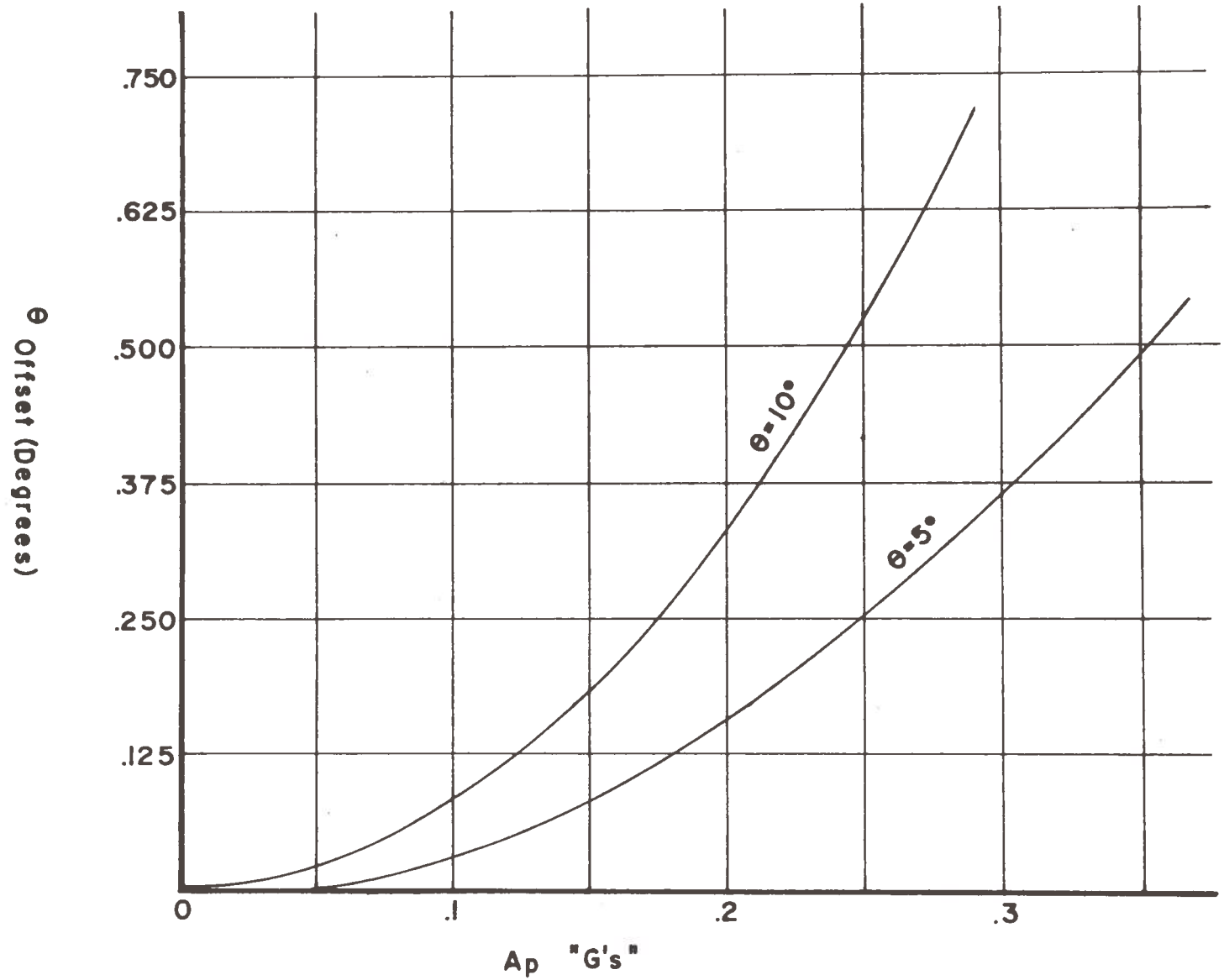

Figure 48. θ_{Offset} Case III

Table 7. Neutral Angle Test Data

Neutral Angle			
Test	Pitch	Roll	Remarks
A11	.62°	.48	No chain tension imparted by the tractor. Random motion, very sluggish.
A21	.71°	1.48°	Chain tension added, movement still sluggish.
A31	-.22°	2.17°	Motion extremely sluggish. Two long pauses in the positive roll plane.
A41	.80°	1.15°	Addition of a rope to the 1st tier of the superstructure. When pulled by men on shore, the buoy pitched and rolled dependent upon the rotational orientation of the buoy with the shore. Created more active angular excursions.
A71	.45		Rope was moved to the top of the superstructure increasing the moment arm and allowing for even more active excursions.
A81		2.30°	Buoy oriented such that pulling on rope caused positive excursions. Active motion apparent.
A91	.19°	3.24°	Buoy oriented such that pulling on rope caused negative pitch and positive roll excursions.
A10-1	-.80°	2.72°	
A11-1	-.53°	3.28°	

Analysis of the data from the A test indicates a neutral roll angle greater than the neutral pitch angle. This is to be expected from the test set-up as shown in figure 49. The axis of rotation of the bridle at the upper attach points was parallel to the roll axis. Also the bridle-chain interface did not clear the lower end of the counter weight and rested against the positive roll side. This constantly restricted negative roll motion but induced no hindrance to positive roll motion. Consequently, the buoy was rolling positive more often than negative, when a chain tension was imparted.

Observation of the data also reveals that the lateral accelerometers closely follow the output of the inclinometers. Small deviations are present because the inclinometer output is linear for angular input and the accelerometer senses the sine of the angular input. At an input angle of 18°, the output of the accelerometer multiplied by the radian conversion factor yields 17.7° or less than 2% error.

Considering the use of an accelerometer in place of an inclinometer, it is obvious that heave motions in the direction of the buoy vertical axis will not affect the output except by a small amount determined by the cross-axis sensitivity. Also angular acceleration components will time average to zero. Therefore, the errors produced in Cases I-III will not be present, but an inherent error does exist because of the non-linearity of the sine function. If the buoy is sinusoidally pitching from 0° to 30° with a neutral pitch angle of 15°, averaging the accelerometer output yields a value of .25408 G's, the arc sin of which is 14.719°, or an offset error of .281°. Another error is introduced when a vertical motion is superimposed upon a non-centered pitching motion. Let the following relations define this condition.

$$\phi_p = \theta \sin\omega t + \theta$$

$$A_V = -A_{PEAK} \cos 2\omega t$$

In this case, A_V defines the acceleration in the local vertical direction. Again using the average values shown in figure 47, the offset error can be approximated:

$$\theta_{OFFSET} = \frac{.636\ A_p[\sin(1.9\theta) + \sin(.1\theta) - 2\sin\theta]}{2} \qquad (25)$$

For a θ equal to 10°, the error at A_p equal to .50 G is less than 0.1°. The maximum static error band of the potentiometric lateral accelerometers is .15 G which could result in an offset angle error of 8°. For this reason, the accelerometer data was not averaged for comparison with the inclinometer

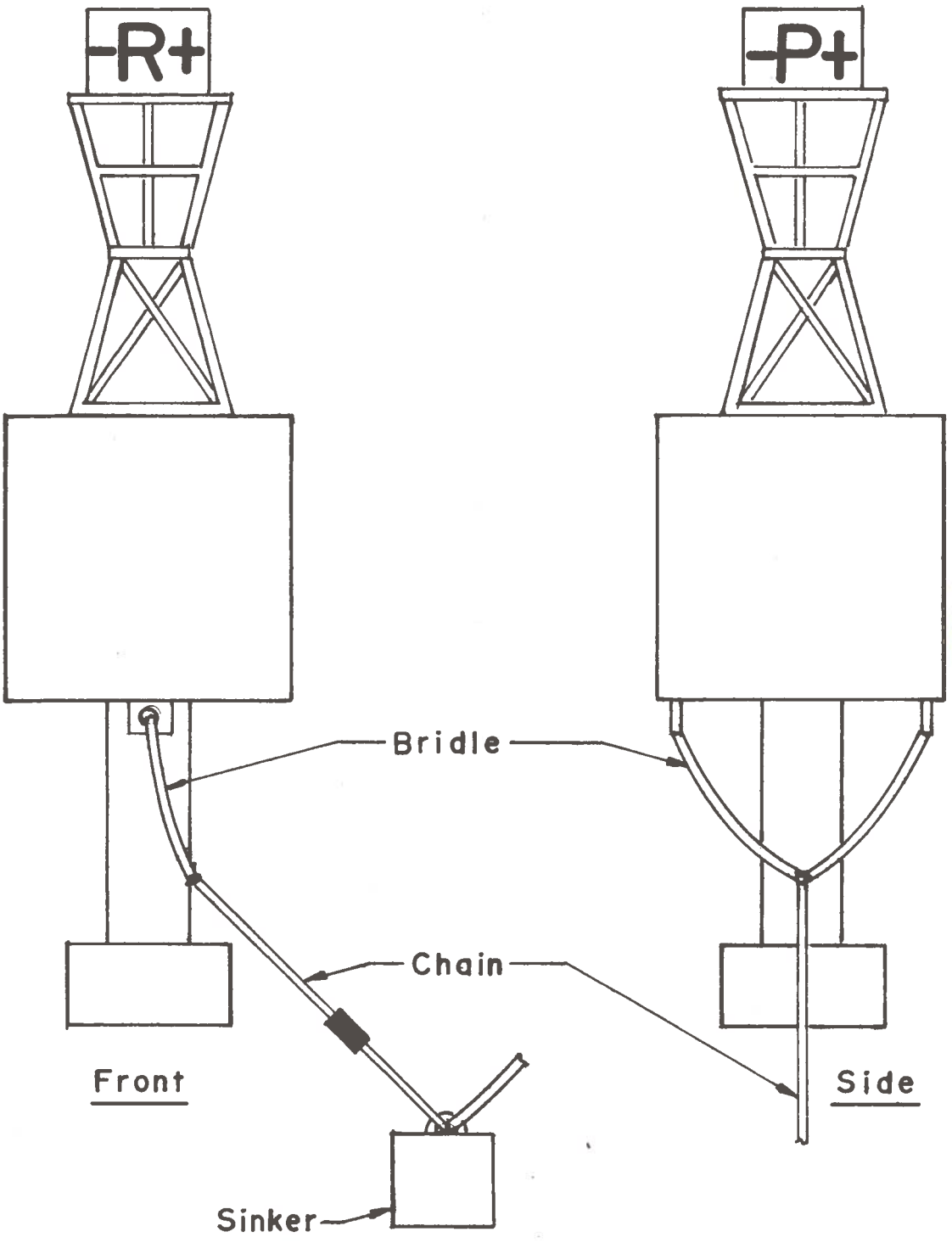

Figure 49. Mooring Configuration Prototype Test

data. Instruments are available with a static error band of .05% of the full range or .001 G on a + 1G unit. This would contribute less than 0.1% error to the offset angle determination. In a progress report concerning the Ocean Environmental Sensing Equipment developed by the Instrumentation Laboratory at The Massachusetts Institute of Technology in Cambridge, Massachusetts, the authors utilize the average of the accelerometer outputs to determine the initial orientation of a rate sensing device. They state that the "accuracy of this method is characterized by the following errors in determination of attitude: 0.3 deg. of vertical..."

From the previous discussion, it is indicated that the pendulum inclinometers or lateral accelerometers do furnish adequate data to determine the neutral pitch or roll angle of a buoy. Furthermore, knowledge of the acceleration parameters will allow an estimation of the error in these measurements and under most conditions, the error will be less than 0.5 degree.

ANGULAR EXCURSIONS

The vertical gyros discussed in the transducers section of this report were used to measure the amplitudes of angular motion. Although the gyros are designed to maintain a vertical reference within 1 1/2 degree, the introduction of gimbal errors must be considered when evaluating their performance. In this application, two forms of gimbal errors are present.

First consider the case in which the spin axis is not aligned with vertical. Defining the axis in which the pendulum vertical erection occurs as pitch and the case alignment axis as roll, a non-vertical spin axis can result from limitations of the unit up to 1 1/2° and the occurrence of a neutral roll angle other than 0°. Letting the spin axis tilt angle be 5° in the roll plane, a 90° yaw, remembering the property of the gyro to maintain its spatial alignment, causes the 5° angle to be transferred to the pitch axis when, in reality, no pitching motion had occurred. Knowledge of the neutral roll angle from the inclinometer or accelerometer data can yield the maximum error in the magnitude measurements. Minimizing the neutral roll angle can decrease the maximum possible error. This can be accomplished by placing the roll axis parallel to the axis of symmetry of the mooring chain. It is also noted that yaw motions of $\pm$ 90° occurring in phase with the pitch motions are improbable and therefore a smaller error can be expected.

A second gimbal error results because the output of the pitch axis does not remain in a vertical plane but is tilted according to the roll angle. Since the roll pot is located on the inner gimbal, it does yield a vertical reference. Therefore

$$\phi_{RINC} = \phi_{RG} \tag{26}$$

but,

$$\phi_{PINC} = \text{Arcsin}\,[\sin\phi_{PG}\cos\phi_{RG}] \tag{27}$$

ϕ RG = Roll gyro

ϕ RINC = Roll inclinometer

ϕ PG = Pitch gyro

ϕ PINC = Pitch inclinometer

For roll angles, ϕ_R, less than 18°, ϕ_{pinc} can be approximated by ϕ_{PG} with less than 5% error. Analysis of the prototype test data utilized this approximation with the results given in table 8, from the A series of tests. Referring to the remarks in table 8, the amplitude values appear reasonable.

Because of the inaccuracies probable in the inclinometer measurements, the use of a vertical gyro is necessary to determine the orientation of the accelerometer triad. Ideally, the spin axis would remain aligned with the local vertical but practically this is not accomplished because of inadequacies in the erection system. The simultaneous reduction of the five data channels with the spin axis non-vertical is analogous to a single vertical accelerometer stabilized at the same non-vertical angle. This accelerometer, assuming a 1 G bias, senses a component of gravity dependent upon the non-vertical angle and is equal to $[1-\cos\phi_{v\text{-}error}]$. For angles from 0° to 10°, this component varies from 0 g to 0.015 g. By minimizing the precession rate and mounting the gyro near the center of rotation, the response of the spin alignment mechanism to angular accelerations is minimized and the gravity component can be assumed constant and removed in a data averaging process. Another error results because the accelerometer does not sense the vertical acceleration but a cosine dependent component. If the spin is misaligned by 10°, the maximum error is equal to 1 1/2% of the indicated value. Gimbal errors are eliminated in the system equations.

It is expected that the gyros procured for the prototype unit will remain vertical within a 10° cone and the errors introduced will be small. To speed initial erection of the gyro, a reduced voltage may be applied to the rotor decreasing the angular momentum, $\bar{H}$, thereby increasing the precession velocity, ω_p. An actual ocean test is mandatory to adequately evaluate the performance and with this information the dynamic environment can be specified for laboratory simulations and absolute error determination.

ANGULAR RATES

The pitch and roll rates can be obtained by differentiating the gyro data graphically or by approximating the gyro data by a sine function and noting the period of motion to be 6 seconds. Using the latter method, the angular rate is given by equation 28.

$$\dot{\phi} = \phi_{PEAK}\omega \cos\omega t \qquad (28)$$

From this equation, it is seen that the peak rate is proportional to the peak excursion and by averaging the peak excursions as in the previous section and multiplying by the natural frequency of oscillation, an average value for the peak angular rate is obtained. While incremental differentiation can be accomplished by noting the slope of the curve at various points, equation 28 is used in evaluating the 8x26 test data which largely exhibited sinusoidal motion. The results of the angular rate calculations are included in table 8.

Table 8. Angular Data, Test A1 thru A4

TEST	Amplitude (Deg)		Rate (Deg/Sec)	
	ϕ_P	ϕ_R	$\dot{\phi}_P$	$\dot{\phi}_R$
A11	11.2	10.8	11.8	11.3
A21	7.6	9.3	8.0	9.8
A31	4.7	6.6	4.9	6.9
A41	13.4	5.4	14.1	5.7

MOORING LINE TENSION

The mooring line tension information was transmitted continuously during the prototype tests. Because of the test configuration, the chain tension data was largely composed of sudden impulses corresponding to the jerks of the tractor and did not simulate a moored environment. The average spike was 0.5 seconds in length and 3000 pounds maximum amplitude. Referring to figure 50, it can be seen that the vertical accelerometer data can be correlated qualitatively with the tension data, but because of the possible acceleration error, numerical correlation is not attempted. From the manufacturer's test data, the maximum error in the test cells was less than 50 pounds.

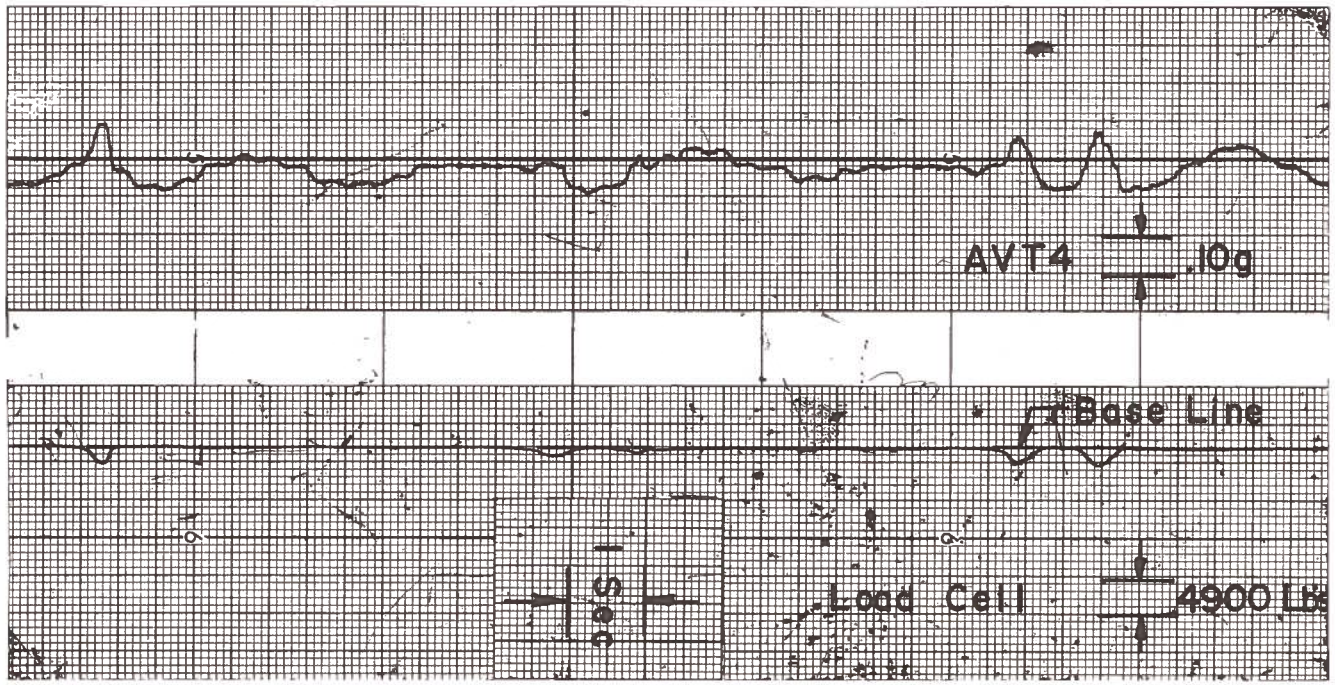

Figure 50. Load Cell and Accelerometer Correlation

10.0 ALTERNATE APPROACHES

Measuring the attitude and displacements of a buoy is a relatively new field and the basic approaches to date have utilized instrumentation originally designed for aircraft use. The most desirable means of obtaining the information required would be the use of a stable inertial platform such as those used on large aircraft or space vehicles. Angular data can be read directly and the heave motion measured with a vertically stabilized accelerometer eliminating the need for lateral accelerometers and simultaneous reduction of five data channels. Economic considerations forced abandonment of this approach.

Recently, however, gyro companies have begun to fabricate "poor man's platforms" consisting of a vertical gyro with an accelerometer mounted on the inner gimbal and hence vertically stabilized. It is obvious that while the motions of an aircraft are somewhat predictable, the open seaway imparts a random behavior to a moored buoy. It is this random behavior that causes difficulty in establishing a local vertical reference. Specifically, the vertical erection of a gyro is complicated by three factors.

a. The vertical sensor is a pendulum type device and therefore, subject to the errors discussed in the previous section. Increasing the damping coefficient reduces these errors but does not eliminate them.

b. The torquing motors used to precess the spin axis into alignment with the gravity sensor may exert a larger torque in one direction than the other. In this case, an offset angle can result even if the lateral accelerations average to zero.

c. Lateral translational acceleration is sensed on the rotor as an angular error and the gyro is precessed to align with this false vertical. Correction for this acceleration in aircraft is to simply turn off the erection system during turning or similar maneuvers and allow the gyro to drift freely during this period. Following completion of the maneuver, the erection system is re-activated and appropriate corrections applied. Such an option is not presently feasible on an ocean buoy because the motions are not adequately defined.

As a result of these error possibilities, no gyro stabilized accelerometer manufacturer contacted could guarantee erection of a standard unit to within 0.5 degree of vertical under the random dynamic conditions, although many units exhibited a non-verticality of less than 0.25 degree under controlled conditions. This accuracy uncertainty together with the cost factor similarly prohibited continuance of this approach.

An alternate method considered for determining the heave motion utilized wave measuring staffs, either resistive or capacitive in nature. By attaching one or several of these staffs to the candidate buoy and comparing the output to that of a staff attached to an offshore platform, the response of the buoy can be obtained. If the buoy exactly followed the wave action, a zero output of the staff would result and it would be apparent that the buoy motion paralleled the output of the stabilized staff. However, if the output of both staffs was identical, it would be obvious that the buoy was as stable as the offshore platform. The actual response lies between these extremes.

While this system offers absolute dc response and sensitivity to even tidal induced motions the errors caused by angular motion are significant. Since the staff cannot easily be attached to coincide with the buoy axis of symmetry, and more likely would have to be placed along the buoy exterior nearly five feet from this axis, any tilt of the buoy creates an amplified mock depth on the staff. Correction for this effect requires simultaneous reduction of the staff data with the pitch and roll information. Another disadvantage to this method is the susceptibility of the staff to fouling by marine life and oil.

11.0 CONCLUSIONS

Analysis of data from the prototype test resulted in the following conclusions:

a. The ranges of the angle measuring devices proved satisfactory, but a 20% reduction in the inclinometer range to ± 35° could be tolerated with a resultant 20% decrease in error margin. The magnitudes of the tangential components of angular acceleration dictate that the inclinometers cannot be used for instantaneous angle measurement because of the errors introduced but it has been shown analytically that averaging the output yields the neutral angle within the 0.5 degree accuracy requirement under expected G ranges. The use of low range accelerometers has also beeen proposed for this purpose both analytically and upon observation of the test data.

b. The ranges of the accelerometers proved to be much too great to adequately represent the buoy motions. The maximum accelerations of the test buoy were less than 10% of the sensor range of ± 5 G's. A reduction in range is obviously indicated.

c. The sensitivity of the angular devices proved satisfactory and utilized nearly 50% of the telemetry 0-5 VDC range for good resolution. Reduction in the range of the instrument will also increase the sensitivity and therefore the resolution.

d. The sensitivity of the accelerometers was inadequate and because of the very low G ranges experienced in the prototype tests, the use of potentiometric devices with the inherent friction is not advisable. Also, the accelerations utilized only 10% of the telemetry band and the error margins introduced here can also be alleviated by decreasing the range.

e. The use of a gyro to determine the amplitudes of angular motions is required because of the acceleration induced errors on the inclinometers. The dc gyros purchased for the prototype can be utilized for this purpose if oriented to place the case erection axis parallel to the mooring line plane to minimize yaw induced errors. The error of these measurements can be related to the neutral angle

in this plane.

Output from the gyros can also be differentiated to yield values for the pitch and roll rates. Because of the sinusoidal motion of the test buoy, rate values were calculated for this evaluation, although an incremental differentiation can be undertaken.

f. The dynamics of the prototype test did not induce representative lateral translations and therefore conclusions relating to this motion are not extended.

g. Observation of the angular motion in the prototype test was predominately sinusoidal and a maximum angular acceleration of 0.346 radians per second per second was calculated. The peak instantaneous error introduced to the inclinometer, or, accelerometer used for angular measurement, is nearly 6°. Because the translational accelerations will similarly degrade this performance, the use of a vertical gyro for absolute angle measurement is dictated. Compensation for non-verticality errors can be accomplished by data averaging.

h. Determination of the heave displacement and rate was complicated by the accelerometer inaccuracy but values were obtained that roughly correlated with the movie film values. By placing the instrument package at the center of rotation two advantages result.

    1. The heave movement sensed by the instrument is translational and not influenced by the angular excursions.

    2. The dynamic environment of the gyro would be less violent, thus aiding the erection to a vertical reference.

i. The mooring line tension data was definitely not representative of a moored situation but the results obtained indicate satisfactory operation.

j. The telemetry data transmission system operated satisfactorily with any drifts of the system periodically removed by the stepping switch calibration position. Battery voltage information was also relayed for instrument calibration.

k. The command system functioned properly after an initial low battery voltage difficulty was eliminated by the addition of more series cells.

l. The transducers functioned properly electrically except for a slight drop-out of signal in the pitch inclinometer that occurred at the + 10° position. Graphically compensating for this effect was easily done. It is also noted that the step-like character of the acceleration data from the potentiometric devices was due to the resolution of the instruments in the low acceleration ranges. This enabled the motion of the wiper arm to be seen over the individual wires of the potentiometer.

m. The low battery drain will allow the final tests to be run for six months on a single set of batteries.

n. Use of a pressure tight (10_{psi}) container will completely eliminate the possibliity of instrument contamination from the environment.

12.0 RECOMMENDATIONS

The prototype package should be modified as follows:

a. Replacement of present accelerometers with three more-sensitive units with specifications as shown in Table 9 with self-test calibration feature.

b. A reduction in the erection speed to 5°/minute for the gyro oriented with the inner gimbal axis parallel to the plane of the mooring line.

c. Rewiring of stepping switch to incorporate the new accelerometers and calibration features.

d. Replacement of enclosure with pressure tight case if indicated as a result of additional testing.

With these modifications complete, an ocean test should be performed with the buoy in an actual deep moored environment with the instrument package located at the apparent center of rotation. Data reduction will again be manual with the results used to evaluate the instrumentation and also to specify the dynamic environment for laboratory accuracy tests. Knowledge of this environment is also helpful, when specifying the characteristics of additional sensors if required.

Table 9. Accelerometer Specifications
Prototype Modification

PHYSICAL RANGE	
Vertical	0-1.5 g
Lateral	± .75 g
Voltage Output (nominal)	Telemetry: +0.2 to +4.8 VDC
Input Power	Telemetry: +28 VDC ± 10%, at 20 ma
Electrical Connector	Solder Terminals
Case Alignment	± 1° to True Sensitive Axis
Weight	2 oz.
Physical Configuration	Rect. Case: Electrically Damped
ACCURACY	
Non-Linearity B.F.S.L.	<0.015% of F.R.
Hysteresis	<0.01% of F.R.
Resolution	<0.001% of F.R.
Non-Repeatability	<0.01% of F.R.
Zero Output (Null)	<0.05% of F.R.
Temperature Coefficient of Null:	<0.001% of F.R./°F From -40° to +160°F
Temperature Coefficient of Scale Factor	<0.005% of F.R./F° From -40° to +160°F
Output Noises (RMS volts)	<0.05% of F.R.
Cross Coupling	<0.002 g/g at F.S.I. on SA
Vibration Rectification	1.0×10^{-3} g/g^2

Table 9. Accelerometer Specifications
Prototype Modification (Continued)

Natural Frequency 90° Phase Shift @ 72°F. (dependent on range)	E.D.: 150 to 250 Hz
Damping Ratio @ 72°F.	E.D.: 0.7 $\pm$ 0.1
ENVIRONMENTAL	
Temperature Range	Storage: -65°F to -200°F Operating: -40°F to +200°F
Shock Survival	100 g, 11ms
Vibration Survival	15g RMS, 20-2000 Hz
Humidity, Salt Spray, Fungus, Sand, Dust	Hermetically Sealed (Meets MIL-E-5272C)
Ambient Pressure	0 to 5 Atmospheric Absolute

REFERENCES

1. Waid, R. L., and Webster, Dr. W. C.: *An Experimental Study to Determine the Motions and Mooring Tensions of Three Buoys*, Report No. LMSC/DO22460, Lockheed Missiles and Space Company, Sunnyvale, California, 1968.

2. Toth, W., and Vachon, W.: *Progress Report on WHOI Contract PO17052, OESE and Geodyne Current Meter*, Report No. E-2229, Instrumentation Laboratory, MIT, Cambridge, Mass, 1968.

3. Dinter, Henry A.: *Inertial Sensors, Theory and Application*, Document No. AM-62, Honeywell, Aerospace Division, Minneapolis, Minnesota, 1967.

4. Thomson, William T.: *Vibration Theory and Applications*, New Jersey, Prentice-Hall, 1965.

5. Lichtenstein, Bernard: *Gyros Platforms Accelerometers*, Fifth Edition, Kearfott Division, General Precision, Inc., Little Falls, New Jersey, 1962.

APPENDIX A

TAPE SPEED COMPENSATION

TAPE SPEED COMPENSATION

In an earlier section of this report it was pointed out that with multiple buoy systems there were advantages to recording the data at the output of the fm receivers. To summarize; a multichannel recorder preserves time coherence, a permanent record is obtained which may be processed at a future date, and finally only one set of subcarrier discriminators is required since each tape track may be processed separately.

The bandwidth of information to be recorded on any one track must span from the lowest excursion of the first subcarrier oscillator to the highest excursion of the channel six oscillator which is a range of from 370 Hz to 1828 Hz. No other frequency components should be present because all of the subcarrier frequencies were mixed in a truly linear fashion. The recording and playback of this part of the spectrum should present no difficulties with any good quality instrumentation type tape recorder, however this may not be the case with a recorder of lower quality. Distortions due to the wow and flutter characteristics of the recorder may be unacceptable thus requiring corrective measures. This is mentioned primarily because the capability exists with the present discriminators to achieve significant improvements with the addition of several modules. This is shown in figure A-1. Parts A and B of this figure were added for clarity. The procedure is to record a known precision frequency along with the data. This frequency may be mixed with the data or recorded on a separate track. In playback this frequency will experience the same distortive effects as the data. If now a discriminator is used to process this frequency, an error signal will be generated which can be applied to the data discriminators to compensate for the original distortions. It should be noted that the reference frequency must be higher than the highest subcarrier frequency. A delay line is necessary to adjust conditions to where the error signal is applied at precisely the correct time. With this type of system a 30dB improvement is possible for tape-speed errors as large as the channel deviation, up to $\pm$ 7.5%.

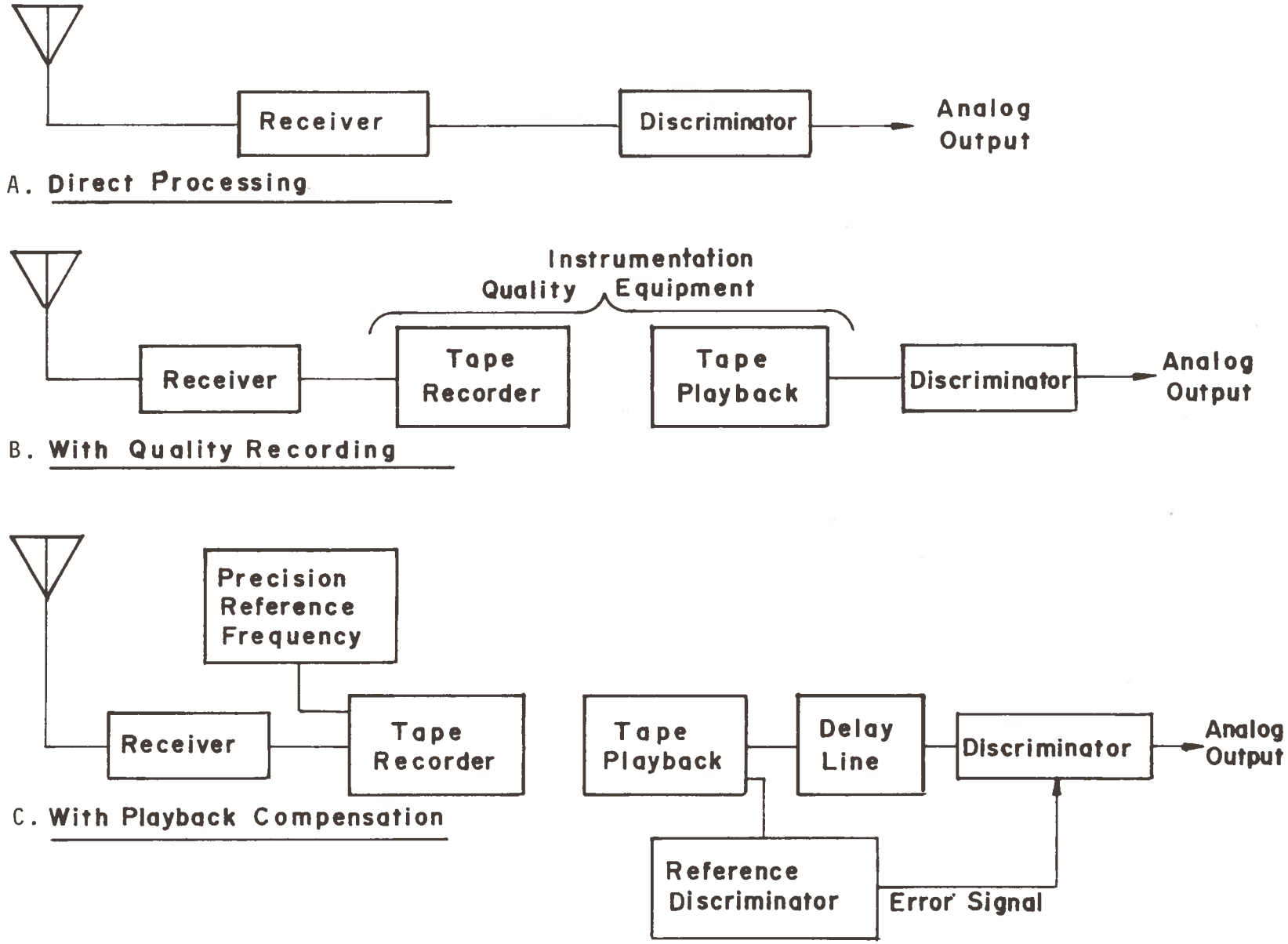

Figure A-1. Tape Speed Compensation

APPENDIX B

PROTOTYPE TEST PLAN

PROTOTYPE TEST PLAN

OBJECTIVE

The objective of this test is to determine actual sensor selection and package placement on a buoy. The sensors selected will be those that provide the best data to adequately describe the statistical parameters of dynamic buoy motion. Based on the data collected during this test a decision on whether or not to outfit additional buoys with a similar package will be made. A test plan for Phase III is to be developed.

TEST SITE

Per mutual agreement the test site has been chosen to be the Field Test and Development Center (FTDC) at the United States Coast Guard Station, Curtis Bay, Baltimore, Maryland.

PARTICIPANTS

Transportation Systems Center (TSC) will be represented by Lowell V. Babb, Mechanical Design Engineer and Robert W. Wilmarth, Electrical Design Engineer who will jointly direct the tests. Coast Guard personnel involved are expected to be LCDR William Newland and a contingent of Coast Guard technicians, the exact number dependent upon the task. A Coast Guard photographer will record the tests on movie film for future reference.

DURATION

It is anticipated that the initial set-up, check-out, and data collection will last about 10 days. Data analysis and recommendations for final design will begin subsequently and continue approximately two more weeks.

EQUIPMENT REQUIRED

The Coast Guard will furnish the following:

a. Test Equipment

1. Digital Volt Meter, 0-30 VDC Range, Floating Input
2. Power Supply - 28 VDC, 4 AMP capacity
3. Function Generator
4. Frequency Counter
5. Oscilloscope

b. Electrical and Mechanical Hardware

c. Tools

   1. Common electrical and mechanical technician type.

d. Operations Building - To house above equipment and be used as a ground base for telemetry and data collection. Coast Guard to furnish RG-8 cable for ground base antennas.

e. Candidate Buoy - 8x26 with following modifications:

   1. One mounting plate per TSC information
   2. Pitch and roll signs (TSC furnished, C.G. installed)
   3. Antennas and cables (TSC furnished, C.G. installed)
   4. Suitable batteries per TSC information
   5. Load Cell (TSC furnished, C.G. installed)
   6. Routing of cables (Load Cell, power, antennas)

f. Suitable equipment to launch and moor buoy and to impart motion.

g. Voice communications link between test conductor, dock site and photographer.

h. Magnetic tape recording equipment.

TSC will furnish:

a. Instrument Package with associated spare parts.
b. Test Apparatus for Package check-out.
c. Telemetry base station with appropriate interface connectors. [RG-58 cable and RF connectors]
d. 8-Channel Strip Chart Recorder for Data Analysis.

PRELIMINARY CHECKOUT

Following interface checks to the candidate buoy modified as listed above and insertion of the load cell in the mooring chain, the preliminary check-out can begin.

Both the buoy and the ground station antennas will be set-up at the building facility and power to the package will be furnished by:

1. 28-VDC power supply
2. buoy batteries

The current and voltages will be monitored and the calibration procedure performed by TSC. Output of all transducers will be monitored sequentially via telemetry link. Should problems arise, a direct check-out will be initiated omitting the telemetry link.

Assuming satisfactory performance at this stage, the batteries will be loaded into the buoy and the buoy deployed at a Coast Guard determined location. Coast Guard personnel, per TSC information will then attach the instrument package to the gong pad, the buoy antennas to the mast and the appropriate connectors to the package.

The ground station conductor will then command the package into operation to check the system. Proper operation of the magnetic tape recorder will also be verified.

Assuming correct operation of the system, the battery voltage and transducer voltage will be recorded.

ACTUAL TEST

The rotary switch will be placed in position one and approximately 30 seconds of data will be recorded on the magnetic tape, strip chart recorder and movie film. Documentation will be as follows:

a. Magnetic tape - prior to recording of data, voice input will be made to denote rotary switch position.

b. Strip chart - Marking pens will note on the chart:

    1. Switch position
    2. Channel sensitivity
    3. Paper speed

c. Movie film - Signs will be used to denote switch position.

d. Written log - Test conductor on scene will describe motions in log.

Synchronization of events will be via the communications link.

The above will be done for each of the twelve switch positions (see Table 1) with repetition possible at the discretion of the test conductors.

The package will now be mounted on the lantern pad and the above test repeated.

Based on preliminary findings the better package location and best appropriate sensors will be selected. The stepping switch will be bypassed to allow direct recording of the selected six sensors. Another test run will then be conducted using a 6 track magnetic tape recorder (GFE) to record the simultaneous output from the selected sensors. Data reduction on this tape will be a Coast Guard effort.

DATA REDUCTION

The purpose of this test is to determine if the sensors furnish adequate data to define the stability of the buoy. Specific items to be checked include:

1. Sensor Range - acceleration, angular
2. Sensor sensitivity
3. Necessity of Gyros
4. Magnitude of Lateral accelerations
5. Magnitude of angular accelerations

By visually examining the strip chart recording and utilizing a programmable calculator, vertical acceleration data can be found. Integration of this data, with planimeter, will yield heave rate and heave displacement. By comparing the heave data and angular data to the movies, instrument system accuracy can be surmised. Chain tension data from the strip chart recording will be compared to existing data for gross error determination.

TIME SCHEDULE

The tests are to be conducted during the period 7-16 June 1971. The first 2 days are for initial check out and calibration of equipment at the site. The remaining days are for launching the buoy (9 June) and conducting the water borne test.